

T-4340

INTEGRATED GEOPHYSICAL
INVESTIGATION OF A SHALLOW AQUIFER AT
ROCKY MOUNTAIN ARSENAL,
DENVER, COLORADO

ARTHUR LAKES LIBRARY
COLORADO SCHOOL OF MINES
GOLDEN, CO 80401

by

Nicholas E. White

ProQuest Number: 10783885

All rights reserved

INFORMATION TO ALL USERS

The quality of this reproduction is dependent upon the quality of the copy submitted.

In the unlikely event that the author did not send a complete manuscript and there are missing pages, these will be noted. Also, if material had to be removed, a note will indicate the deletion.



ProQuest 10783885

Published by ProQuest LLC (2018). Copyright of the Dissertation is held by the Author.

All rights reserved.

This work is protected against unauthorized copying under Title 17, United States Code
Microform Edition © ProQuest LLC.

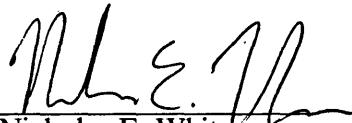
ProQuest LLC.
789 East Eisenhower Parkway
P.O. Box 1346
Ann Arbor, MI 48106 – 1346


T-4340


A thesis submitted to the Faculty and the Board of Trustees of the Colorado School of Mines in partial fulfillment of the requirements for the degree of Master of Science (Geophysical Engineering).

Golden, Colorado

Date 29. AUG. 95

Signed: 
Nicholas E. White

Approved: 
Dr. Frank Hadsell
Thesis Advisor
29 Aug '95


Dr. Phillip R. Romig
Department Head
Geophysics Department

ABSTRACT

This document evaluates the feasibility of integrating several geophysical methods to characterize geologic and hydrologic features, that are associated with a shallow paleochannel in the Denver Formation near Rocky Mountain Arsenal (RMA), Denver Colorado. The site is located in Section 13, Township 2 South, Range 67 West of the Rocky Mountain Arsenal's Offpost Study Area. The application of geophysical methods is desired to supplement geologic data, derived from soil borings and wells, pertaining to shallow groundwater aquifers (approximately 20 to 100 ft depth) at RMA. Surveys were designed, implemented, and evaluated for five geophysical methods: seismic refraction, seismic reflection, direct current (DC) resistivity, gravity, and frequency-domain electromagnetics (EM).

Survey design was aided by the creation of forward models and by field testing. Data acquisition was carried out along three intersecting profiles, one of which is near five soil boring locations. Data interpretation began with a geophysical model that was created from existing geologic information. Results from the five geophysical methods were then integrated to form an interpreted geologic model that correlates with existing borings and wells.

The subsequent evaluation of the geophysical methods reveals that P-wave refraction is successful in delineating the surface of the groundwater aquifer within the

boundaries of the paleochannel, and is successful in delineating the surface of the Denver Formation in regions where it subcrops above the aquifer surface (outside of paleochannel boundaries). The S-wave refraction method is shown to be useful in defining the surface of the unweathered Denver Formation. DC soundings alone yield ambiguous information on the depths and resistivities of the Denver Formation and overlying alluvial units. However, when DC sounding interpretations are constrained with the depth of the Denver Formation, known from borings and seismic methods, a complex alluvial structure is defined with more detail than any of the other four methods. The gravity method is used to delineate the surface of the Denver Formation. Frequency-domain EM profiles are successful in defining the shape of the Denver Formation, but are not successful in determining accurate depths to its surface. Seismic reflection methods (P-wave and S-wave), as implemented in this study, are shown to be ineffective tools for characterization of the shallow paleochannel.

TABLE OF CONTENTS

	Page
ABSTRACT	iii
LIST OF FIGURES AND TABLES	vii
ACKNOWLEDGMENTS	x
Chapter 1. INTRODUCTION	1
Study Objectives	3
Summary of Results	6
Chapter 2. GEOLOGY	7
Introduction	7
Unconsolidated Sediments	7
Denver Formation	9
Chapter 3. SURVEY DESIGN	13
Introduction	13
The Geologic Model	13
The Geophysical Model	15
Physical Parameters	17
Seismic Velocity	17
Electrical Resistivity and Conductivity	18
Density	19
Magnetic Susceptibility	19
Geophysical Method Selection	19
Geophysical Modeling and Field Testing	20
Seismic Models and Testing	21
P-wave Model	21
S-wave Model	23
Seismic Field Tests	23
Resistivity Model	28

Gravity Model	32
Electromagnetic Model	34
Chapter 4. DATA ACQUISITION AND PROCESSING	38
Introduction	38
The Positional Survey	38
P-wave Data Acquisition and Processing	40
P-wave Acquisition Equipment	40
P-wave Acquisition Geometry	41
Continuous Refraction Profiling	41
P-wave Data Processing	42
P-wave Refraction Processing	42
P-wave Reflection Processing	43
S-wave Data Acquisition and Processing	43
S-wave Acquisition Equipment	45
S-wave Acquisition Geometry	45
S-wave Data Processing	46
DC Sounding Acquisition	48
Gravity Data Acquisition	49
Electromagnetic Data Acquisition	50
Chapter 5. RESULTS AND INTERPRETATION	52
Introduction	52
Interpretation of P-wave Refraction Data	52
Interpretation of S-wave Refraction Data	56
Interpretation of Direct Current Resistivity Data	61
Interpretation of Gravity Data	69
Interpretation of Electromagnetic Data	70
Integrated Geologic Interpretation	77
Chapter 6. CONCLUSIONS	83
REFERENCES CITED	88
APPENDIX	91
DC Resistivity Data and Sounding Curves	92
Gravity Data	140
Electromagnetic Data	143

TABLE OF FIGURES

	Page
Figure 1. Location map for site of geophysical investigation.	2
Figure 2. Detailed site map showing survey line locations.	4
Figure 3. Generalized east-west cross-section from the South Platte River to the northeast corner of Rocky Mountain Arsenal (Source: Guest, 1988).	5
Figure 4. Quaternary columnar section (Modified from Guest (1988)).	8
Figure 5. The Unified Soil Classification System (ASTM D-2487) is used at RMA to classify unconsolidated sediments.	10
Figure 6. Bedrock surface elevation map in the Offpost Study Area near the RMA northern boundary (Source: RMA CAD drawing, region.dwg (dated 5/27/94)).	12
Figure 7. Geologic cross-section (east-west) across the northern boundary of the site (Source: ESE, 1988).	14
Figure 8. Denver Formation sandstone unit subcrop map (Source: ESE, 1988).	16
Figure 9. Modeled P-wave seismic record created with <i>cshot</i>	22
Figure 10. Modeled S-wave seismic record.	24
Figure 11. P-wave record obtained during field testing (sledge hammer source at Site 1)..	27
Figure 12. The Schlumberger electrode array was used to acquire DC resistivity data. The potential electrodes, M and N, are kept near the center of the array. The current electrodes, A and B, are placed much farther away from the center point.	29

Figure 13. A family of modeled apparent resistivity curves. Each model is such that $\rho_1 > \rho_2 > \rho_3$. Only the thickness of the middle layer is varied. 30

Figure 14. Chart of percent change in apparent resistivity versus $AB/2$ distance for varying thicknesses of the unconsolidated saturated zone (± 10 percent and ± 20 percent change in the thickness of the second layer). 31

Figure 15. (a) Density model based on the depth to the Denver Formation as given in the five wells/borings along Line 1. (b) Modeled Bouguer gravity showing a large anomaly resulting from a high in the Denver Formation at the west end of the line. 33

Figure 16. Cumulative response curves showing the relative contribution to measured apparent conductivity of all material below a given depth. The horizontal axis (z) is depth divided by the coil spacing. $R_v(z)$ is the cumulative response function for VMD orientation and $R_h(z)$ is the cumulative response function for HMD orientation. 37

Figure 17. Location of survey lines with state plane coordinates. 39

Figure 18. Typical P-wave record from Line 1 showing noise levels. 44

Figure 19. Reversing the direction of the sledge hammer impact reverses the polarity of the recorded SH-waves. 47

Figure 20. P-wave (refractor) and S-wave velocities of Line 1. P-wave velocity of surface layer averaged 1,200 ft/s. 54

Figure 21. Interpreted P-wave refractor for Line 1, P1-1. 55

Figure 22. Interpreted P-wave refractor for Line 2, P2-1. 57

Figure 23. Interpreted P-wave refractor for Line 3, P3-1. 58

Figure 24. Calculated P-wave and S-wave velocities for Line 2. 59

Figure 25. Interpreted S-wave refractor for Line 2, S2-1. 60

Figure 26. Interpreted S-wave refractor for Line 1, S1-1. 62

Figure 27. Two type-curves which are representative of the observed apparent resistivity curves. The apparent resistivity curve on the left is a KH-type curve and the curve on the right is a Q-type curve. 63

Figure 28. DC resistivity sounding interpretation for Line 1. The interpreted resistivity models are superimposed on the cross-section at each sounding location. 65

Figure 29. DC resistivity sounding interpretation for Line 2. The interpreted resistivity models are superimposed on the cross-section at each sounding location. 67

Figure 30. DC resistivity sounding interpretation for Line 3. The interpreted resistivity models are superimposed on the cross-section at each sounding location. 68

Figure 31. Interpreted surface of the Denver Formation from gravity data. 71

Figure 32. HMD conductivity measurements for Line 1 (EM-31 and EM-34). 73

Figure 33. VMD conductivity measurements for Line 1 (EM-31 and EM-34). 74

Figure 34. Interpreted surface of the Denver Formation along Line 1 based only on EM data. 76

Figure 35. Interpreted conductivities for Line 1. 78

Figure 36. Combined interpretations for Line 1. The EM surface has been manually shifted downward to agree with S-wave and gravity interpretations. 80

Figure 37. Integrated interpretation for Line 2. 81

Figure 38. Integrated interpretation for Line 3. 82

Table 1. Comparison of calculated apparent conductivity values. 36

ACKNOWLEDGMENTS

I am extremely grateful to Katherine Cain and Paul Lucas from the Office of the Program Manager, Rocky Mountain Arsenal. The funding and support offered by Rocky Mountain Arsenal opened the door to graduate school as well as a career in engineering / environmental geophysics. I thank the graduate students who provided help when I was in the dark: Will Barnard, Craig Artley, Mike Powers, Gary Elkington, Rob Kendall, Asbjorn Christensen, and many others. Obviously many professors deserve my gratitude. In particular, many thanks to Dr. Wahid Ibrahim for initiating the project and Dr. Frank Hadsell for ending it! Special thanks to Dr. David Butler, my geophysical mentor, for providing me with valuable experience and support. I wish to thank my parents and family for heralding education as an important and noble pursuit. Finally, I have to thank all of the friends who helped me drag out my graduate school experience by enticing me to have fun: the Oyster Club crew, Glen DiCostanzo, the students mentioned above, the Christines, Trish Green, and many more. We had a good time, and for that I'm grateful.

Chapter 1

INTRODUCTION

The Rocky Mountain Arsenal (RMA), located adjacent to Commerce City, Colorado, was the site of an investigation that evaluates the effectiveness of using several geophysical methods to characterize the geologic and hydrologic structure of a shallow groundwater aquifer. A system of shallow, unconfined aquifers in the Offpost Study Area of RMA was identified as a transport mechanism for contaminants that originated from on-site RMA (ESE, 1988). Successful remediation of these contaminated groundwaters is best served by detailed knowledge of the geologic materials that compose the aquifers and an understanding of how these materials influence the groundwater system.

In this study, five individual geophysical methods were used to delineate shallow geologic features: seismic refraction, seismic reflection, direct current (DC) resistivity, gravity, and frequency domain electromagnetic (EM) methods. The study site, located over the western boundary of a contaminated aquifer, occupied the north half of the southwest quarter of Section 13, approximately one-quarter mile north of the northern RMA boundary, on the east side of Peoria Street (**Figure 1**). During the summer of 1992, geophysical data were acquired along three intersecting lines. Line 1 was located coincident with five pre-existing and two post-acquisition (placed after the geophysical survey) soil borings (**Figure 2**). Line 2 was located one-quarter mile south of Line 1. Line 3 was perpendicular to and intersected Lines 1 and 2.

This document describes the survey design process, provides data acquisition parameters, presents the acquired data, and provides possible interpretations for observed

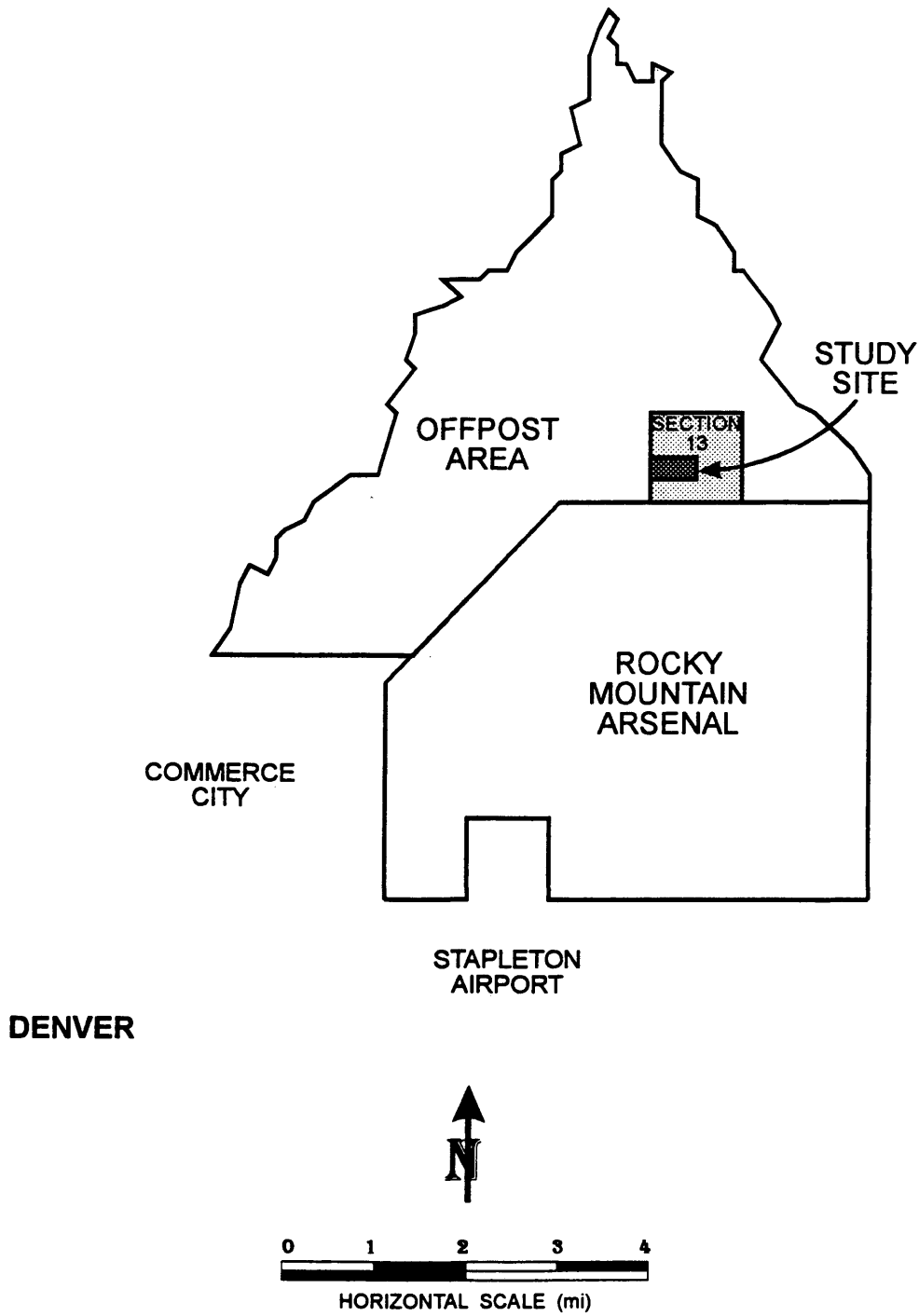


Figure 1. Location map for site of geophysical investigation.

geophysical anomalies. No individual geophysical technique can provide a unique geologic solution without external constraints, and each technique responds to different physical properties of the subsurface. Therefore, the design and interpretation processes were benefited by the integration of the results from each of the geophysical techniques and by the integration of known geology with the final geophysical interpretations.

Study Objectives

The shallow groundwater system at RMA is predominantly controlled by the ancient eroded surface of the Denver Formation claystone. A system of stream channels was eroded into the Denver formation by the ancestral South Platte River during the Quaternary period (ESE, 1988). A complex package of unconsolidated alluvial and eolian units now overlies the eroded surface of the Denver Formation and serves as the host material for an unconfined aquifer, with the underlying Denver claystone serving as the aquifer's impermeable base (Guest, 1988) (**Figure 3**). Topographic highs in the Denver Formation subcrop above the groundwater surface to form lateral aquifer boundaries. The primary objective of this geophysical investigation was to identify geophysical techniques that aid in identifying clays and sands in the unconsolidated portion of the aquifer. Additionally, any geophysical techniques that delineate the surfaces of the Denver Formation and the water table were to be identified.

The motive for defining unconfined aquifer boundaries and aquifer host materials is to find the most effective location of remediation wells, either injection or removal. Wells located in the unconfined aquifer's permeable sand and gravel units are more effective than those located in its impermeable clays or in Denver Formation highs.

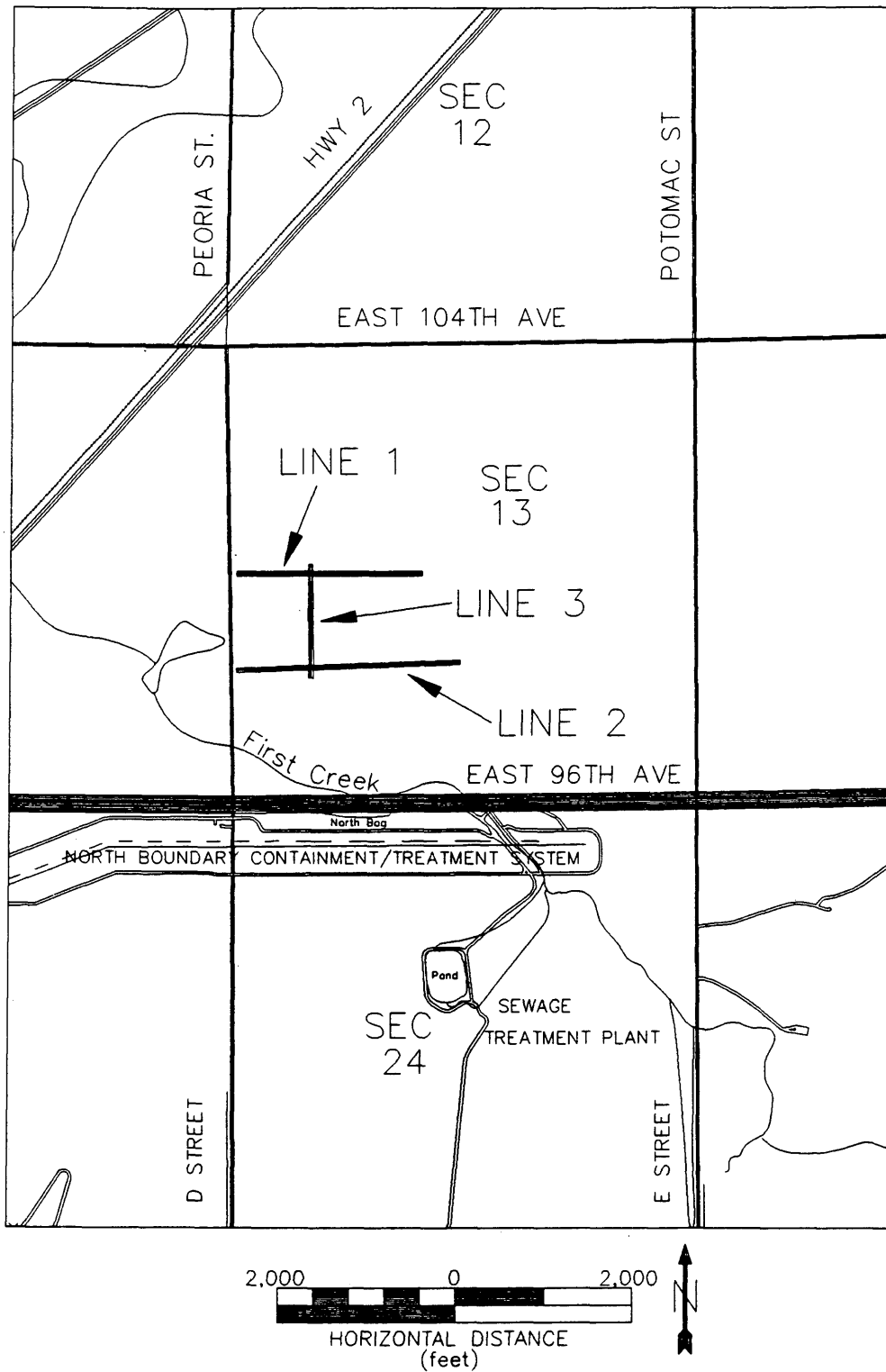


Figure 2. Detailed site map showing survey line locations.

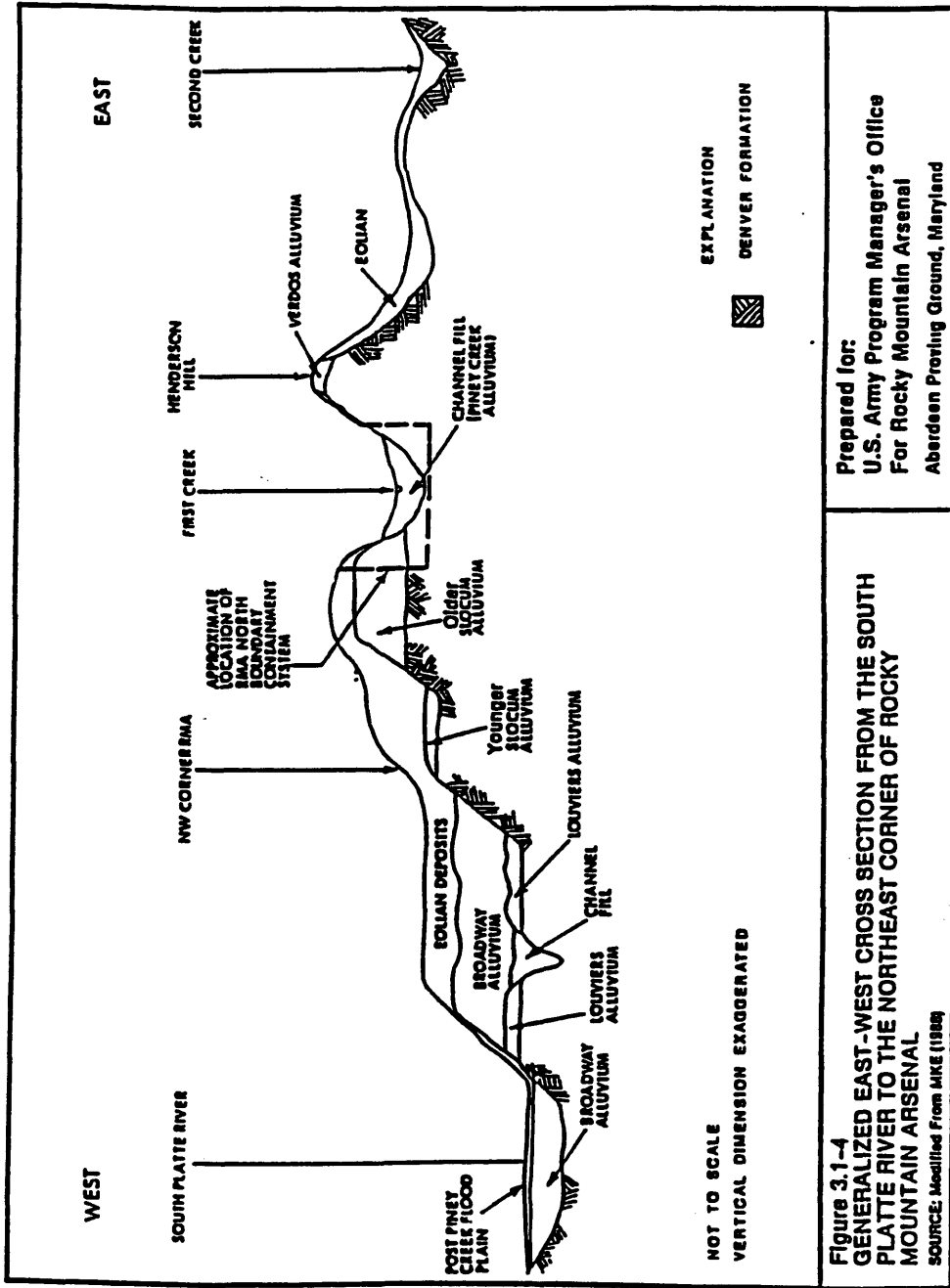


Figure 3. Generalized east-west cross-section from the South Platte River to the northeast corner of Rocky Mountain Arsenal (Source: Guest, 1988).

Summary of Results

The final results of the investigation reveal that several of the applied geophysical techniques were effective in meeting some of the stated objectives. Specifically, P-wave refraction was successful in delineating the surface of the groundwater aquifer within the boundaries of the paleochannel, and was successful in delineating the surface of the Denver Formation in regions where it subcrops above the aquifer surface (outside of paleochannel boundaries). The S-wave refraction method was shown to be useful in defining the surface of the unweathered Denver Formation. DC soundings, by themselves, were found to yield ambiguous information about the depths and resistivities of the Denver Formation and overlying alluvial units. However, when DC interpretations were constrained with the known depth of the Denver Formation from borings and seismic methods, a complex alluvial structure was defined with more detail than any of the other four methods could provide. The gravity method was used to define the surface of the Denver Formation, and EM methods were successful in defining the shape, but not the depth, of the Denver Formation. Seismic reflection methods (P-wave and S-wave), as implemented in this study, were determined to be ineffective tools for the characterization of the shallow paleochannel.

Chapter 2 GEOLOGY

Introduction

The starting point for the design of this geophysical survey is the characterization of the local geologic and hydrogeologic system at Rocky Mountain Arsenal. A thorough understanding of the lithologic and hydrologic properties of the shallow subsurface will be the starting point for geophysical modeling and testing, and will be integrated into the final interpretation of geophysical results. The geologic units of primary concern to this study can be divided into two groups: the unconsolidated surface materials and the underlying Denver Formation.

Unconsolidated Sediments

The unconsolidated sediments at RMA are made up of a complex sequence of terrace gravel, colluvium, eolian sand, loess, and fluvial sediments (Romero, 1976). Surficial units are primarily alluvial and eolian units of the Quaternary period (Pleistocene and Holocene epoch, **Figure 4**) (May, 1982). Pre-Wisconsinan sediments consist of fluvial silts, sands, and gravels that were deposited as glacial outwash (May, 1982). Post-Wisconsinan eolian sediments were generated from the weathered glacial outwash materials (Guest, 1988).

In the area of Section 13, the unconsolidated sediments are stratified into two layers. The upper unit corresponds to the post-Wisconsinan wind-blown sediments and consists of approximately 15 ft of eolian silt and clay (Guest, 1988). The lower unit consists of well-sorted fluvial sand and gravel and is associated with the Pleistocene

ERA	PERIOD	EPOCH	AGE	FORMATION		
CENOZOIC	QUATERNARY	HOLOCENE		Post Piney Creek Alluvium		
				Piney Creek Alluvium		
				Eolian		
		PLEISTOCENE		Wisconsinan	Loess	
					Broadway Alluvium	
				Illinoian	Louviers Alluvium	
					Slocum Alluvium	
					Verdos Alluvium	
				Kansan		

NOT TO SCALE

Figure 4. Quaternary columnar section (Modified from Guest (1988)).

Slocum Alluvium or with the Holocene Piney Creek Alluvium. The Slocum Alluvium consists of coarse gravel interlayered with lenses of arkosic sand, and the Piney Creek Alluvium is commonly thin, fluvial sands, silts, and clays with gravelly lag deposits at its base (Guest, 1988).

The Unified Soil Classification System (ASTM D-2487) is used at RMA to classify the unconsolidated sediments according to grain size, organic material content, and degree of sorting (**Figure 5**). The thickness of unconsolidated overburden varies from approximately 120 feet in the southwest portion of RMA (Lindvall, 1983) to nearly non-existent, north of the Northern Boundary Containment System (ESE, 1988).

Denver Formation

The Denver Formation was deposited in a continental environment that included braided stream, low-gradient stream, overbank, and marsh depositional environments. This complex depositional environment is reflected in the lithologic components of the Denver Formation that include the conglomerate and sandstone beds resulting from the braided streams near the uplifted mountains of the Laramide Orogeny (50 to 60 m.y. ago), and the siltstone, claystone, and lignites of the alluvial plain farther to the east of the Laramide mountains (Kirkham & Ladwig, 1979).

The surface of the Denver Formation has been shaped by extensive Quaternary erosional processes. A system of channels and associated interchannel highs has been incised into the surface of the Denver Formation during the development of the South Platte River valley (Romero, 1976). As a result of extensive erosion, the surface of the Denver Formation is often weathered. A shallow, predominately unconfined, aquifer is contained within the unconsolidated alluvial sediments and bounded by the Denver Formation. Topographic bedrock highs create unsaturated zones within the

MAJOR DIVISIONS			TYPICAL NAMES	
COARSE-GRAINED SOILS MORE THAN HALF IS COARSER THAN NO. 200 SIEVE	GRAVELS MORE THAN HALF COARSE FRACTION IS LARGER THAN NO. 4 SIEVE	CLEAN GRAVELS WITH LITTLE OR NO FINES	GW	WELL GRADED GRAVELS WITH OR WITHOUT SAND, LITTLE OR NO FINES
			GP	POORLY GRADED GRAVELS WITH OR WITHOUT SAND, LITTLE OR NO FINES
		GRAVELS WITH OVER 12% FINES	GM	SILTY GRAVELS, SILTY GRAVELS WITH SAND
			GC	CLAYEY GRAVELS, CLAYEY GRAVELS WITH SAND
	SANDS MORE THAN HALF COARSE FRACTION IS SMALLER THAN NO. 4 SIEVE	CLEAN SANDS WITH LITTLE OR NO FINES	SW	WELL GRADED SANDS WITH OR WITHOUT GRAVEL, LITTLE OR NO FINES
			SP	POORLY GRADED SANDS WITH OR WITHOUT GRAVEL, LITTLE OR NO FINES
		SANDS WITH OVER 12% FINES	SM	SILTY SANDS WITH OR WITHOUT GRAVEL
			SC	CLAYEY SANDS WITH OR WITHOUT GRAVEL
FINE-GRAINED SOILS MORE THAN HALF IS FINER THAN NO. 200 SIEVE	SILTS AND CLAYS LIQUID LIMIT 50% OR LESS	ML	INORGANIC SILTS AND VERY FINE SANDS, ROCK FLOUR, SILTS WITH SANDS AND GRAVELS, LEAN CLAYS	
		CL	INORGANIC CLAYS OF LOW TO MEDIUM PLASTICITY, CLAYS WITH SANDS AND GRAVELS, LEAN CLAYS	
		OL	ORGANIC SILTS OR CLAYS OF LOW PLASTICITY	
	SILTS AND CLAYS LIQUID LIMIT GREATER THAN 50%	MH	INORGANIC SILTS, MICACEOUS OR DIATOMACEOUS, FINE SANDY OR SILTY SOILS, ELASTIC SILTS	
		CH	INORGANIC CLAYS OF HIGH PLASTICITY, FAT CLAYS	
		OH	ORGANIC SILTS OR CLAYS OF MEDIUM TO HIGH PLASTICITY	
HIGHLY ORGANIC SOILS			Pt	PEAT AND OTHER HIGHLY ORGANIC SOILS

Figure 5. The Unified Soil Classification System (ASTM D-2487) is used at RMA to classify unconsolidated sediments.

unconsolidated sediments. A general northwest dip in the bedrock surface and the paths of the bedrock paleochannels control the flow direction of local groundwaters. Two paleochannels are identified in the vicinity of Section 13. The largest channel is the First Creek Paleochannel, which approximately parallels the path of the current First Creek drainage (**Figure 6**). The second channel, referred to as the Northern Paleochannel, extends north through Section 13 from the northern RMA boundary. The site for this geophysical investigation is located over the western boundary of the Northern Paleochannel.

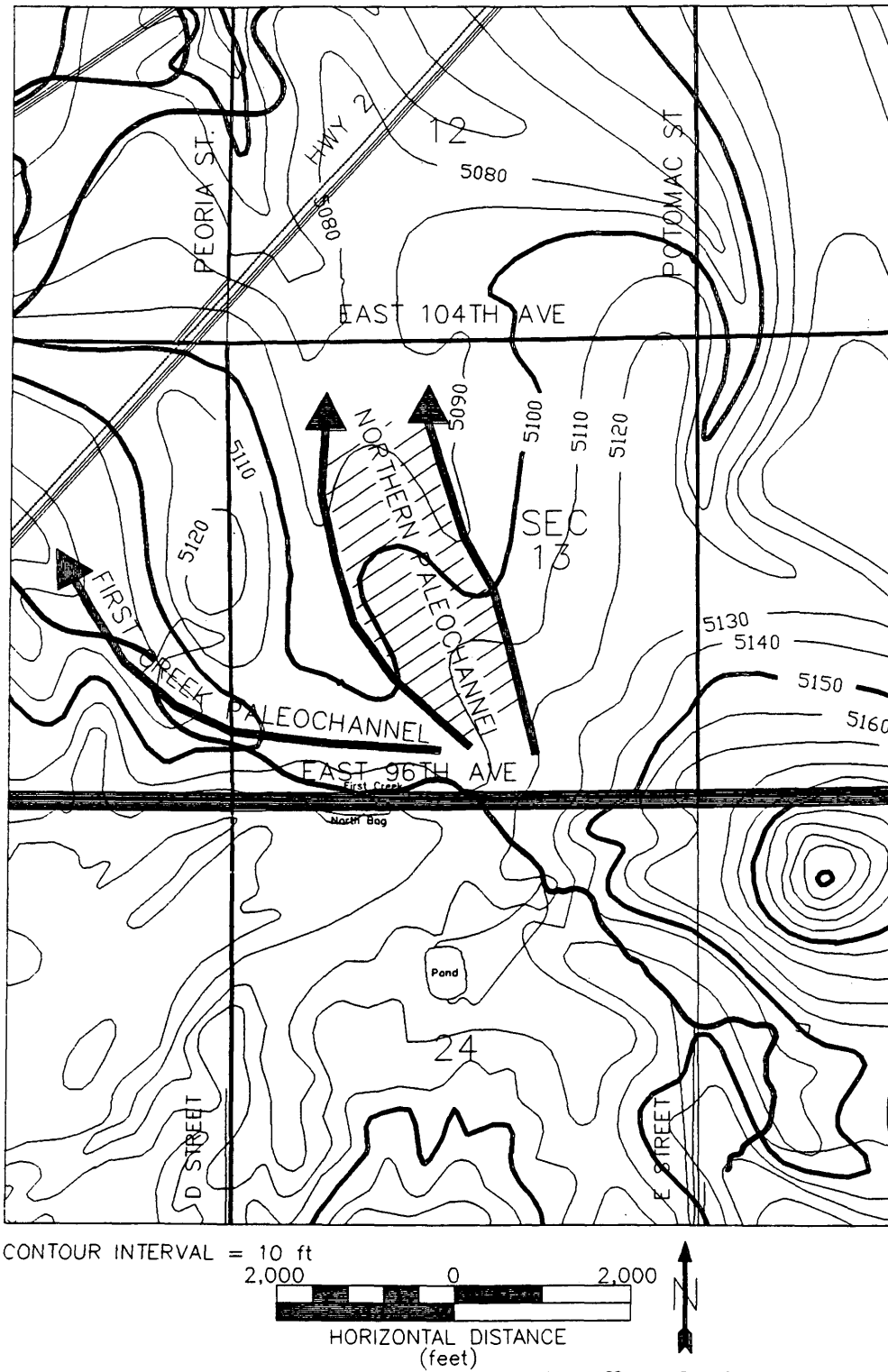


Figure 6. Bedrock surface elevation map in the Offpost Study Area near the RMA northern boundary (After: RMA CAD drawing, region.dwg (dated 5/27/94)).

Chapter 3

SURVEY DESIGN

Introduction

This chapter documents the geophysical survey design process. Survey design began with a review of previous geological and geophysical studies at RMA. A list of geophysical methods that were likely to be successful was generated based on a general concept of the site geology and estimated physical properties of the subsurface. Forward modeling, based on an initial geologic model, was used to verify that the contrasts in physical properties between targeted geologic units were large enough to be observed with geophysical methods. Forward modeling also guided the design of survey geometry parameters, such as geophone spacing for the seismic surveys and electrode spacing for electrical soundings. Finally, field testing further refined acquisition parameters.

The Geologic Model

The geologic model was derived from geologic logs from the five borings/wells located along the northern boundary of the site. A geologic cross-section (HLA, 1988) constructed from these wells characterizes a portion of the Northern Paleochannel (**Figure 7**). Three dominant lithologies are defined: (1) a fine-grained unconsolidated unit that is predominantly unsaturated (eolian), (2) a coarse-grained alluvial unit that is saturated (Slokum Alluvium), and (3) the underlying Denver Formation that is saturated in the area of the paleochannel and unsaturated where the top of the Denver is higher in elevation.

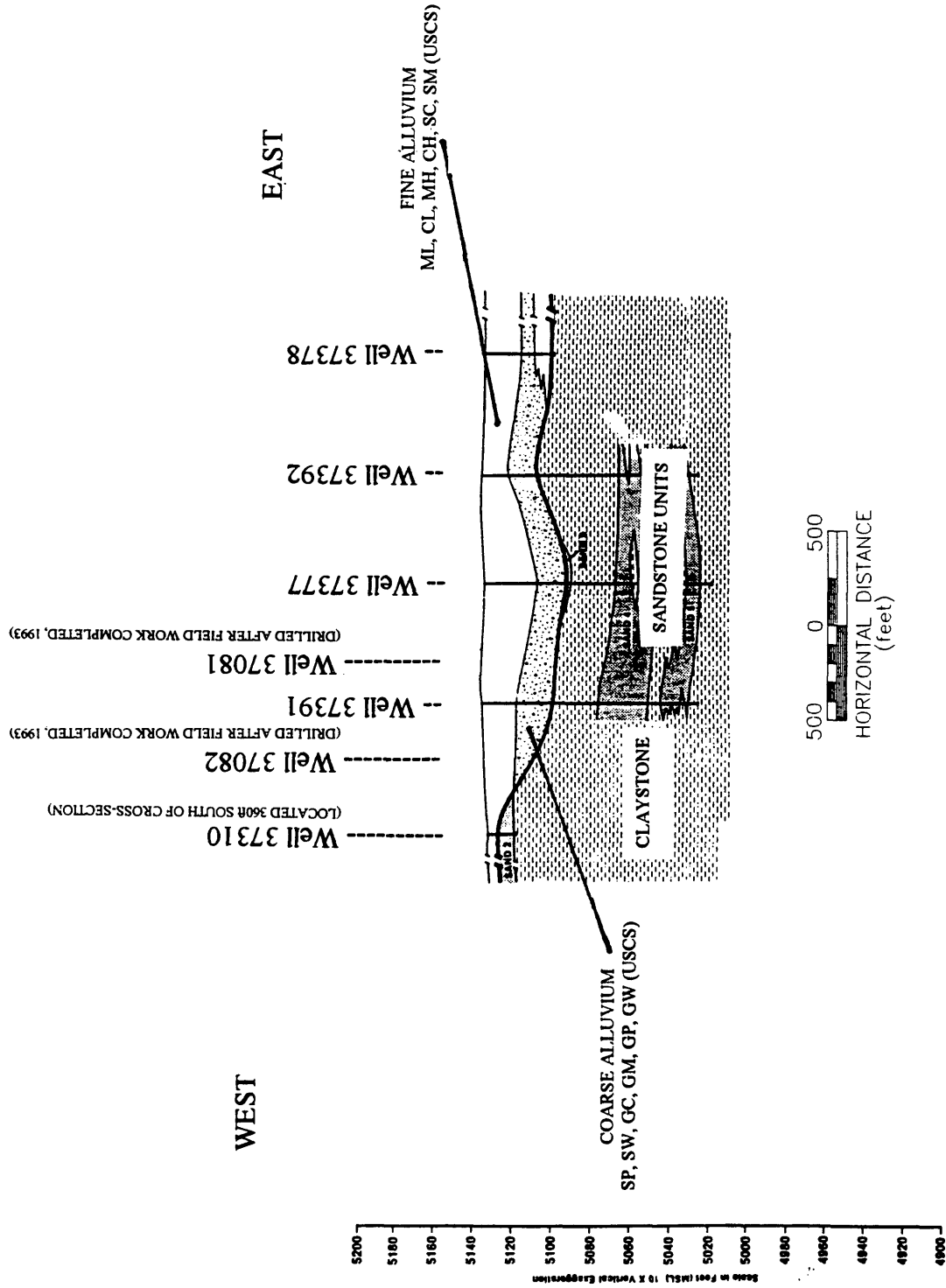


Figure 7. West-east geologic cross-section across the northern boundary of the site (After: ESE, 1988).

The west end of the cross-section is an interchannel high with the fine-grained eolian unit lying directly on top of an unsaturated portion of a Denver Formation sandstone. At some point between wells 37310 and 37391, the bedrock surface dips to the east and defines the western edge of the paleochannel. The coarse-grained alluvial unit appears between the Denver Formation and the overlying fine-grained unit as the bedrock surface deepens to form the paleochannel. The central and eastern portions of the cross-section show approximately 40 feet of unconsolidated sediments (fine and coarse-grained) overlying Denver Formation claystone.

Interbedded sandstone units within the Denver Formation are numbered NBW#1 and NBW#2 (ESE, 1988). Sandstones associated with sandstone unit NBW#2 are interbedded in the claystone in the central portion of the Section 13 but do not appear to subcrop at the bedrock surface (**Figure 8**). Unidentified Denver Formation sandstone units subcrop at well 37377 and at the interchannel high at the west end of the cross-section (well 37310). Sandstone units NBW#1 and NBW#2 have been projected to subcrop within the site boundaries (ESE, 1988).

The Geophysical Model

The initial model used for geophysical modeling is based on the central portion of the paleochannel near well 37377. This location represents target units in terms of the types of lithologies, hydrologic conditions encountered, and depths to interfaces in the Northern Paleochannel. A horizontally layered structure consisting of three layers was used for modeling seismic, DC resistivity, and EM results. The top layer of the model represents the dry, fine-grained eolian sediment and extends from the surface to a depth of 24 feet. The second layer represents a saturated, coarse-grained sediment, which extends from a depth of 24 feet to a depth of 40 feet. The top of the Denver Formation is

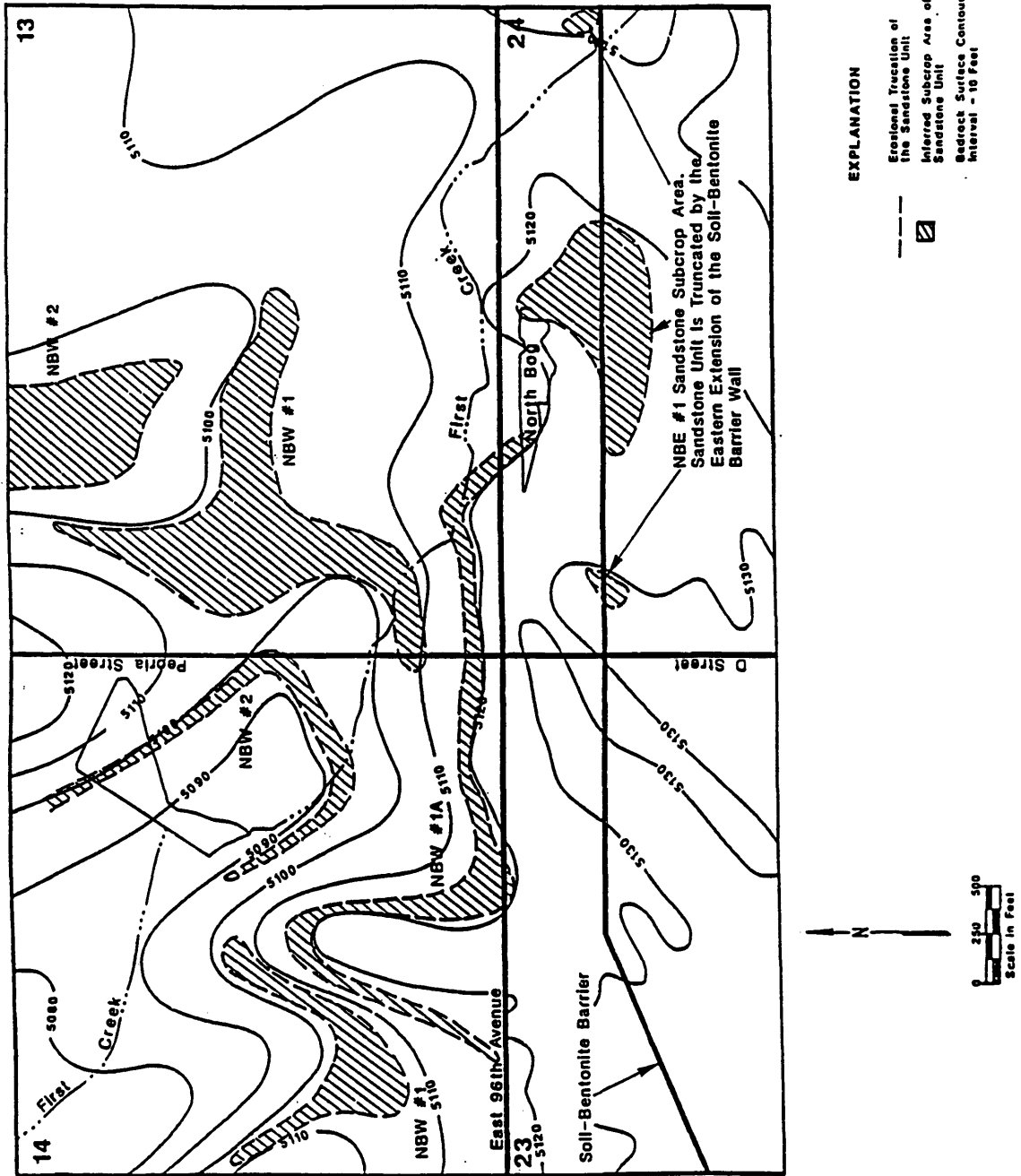


Figure 8. Denver Formation sandstone unit subcrop map (Source: ESE, 1988).

placed at 40 feet and is modeled as an infinite half-space. A two-layer model with topographic relief on the layer surfaces was used for gravity modeling. The upper layer of that model represents the unconsolidated sediments, and the lower layer represents the Denver Formation and includes the topography of the Denver Formation surface.

Physical Parameters

After the model geometry was defined, physical properties were estimated for each of the model units. The first estimates of geophysical properties were estimated from standard references (Clark, 1966) for each of the units in the geologic model. These estimates were necessary for method selection and survey parameter design, but were replaced with more accurate values as data became available. The magnitude of contrasts in the physical properties of targeted units ultimately determines the success of geophysical methods.

Seismic Velocity

A longitudinal wave (P-wave) seismic velocity was assigned to each of the three model layers. A velocity of 1,400 ft/s was assigned to the unsaturated, fine-grained unit; however, seismic velocities in unconsolidated, unsaturated sediments can vary widely (1,000 to 4,000 ft/s). A velocity of 5,000 ft/s was assigned to the saturated, coarse-grained alluvial unit. The velocity of the saturated zone in unconsolidated materials is determined primarily by percent saturation, and is less dependent on grain matrix properties (Burger, 1992). A velocity of 6,800 ft/s, representative of a shallow claystone (Clark, 1966), was assigned to the Denver Formation claystone.

S-wave seismic velocities assigned to the three layers were based on the P-wave velocities and the following general empirical relationship (Burger, 1992):

$$\frac{V_s}{V_p} = 0.4$$

where V_s is the S-wave velocity and V_p is the P-wave velocity. The above relationship corresponds to a Poisson's ratio of 0.4, which is typical for unconsolidated and near-surface sediments. The fine-grained, unsaturated unit and coarse-grained, saturated units were assigned an S-wave velocity of 600 ft/s. No significant S-wave velocity change was expected with the change in unconsolidated sediment lithology, and a change in water saturation has little effect on S-wave velocity (Domenico, 1976). Therefore, the two unconsolidated model units are considered to be one unit in terms of S-wave velocity. An S-wave velocity of 3,000 ft/s was assigned to the Denver Formation.

Electrical Resistivity and Conductivity

Electricity is conducted mainly through the fluid present within pore spaces (Zohdy, 1974). Therefore, the electrical resistivity is controlled by the amount of fluid saturation and by salinity. The presence of clay minerals and fine grained sediments tends to reduce resistivity because of the cation exchange capacity of these minerals (Burger, 1992).

A model resistivity of 70 $\Omega \cdot m$ was assigned to the fine-grained, unsaturated unit. The coarse-grained alluvial unit was assigned a lower resistivity of 30 $\Omega \cdot m$ due to the presence of water. A low resistivity of 5 $\Omega \cdot m$ was assumed for the Denver Formation

claystone based on several factors: complete water saturation, the presence of clay minerals, high porosity due to weathering, and resistivity logs of the Denver Formation at RMA (Colog, 1993).

Density

The densities of unconsolidated sediments vary widely, but are commonly in the range from 1.7 to 2.3 g/cm³ (Burger, 1992). A density of 1.7 g/cm³ was assigned to the unconsolidated sediments (Irons, 1989). Lithified rocks such as the Denver Formation are generally more dense than unconsolidated sediments due to decreased porosity. A density of 2.1 g/cm³ was assumed for the modeled bedrock based on neutron density logs of the water-saturated Denver Formation at RMA (Colog, 1993).

Magnetic Susceptibility

The magnetic susceptibility of rocks depends on the amount of ferrimagnetic minerals within the rock. The most common ferrimagnetic mineral is magnetite and thus the susceptibility of rocks and sediments depends mainly on the amount of magnetite present (Burger, 1992). Magnetic susceptibility in sedimentary rocks is commonly an order of magnitude smaller than metamorphic and igneous rocks. Both the alluvial units and Denver Formation are sedimentary in origin, therefore the magnitude of susceptibility contrast between these materials was estimated to range between 0 to 40 (10⁻⁶ c.g.s. units).

Geophysical Method Selection

Specific geophysical methods were selected for the modeling phase based on the magnitude of physical contrasts in the geologic model. P-wave seismic methods were

selected because of the velocity contrasts expected between unsaturated, saturated, and bedrock layers. S-wave seismic methods were selected in order to more clearly map the bedrock surface. Since little change in S-wave velocity was expected in the unconsolidated sediments, the primary contrast was expected to occur at the bedrock surface, thereby simplifying interpretation. Both reflection and refraction methods are capable of detecting velocity changes, but refraction methods can only be successful when layer velocities increase with depth. Seismic energy traveling from a high velocity material to a low velocity material is not critically refracted. As a result, the low velocity layer is not interpreted and all depth estimates to refractors deeper than the low velocity layer are in error; those depth estimates are deeper than the actual interface depth.

Direct current resistivity and frequency domain electromagnetic methods were chosen because of the expected resistivity contrasts between unsaturated, saturated, and bedrock units. The gravity method was chosen based on possible density contrasts between lithologic units. The magnetic method was ruled out because magnetic susceptibility contrasts between targeted lithologic units were not expected to be large enough to produce a measurable magnetic field anomaly. Also, the remains of an old wire fence, parallel to Line 1, would have interfered with a magnetic survey.

Geophysical Modeling and Field Testing

Synthetic data created during the forward modeling process was used to verify that the contrasts in physical properties of the geologic model would produce measurable effects. For example, it was useful to observe that a resistivity contrast of 25 $\Omega\cdot\text{m}$ at a boundary that is 40 feet below the surface will result in a detectable change in the measured apparent resistivity values. Acquisition parameters were then designed based

on synthetic data. For example, a simple seismic model of a P-wave refractor aids the determination of proper record length, source-receiver offset, and receiver spacing.

This section presents the forward modeling results and describes the acquisition parameters that were chosen with the aid of synthetic data and field tests. Some parameters, such as the best seismic source type, were best determined by performing field tests.

Seismic Models and Testing

A major goal of seismic modeling was to observe the temporal and spatial relationship between reflection and refraction events and to define an optimum time-offset window that would enable detection of the water table and targeted lithologic units. The program cshot (Docherty, 1991) was used to create synthetic shot records from the input velocity model. Cshot calculates true amplitude seismic records assuming two-and-a-half-dimensional layered acoustic media. Two-and-one-half-dimensional models are of finite dimension in two directions (in the plane of the model) and infinite dimension in the third direction (perpendicular to the plane of the model). Cshot is capable of modeling direct waves, reflected waves, refracted waves, and multiples. Horizontal, homogeneous, and isotropic layers were assumed in the modeling process. For display purposes and to insure that all events were visible at all offsets, the amplitudes of the traces in the synthetic shot records were balanced; relative amplitudes of events within each trace were still preserved.

P-wave Model

The resulting synthetic P-wave record (**Figure 9**) shows that reflections from the top of the saturated zone and the top of the Denver Formation occur near each other in

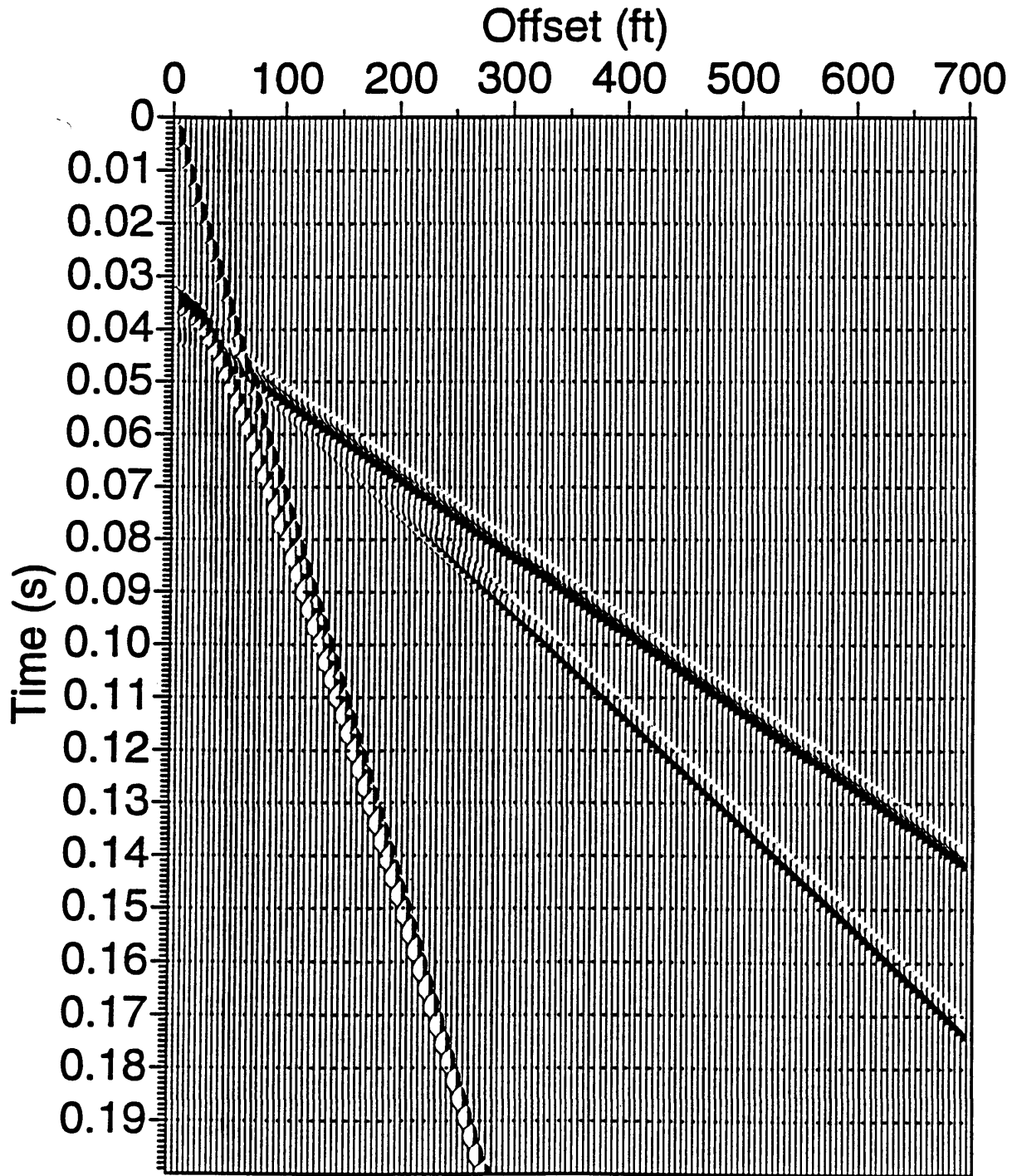


Figure 9. Modeled P-wave seismic record created with cshot.

time . The Denver Formation reflection amplitude is small relative to the amplitude of the water table reflection. Reflected events are best observed within a time window of 30 to 50 ms and within a source-receiver offset window of 0 to 50 ft. The direct wave is clearly defined, as is the refraction from bedrock; however, the refraction from the saturated zone is only observed beyond 200 ft of offset. A refracted event from a slightly thinner saturated zone would not appear as a first arrival in the modeled record; the thin zone would be a hidden layer.

S-wave Model

The resulting synthetic S-wave record reveals that a reflected event is observable from the surface of the Denver Formation (**Figure 10**). Direct arrivals from the unconsolidated layer and a refracted event from Denver Formation are observed. From this modeling result, it was clear that the use of S-waves is advantageous because the saturated zone is not a hidden layer; thus the model is simplified into a two-layer velocity model. It should be noted that mode conversions were not considered in the modeling process. It was assumed that horizontally polarized S-waves with particle displacement parallel to interfaces would be generated; therefore no mode conversions to P-waves would be possible (Aki and Richards, 1980).

Seismic Field Tests

Seismic field tests were conducted at two locations. Test Site 1 was located approximately 100 feet south of well 37377 (see **Figure 17**, Chapter 4, for a map showing well locations). Test Site 2 was located approximately 1500 feet south of well 37377. Testing at Site 2 was not useful for calibration with the initial geologic model

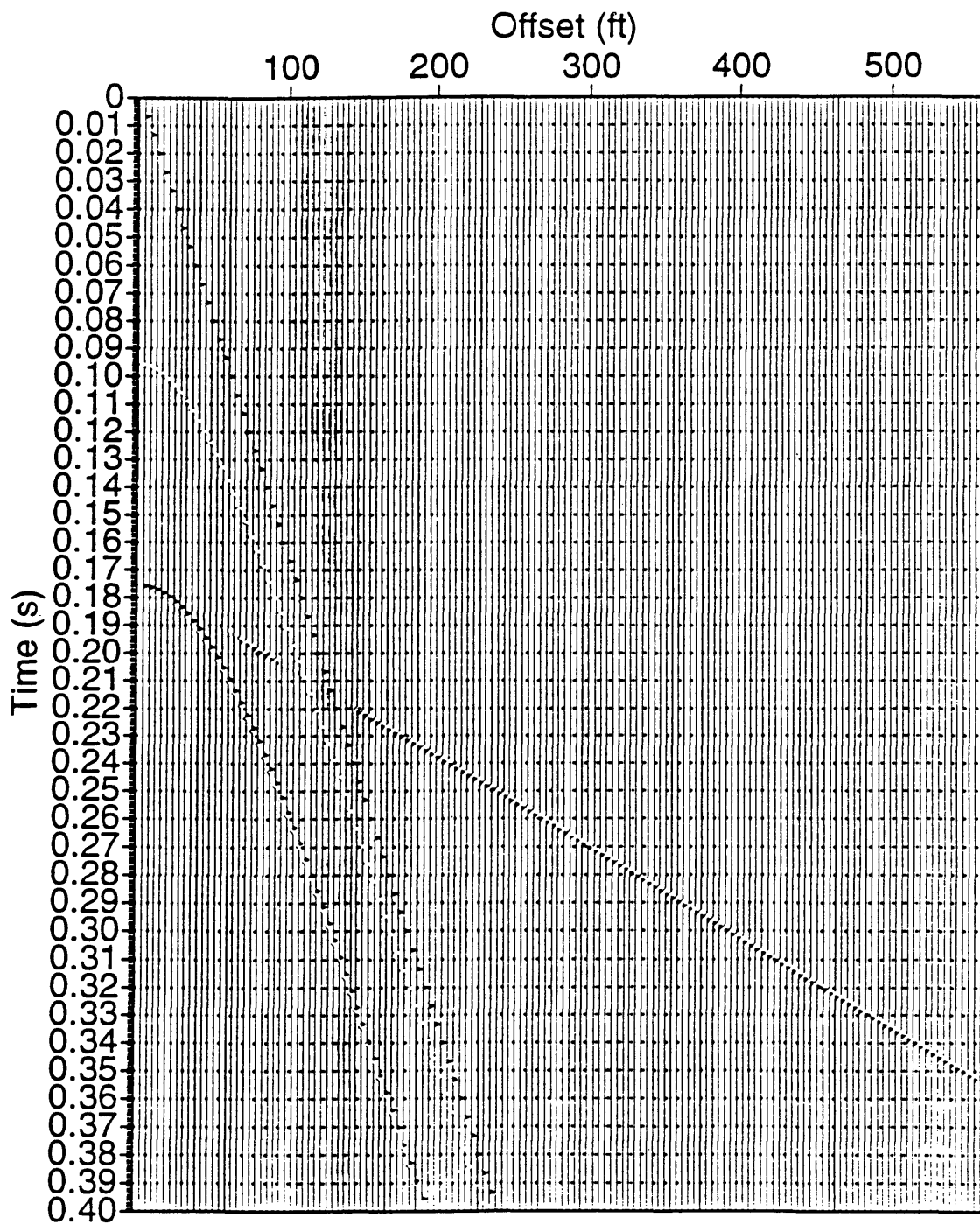


Figure 10. Modeled S-wave seismic record.

because it was located far from the modeled location; however, testing at Site 2 was useful for testing a variety of seismic sources.

The primary goal of seismic field tests was to determine if the modeled refractions were actually observed in the field. Also, it was necessary to experiment with different seismic sources (e.g., a sledgehammer, explosives, and a seismic shotgun) in order to evaluate which source was capable of delivering the highest frequencies and highest energy. Noise reduction techniques such as frequency filtering and geophone burial were tested. A total of 33 test records were acquired at the two testing sites. Besides source variations, these tests reflect changes in geophone interval, source-receiver offset, geophone coupling (surface vs. buried), and frequency filtering.

The Betsy Seisgun was chosen as the source for P-wave refraction and reflection surveys. The Seisgun consists of a vertically mounted 8-gauge shotgun. Commonly, either lead or iron slugs are fired from the gun. The most desirable features of the Seisgun were that it created relatively little airwave and it generated relatively high frequencies. The sledge hammer records appeared to have similar frequency content to the Seisgun records, but higher amplitude airwaves were generated by the sledge hammer. Explosive charges (1/3 lb of Kinepak) created very little airwave, but lacked the high frequency content of the other two sources.

The only available source for the S-wave survey was a sledge hammer. Explosives and the Seisgun are ideally P-wave sources and generate very little S-wave energy. In sharp contrast, the sledge hammer can be utilized to generate S-waves with the aid of a vertically mounted source plate.

The dominant noise sources on P-wave test records are attributed to airwaves, surface waves, and commercial airplane traffic. Several techniques were designed to minimize recorded noise. Geophones were placed in holes that were approximately 0.5 ft

deep in order to shield the geophones from direct contact with the airwave. Due to the proximity of Stapleton International Airport, airplanes were flying directly overhead every minute during peak traffic periods. The only solution to the airplane noise was to record when planes were not overhead. Airplane-generated noise is lower in amplitude on the S-wave test records.

Refracted events are observed on all P-wave test records (**Figure 11**). Interpretation of the refraction records for Site 1 yields an upper layer with a velocity of 1,200 ft/s, and a second layer with a velocity of 5,910 ft/s is interpreted at a depth of approximately 25 feet. The velocities of these two layers are consistent with the velocities of a dry, unconsolidated, fine-grained unit (1,200 ft/s) and a saturated, coarse-grained sand (5,910 ft/s). The apparent velocity of the second layer suggests that it corresponds to the top of the saturated zone.

A refraction from the Denver Formation is not observed in any of the P-wave seismic test records. It is interpreted that the top of the Denver Formation has a velocity that is near the velocity of the overlying saturated sand (5,910 ft/s) due to weathering or fracturing; therefore, there is no significant P-wave velocity contrast between the saturated zone and bedrock. No reflections were identified on the P-wave test records. The time-offset window in which a reflection from the water table would exist is obscured by surface waves and air waves.

A refracted event was observed on all S-wave test records. No reflected energy was observed on the S-wave records because of large-amplitude surface waves that obscure any possible reflections. In general, S-wave signal levels were lower; this phenomenon is attributed to higher attenuation of S-wave energy in the unconsolidated material. Also, at far offsets (approximately 200 ft and greater), the refracted arrivals became exceedingly emergent, which made it difficult to pick accurate first-break times.

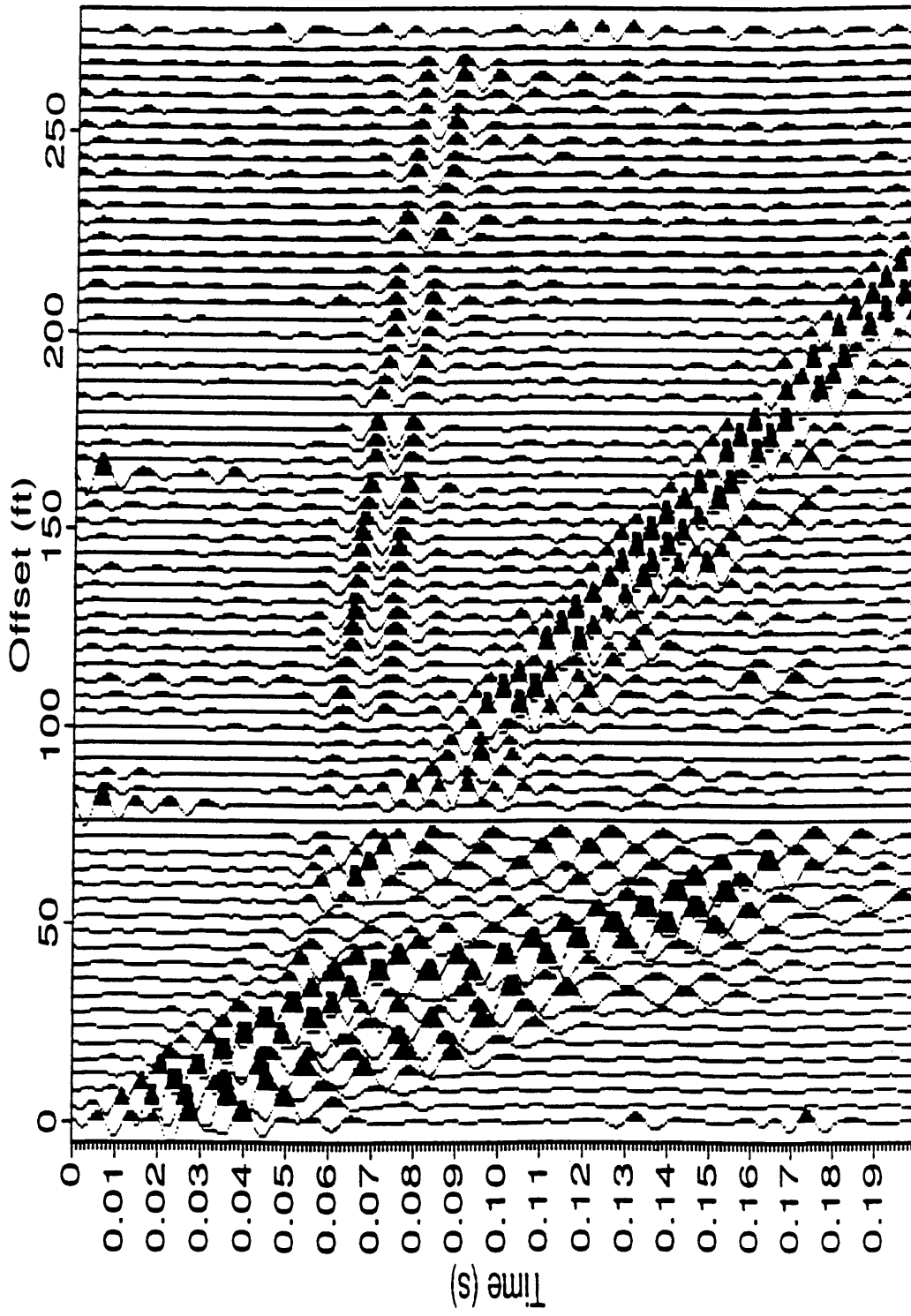


Figure 11. P-wave record obtained during field testing (sledge hammer source at Site 1).

A small amount of P-wave energy, which obscured some near-offset first breaks, was present on some of the S-wave records. Therefore, it was difficult to pick direct arrival energy on some of the near-offset (0 to 40 ft) traces.

Resistivity Model

The primary objective of resistivity modeling was to determine the optimum electrode configuration that would allow for adequate vertical resolution and appropriate depth of investigation. Dcresi[®], a one-dimensional resistivity modeling and interpretation program created by Interpex Ltd., was used to create apparent resistivity curves. Horizontal, isotropic, homogeneous layers and Schlumberger sounding geometry (**Figure 12**) were assumed in the resistivity models.

Synthetic apparent resistivity curves showed that a maximum current electrode half-spacing of 600 feet was large enough to adequately detect the low-resistivity Denver Formation (**Figure 13**). The vertical arrangement of model layers is such that $\rho_1 > \rho_2 > \rho_3$, and the apparent resistivity curve associated with this arrangement is called a Q-type curve. An initial concern with the Q-type curve was that the middle layer ($\rho_2 = 30 \Omega \cdot m$) was not being resolved. A sensitivity analysis revealed that the middle layer was creating a measurable effect on the apparent resistivity curve and that a change in thickness of ± 20 percent in the middle layer produced a ± 10 percent change in the apparent resistivity anomaly (**Figure 14**). Additionally, the sensitivity analysis showed that as many as six sample points were affected by the middle layer over a decade of current electrode half-spacing; therefore, six samples per decade of current electrode half-spacing was chosen as the horizontal electrode spacing interval.

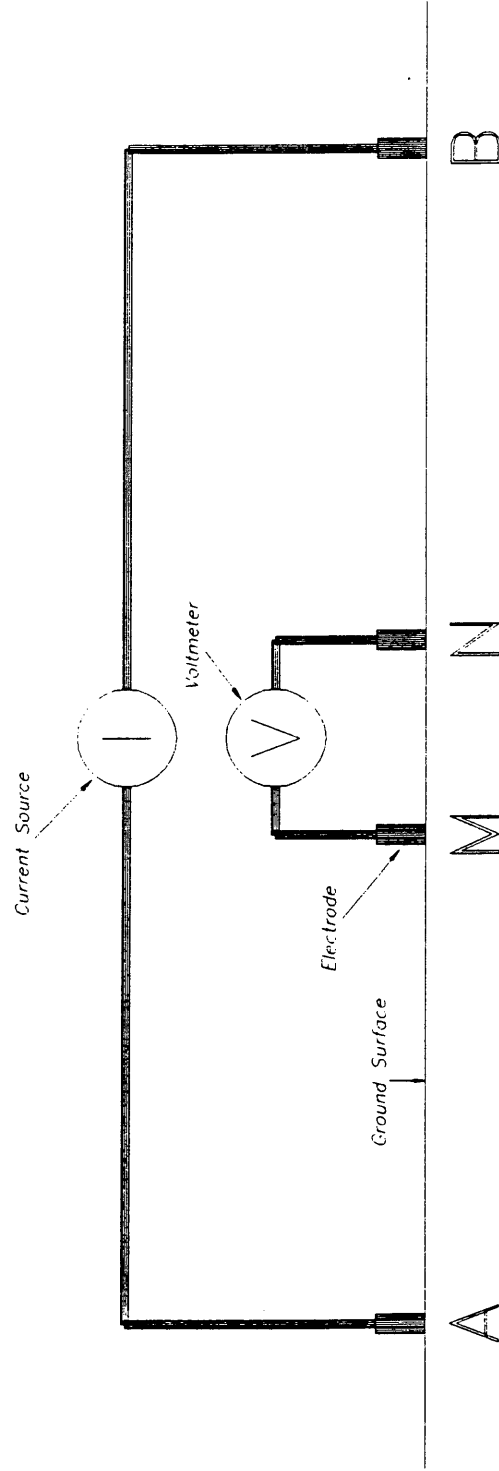


Figure 12. The Schlumberger electrode array was used to acquire DC resistivity data. The potential electrodes, M and N, are kept near the center of the array. The current electrodes, A and B, are placed much farther away from the center point.

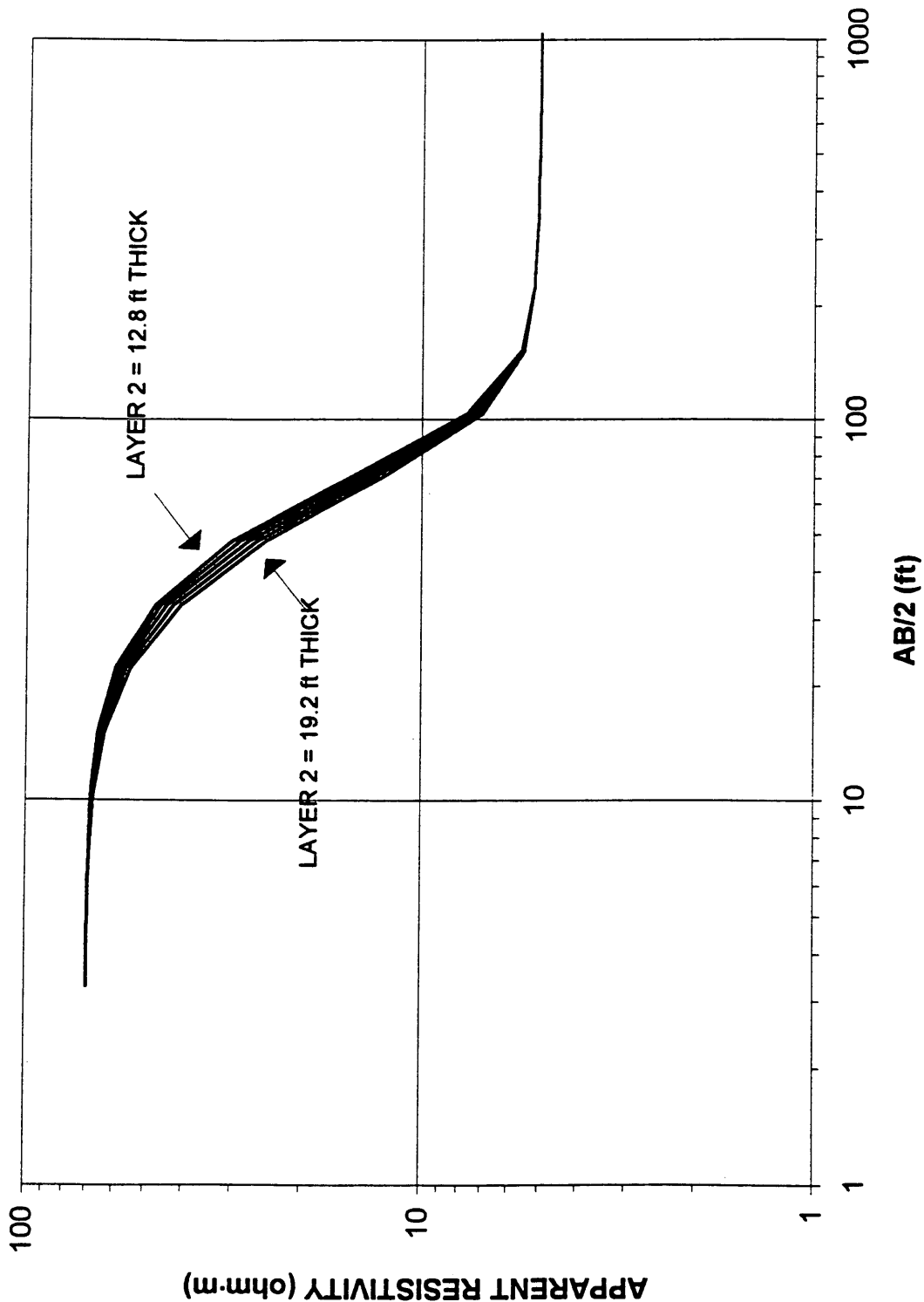


Figure 13. A family of modeled apparent resistivity curves. Each model is constructed such that $\rho_1 > \rho_2 > \rho_3$. Only the thickness of the middle layer is varied.

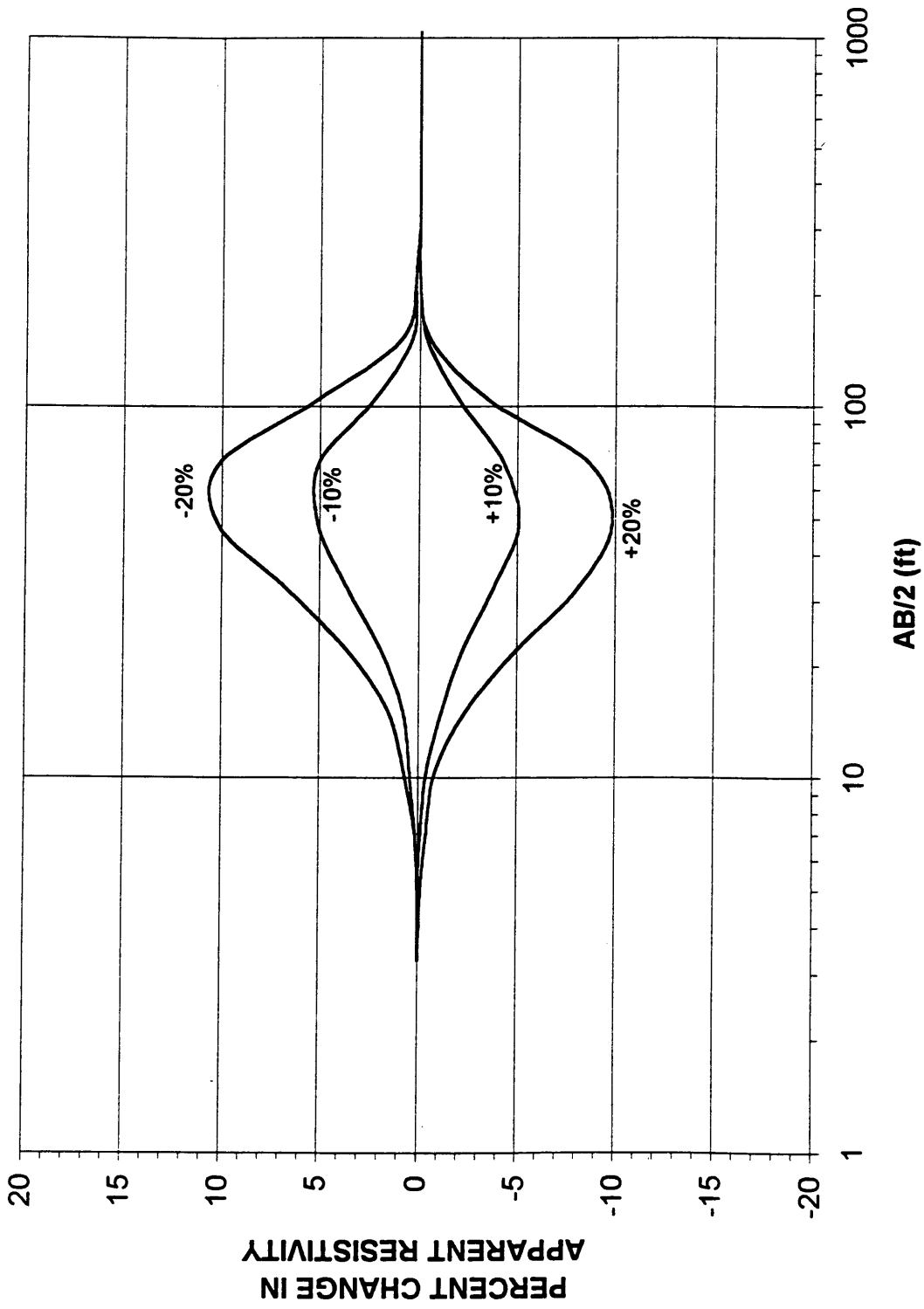


Figure 14. Chart of percent change in apparent resistivity versus AB/2 distance for varying thicknesses of the saturated zone (± 10 percent and ± 20 percent change in thickness of middle layer).

Gravity Model

The primary objective of gravity modeling was to determine the magnitude of the gravity anomaly that could be expected over the Northern Paleochannel. The density model was more complicated than the previous models because it included lateral changes in density; otherwise, no gravity anomaly would exist. A portion of the cross-section for the Northern Paleochannel was digitized and input as the forward gravity model (**Figure 15(a)**). The strike of the model bodies was assumed to be perpendicular to the profile direction.

The Interpex program Magixp[®] performs a forward calculation based on a generalized two-and-three-quarter dimensional Talwani model. A two-and-three-quarter dimensional model is similar to a two-dimensional model except that the strike dimension can be finite rather than infinite and the strike dimension may vary on either side of the profile. The generated profile data shows a maximum anomaly of nearly 100 μGal over the western boundary of the paleochannel (**Figure 15(b)**). A local bedrock high at well 37392 creates an anomaly of approximately 40 μGal . A conventional land gravity survey can realistically provide resolution to the nearest 100 μGal , while a high-resolution gravity survey with a microgravity meter could provide resolution of 5 μGal or less (EDCON, 1991); therefore, a microgravity survey is required. A survey accuracy of $\pm 10 \mu\text{Gal}$ would allow the modeled anomalies to be identified. The required survey accuracy is determined by requiring that the total error between two adjacent measurements must not cause an error in attraction which exceeds half of the targeted anomaly amplitude.

Density estimates were assumed to be accurate to $\pm 0.1 \text{ g/cm}^3$, and station elevations were assumed to be accurate to $\pm 0.02 \text{ ft}$. The combined error associated with

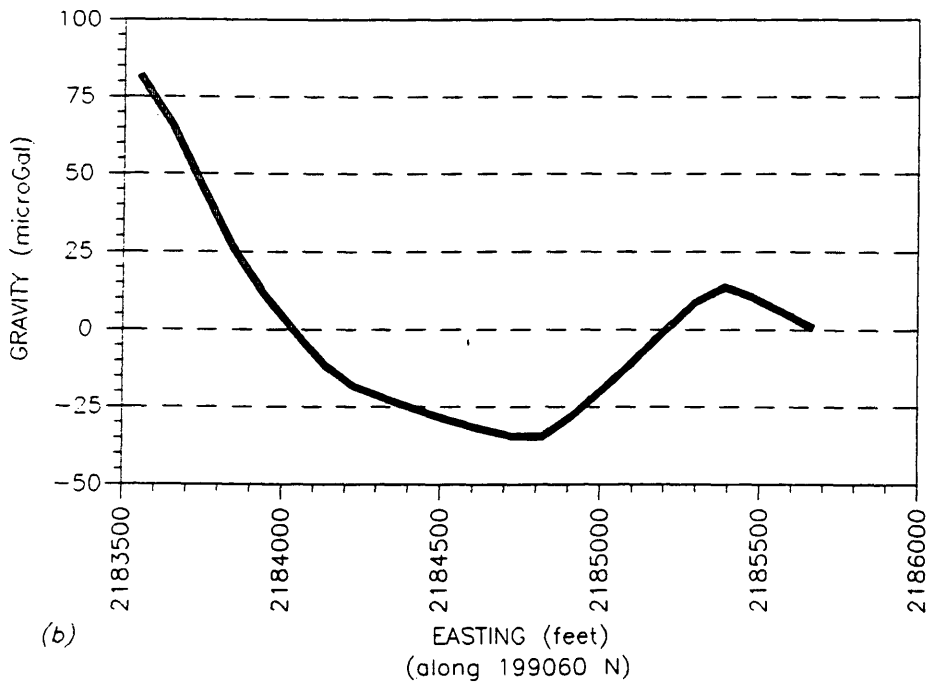
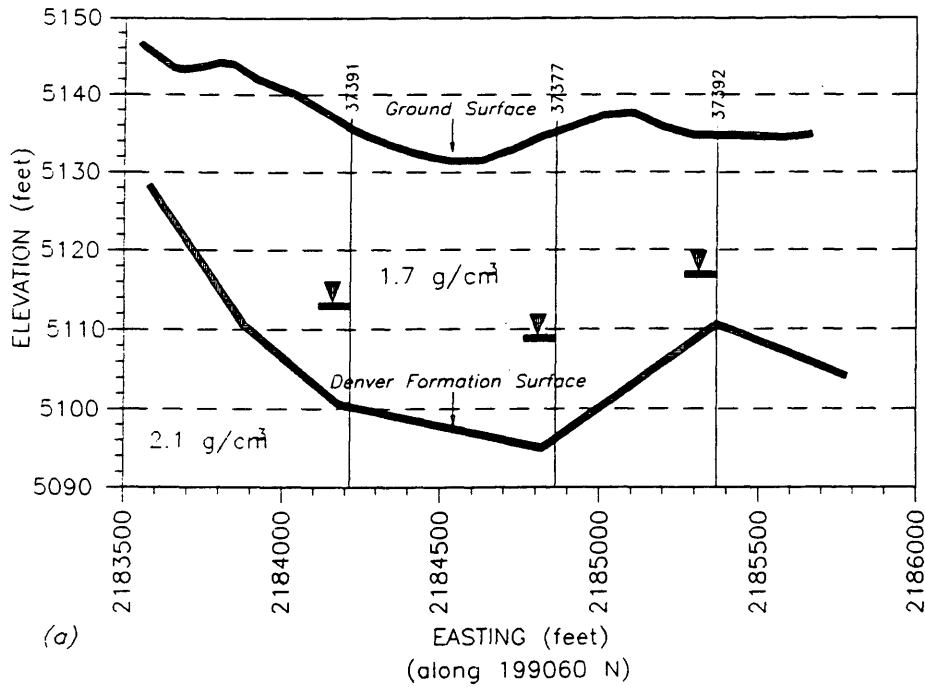


Figure 15. (a) Density model based on the depth to the Denver Formation as given in the five wells/borings along Line 1. (b) Modeled Bouguer gravity showing a large anomaly resulting from a high in the Denver Formation at the west end of the line.

Bouguer slab and free air corrections is $\pm 1.9 \mu\text{Gal}$ and was calculated using the following expression:

$$g_{\text{error}} = g_{\text{free air}} + g_{\text{Bouguer slab}}$$

where:

$$g_{\text{error}} = (0.9406 - 0.01277\rho)(\text{elevation error in feet})$$

A horizontal location accuracy of ± 5 ft introduces a latitude correction accuracy of $\pm 1.2 \mu\text{Gal}$. Meter reading accuracy of $\pm 5 \mu\text{Gal}$ results in an estimated survey accuracy of $\pm 8 \mu\text{Gal}$, which is within the required accuracy range of $\pm 10 \mu\text{Gal}$.

Electromagnetic Model

Choice of frequency-domain electromagnetic (EM) tools was restricted to the EM-31[®] and EM-34[®], which have predefined coil spacings and operation frequencies, so little parameter design was possible. The frequency-domain EM method is based on the induction of electrical currents in subsurface conductors by a time-varying magnetic field generated at the surface. The EM source is commonly a closed loop transmitter in which a controlled alternating current produces a varying magnetic field. The time-variant magnetic field induces alternating currents in subsurface conductors that produce a secondary time-variant magnetic field measured at the surface with another closed loop of wire (receiver).

The secondary magnetic field is not in phase with the primary (transmitted) field and may be divided into the portion of the field that is in phase and the portion that is ninety degrees (90°) out of phase with the primary field. These quantities may be referred to using a variety of names: inphase and quadrature components, or real and

imaginary components. The quadrature component is linearly related to terrain conductivity under normal subsurface conditions. The EM-31[®] instrument measures both inphase and quadrature components, while the EM-34[®] measures only the quadrature component. The output value from both instruments is terrain conductivity in milliSiemen/m (mS/m).

The EM-31[®] instrument has a 3.7 m separation between receiver and transmitter coils and an operating frequency of 39.2 kHz. The EM-34[®] can be used with three different coil separations: 10 m, 20 m, and 40 m. The respective operating frequencies are: 6,400 Hz, 1,600 Hz, and 400 Hz. The coils are kept coplanar and are oriented in the horizontal or vertical plane. Coil orientation is referred to by the axis of the generated magnetic dipole; coils in the horizontal plane generate vertical magnetic dipoles (VMD), and coils in the vertical plane generate horizontal magnetic dipoles (HMD). By combining the measurements from the two instruments at both coil orientations and a total of four coil separations, eight independent measurements are acquired at each station. The larger the coil separation is, the deeper the depth of investigation is. Also, maximum depth of investigation is achieved with VMD coil orientation.

A simple EM forward model calculation was used to calculate the change in measured response with a change in model layer thickness. The function $R(z)$ is defined as the relative contribution to the apparent conductivity from all material below a depth z_d (McNeill, 1980). The expression for the cumulative response function, $R(z)$, is given by

$$R(z) = \int_{z_d}^{\infty} \phi(z) dz$$

where $\phi(z)$ is a function that describes the relative contribution to the secondary magnetic field arising from a thin layer at any depth z , (**Figure 16**). The function $\phi(z)$ is discussed further in Chapter 5.

The apparent conductivity, σ_a , for a three-layered model is calculated from the following expression:

$$\sigma_a = \sigma_1[1 - R(z_1)] + \sigma_2[R(z_1) - R(z_2)] + \sigma_3R(z_2)$$

where z is the layer depth divided by the coil spacing. Apparent conductivities were calculated for the initial geologic model and then again for a model that simulates a bedrock high. Apparent conductivities rose an average of 26 percent in the second model; this result is within the resolving limits of the EM-31[®] and EM-34[®] systems (**Table 1**). Because the existing geologic cross-section shows lateral topographic and lithologic features changing at a spatial wave length of hundreds of feet, an EM station spacing of 30 feet was deemed adequate to sample the targeted lateral lithologic and structural changes estimated to exist within the Northern Paleochannel.

Coil Spacing (m)	Coil Orientation	Model 1 Conductivity (mS/m)	Model 2 Conductivity (mS/m)	Percent Change
3.7	VMD	44	59	34%
10.0	VMD	88	118	34%
20.0	VMD	135	164	22%
40.0	VMD	174	188	8%
3.7	HMD	29	37	28%
10.0	HMD	53	71	34%
20.0	HMD	84	108	29%
40.0	HMD	121	144	19%

Table 1. Comparison of calculated apparent conductivity values.

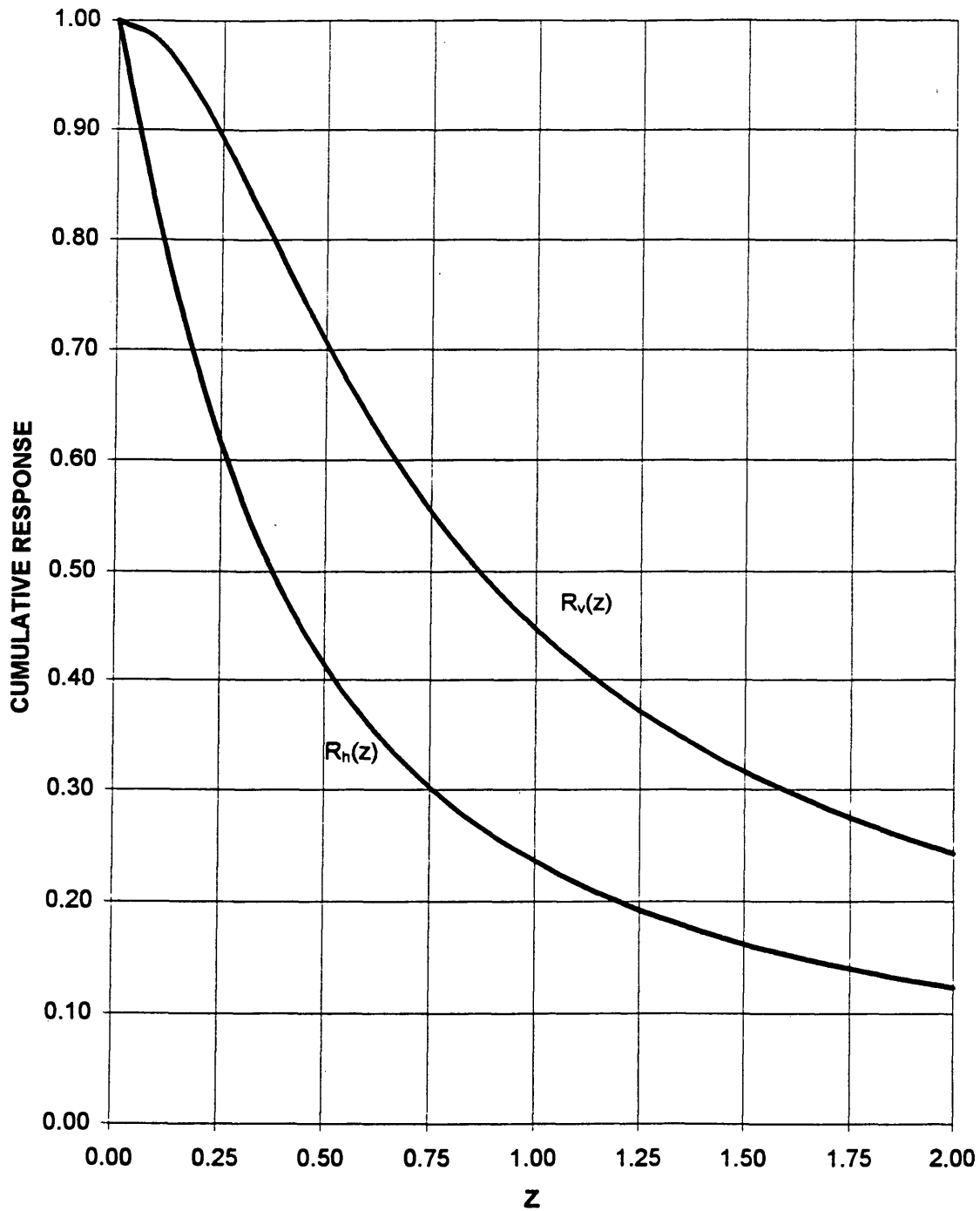


Figure 16. Cumulative response curves showing the relative contribution to measured apparent conductivity of all material below a given depth. The horizontal axis (z) is depth divided by coil spacing. $R_v(z)$ is the cumulative response function for VMD orientation and $R_H(z)$ is the cumulative response function for HMD orientation.

Chapter 4

DATA ACQUISITION AND PROCESSING

Introduction

This chapter begins with a brief discussion of positional surveying techniques, followed by a detailed discussion of data acquisition and data processing. The discussion of data acquisition and processing is organized by the five geophysical methods that were used: longitudinal (P-wave) seismic reflection and refraction, horizontally polarized transverse wave (SH-wave) seismic reflection and refraction, direct current (DC) electrical soundings, microgravity, and electromagnetic (EM) profiling.

The Positional Survey

The site is located in the northern half of the southwest quarter of Section 13, Township 2 South, Range 67 West (N $\frac{1}{2}$ SW $\frac{1}{4}$ S13 T2S R67W). Three survey lines were established for the geophysical measurements. Two parallel lines (Lines 1 and 2), trending from east to west and spaced approximately one-quarter mile apart, are intersected by one line (Line 3) trending from north to south (**Figure 17**). The general trend of the northern paleochannel is from south to north; therefore, Lines 1 and 2 are approximately perpendicular to the paleochannel trend. Line 3 is approximately parallel to the primary axis of the paleochannel.

With the exception of the gravity station location survey, the positional surveying was performed with the aid of an EG&G Electronic Distance Meter (EDM) and nylon measuring tape. The three lines were initially laid out with the measuring tape. The

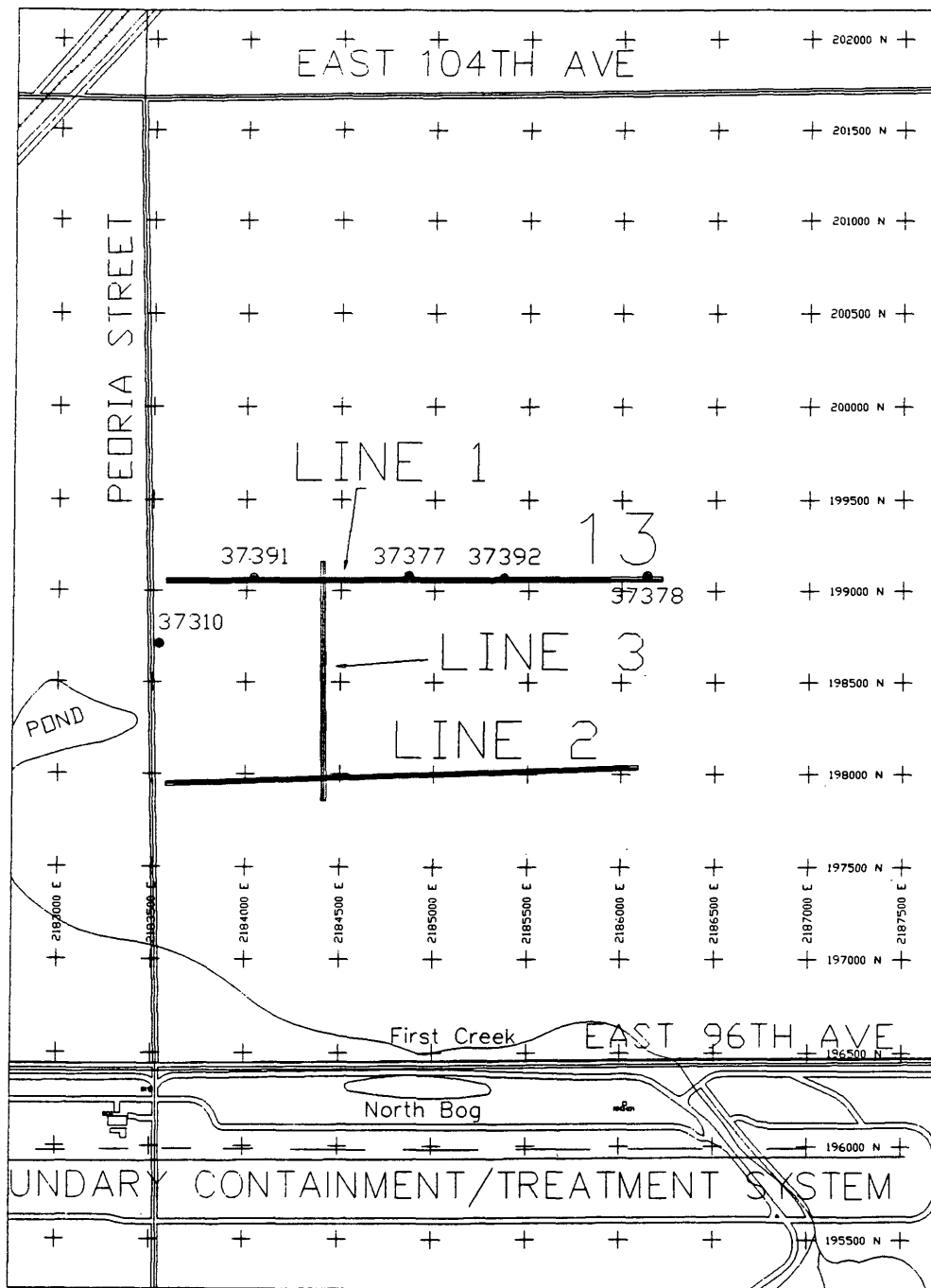


Figure 17. Location of survey lines with state plane coordinates.

EDM was then used to measure station positions at intervals of 120 feet along each line (each seismic spread was 120 feet long) and to measure the angles between the lines. Following the gravity survey, a Nikon Total Station was used to measure the coordinates of the gravity stations and to tie all relative station coordinates (including elevation) to the local state plane coordinate system.

P-wave Data Acquisition and Processing

P-wave seismic data were collected in an effort to map the P-wave velocity structure of the Northern Paleochannel at the study site. It was anticipated that the P-wave velocity structure would aid in the characterization of three subsurface units: unsaturated fine-grained eolian sediments, the saturated coarse-grained Slokum alluvium, and the top of the Denver Formation claystone.

P-wave seismic data were collected on portions of Lines 1, 2, and 3. A total of 343 shot records were acquired on Line 1 for a total coverage of 1,830 ft. A total of 405 shots were recorded on Line 2 for a total coverage of 2,140 ft. Finally, a total of 241 shots were recorded along Line 3 for a total coverage of 1,320 ft.

P-wave Acquisition Equipment

An EG&G 2420, 24-channel, instantaneous floating-point seismograph was used for recording. The data storage device was a reel-to-reel tape recorder. Forty-eight 100-Hz, 0.6 critically damped, vertical-component geophones were used in the P-wave survey. Geophones were spaced at an interval of 5 ft and placed in holes that were ideally 0.5 ft deep. In some areas the soil was very sandy, compact, and dry, which limited the depths of the holes. Cables connected geophones through a switch to the

recording instrument. The switch allowed for the recording of signals from any selected set of 24 contiguous geophones.

The Besty Seisgun source is an 8-gauge shotgun that fires 2-ounce steel slugs into the ground. Although lead slugs provide better impulsive source characteristics because they deform and flatten when they hit the ground, steel slugs were used in an effort to avoid lead contamination of the soil. A geophone was placed next to the base of the Seisgun to serve as a time trigger for the recording unit. An average of two shot records were stacked (summed) at each shotpoint.

P-wave Acquisition Geometry

Both reflection and refraction surveys were desired for this investigation, but time constraints and budgetary limits suggested that performing both surveys would have been impractical. Therefore, an ideal survey configuration was one that would allow for the collection of a reflection data set at the same time as the refraction data set acquisition. Continuous Refraction Profiling (CRP) (Bowers, 1985) geometry was found to meet these criteria.

Continuous Refraction Profiling

CRP acquisition geometry, as used in this application, is identical to an "end-on" reflection survey. The shot is located at one end of a spread of geophones, and the entire setup is moved forward one station location for each subsequent shot. A major advantage of the CRP acquisition method lies in the fact that many different delay times and velocity estimates are found for each station location. Therefore, depth and velocity estimates benefit from the increased redundancy. The fact that the CRP geometry is

identical to an "end-on" reflection survey is a second advantage, because the same data set can be processed as a reflection survey.

In order to use the same data set for both reflection and refraction, the acquisition parameters, such as geophone interval and total offset, must meet the needs of both surveys. For example, if a deep refractor is targeted, a large total offset will be required, and will effectively increase the geophone interval (assuming a fixed number of recording channels). Increasing the geophone interval will increase the spatial sampling, which may inadequately sample a shallow reflection event. Modeling results suggested that identical geometries could be used for reflection and refraction data acquisition; however, the modeling process did not include airwave or ground roll energy, which would have required an excessively small geophone spacing.

P-wave Data Processing

Seismic data were input into ProMAX[®], a commercial seismic processing system from Advance Geophysical. Geometry information was stored in the trace headers, and an initial sort removed bad shot records and bad traces from the data set.

P-wave Refraction Processing

First arrivals were picked for every trace in the data set with the aid of the graphical interface provided with ProMAX[®]. Traces were displayed on the screen, and first arrival times were picked by "pointing and clicking" with the aid of a mouse. Arrival times for the refracted events were then input into an algorithm that solved for a depth model. The algorithm uses the concept of Diminishing Residual Matrices (DRM) to decompose calculated delay times into their shot and receiver components (Gulunay, 1985). The delay time is the additional time required for a wave to travel from the source

along the refractor and to the receiver over the time to travel along the same refractor hypothetically assumed to be at the surface (Sheriff, 1973). The delay time can be divided into a source delay time and a receiver delay time, which when summed are equivalent to the intercept time. After delay times are calculated for each station location, the depth(s) to the refractor(s) can be calculated. Delay time inversion results are presented in Chapter 5.

P-wave Reflection Processing

The key to a successful shallow reflection survey is to minimize the amount of Rayleigh wave and airwave energy. Unfortunately, in this survey, high-amplitude Rayleigh wave and airwave energy appeared in the same time-offset window as the desired reflected energy (**Figure 18**). Some shot records do appear to show strong reflected energy, and attempts were made to enhance the records that do not. A panel of narrow band-pass filtered records revealed that the frequency content of the reflected energy was lower than expected; therefore, attempts to filter out surface wave energy using a high-pass filter resulted in eliminating reflected energy as well. Filtering in the frequency-wavenumber (F-K) domain emphasized apparent reflected energy in some good records, but failed to enhance others. In general, the frequency of any reflected energy and the position of that energy on the shot records overlaps such that the reflection events are unseparable from the surface waves.

S-wave Data Acquisition and Processing

S-wave seismic data were collected in an effort to map the S-wave velocity structure of the Northern Paleochannel at the study site. It was anticipated that the S-

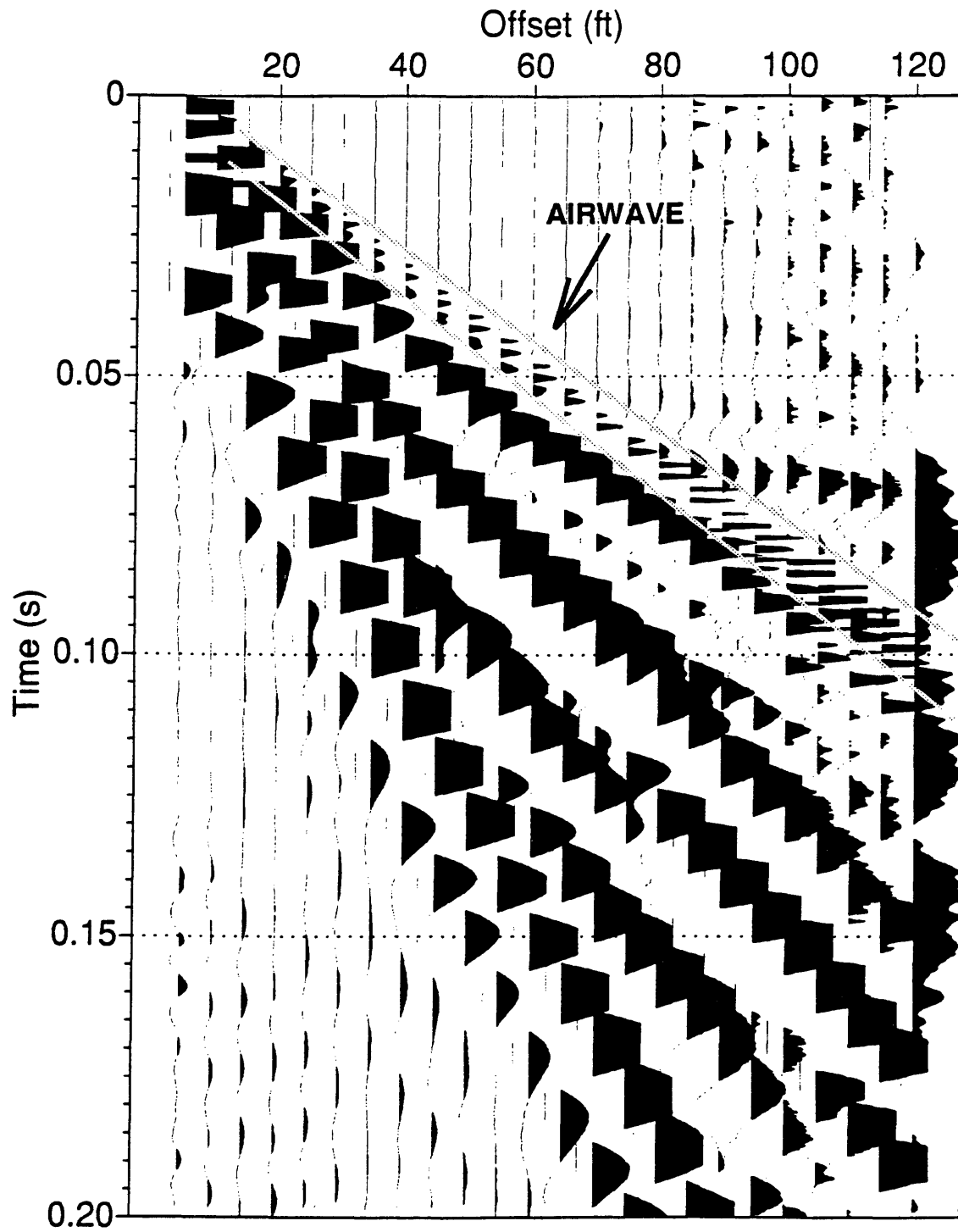


Figure 18. Typical P-wave record from Line 1 showing noise levels.

wave velocity structure would aid in the characterization of unconsolidated alluvial and eolian sediments and the top of the Denver claystone.

S-wave Acquisition Equipment

For the S-wave survey, forty-eight (48) 40-Hz, 0.6 critically damped, horizontal component geophones were used. The same cables and recording equipment that were used in the P-wave survey were used in the S-wave survey. Geophones were buried at a depth of 0.5 ft where soil conditions allowed.

By using transverse receivers with a transverse source, primarily SH-waves were produced and recorded. SH-waves are S-waves with particle motion polarized in the horizontal plane. SV-waves are S-waves with particle motion polarized in the vertical plane. The source consisted of a 12-pound sledge hammer swung against a vertical iron plate that was coupled to the ground with 2-inch-long spikes. SH-waves were used in this study because they do not convert into other waves (i.e., P-waves or SV-waves) when reflected or refracted from a horizontal interface (Aki and Richards, 1980). Ideally, no converted wave energy would have been recorded, which would have simplified the interpretation of the SH-wave data. Practically, some P-wave or SV-wave energy was recorded because no source is a perfect SH-wave source and no geologic boundary is a plane. Reversed shot polarities, discussed below, were used to remedy the mode conversion problem.

S-wave Acquisition Geometry

S-wave data acquisition began on Line 2. CRP geometry was utilized for Line 2, but, because of time constraints near the end of the summer, it was necessary to switch to

the conventional refraction method for Line 1 so that data could be collected over a larger portion of that line.

Two shots were recorded for each station location. The first shot was polarized to the north (transverse to the line direction) and the second shot was polarized to the south. Shot polarity was achieved by striking the source plate from south-toward-north for north polarity and north-toward-south for south polarity. The reason for reversing the shot polarity lies in the fact that the SH-waves produced by the source will have different polarities for different shot polarities (**Figure 19**). Therefore, by looking at two shot records recorded at the same surface location but with different polarities, the true SH-wave events can be identified by their polarity reversals; any P-wave energy on the records will not change polarity with changing shot polarity.

S-wave Data Processing

Airwave contamination was noticeably diminished in the S-wave records. However, surface energy in the form of Love waves dominated and obscured any reflected energy. Refracted arrivals from at least one refractor were evident on all of the records. A P-wave event obscured the S-wave direct arrivals in many instances, so it was necessary to attenuate P-wave energy before picking first arrivals.

P-wave attenuation was achieved by subtracting the south polarity shot record from its north polarity counterpart. Before performing the subtraction, the trace amplitudes were equalized using an root mean square (RMS) trace balance. The RMS value of each trace was calculated (square root of the mean of the sum of all squared sample values for a particular trace) and the traces are normalized so that the RMS value was the same for all traces in the record. After the subtraction of opposite-polarity

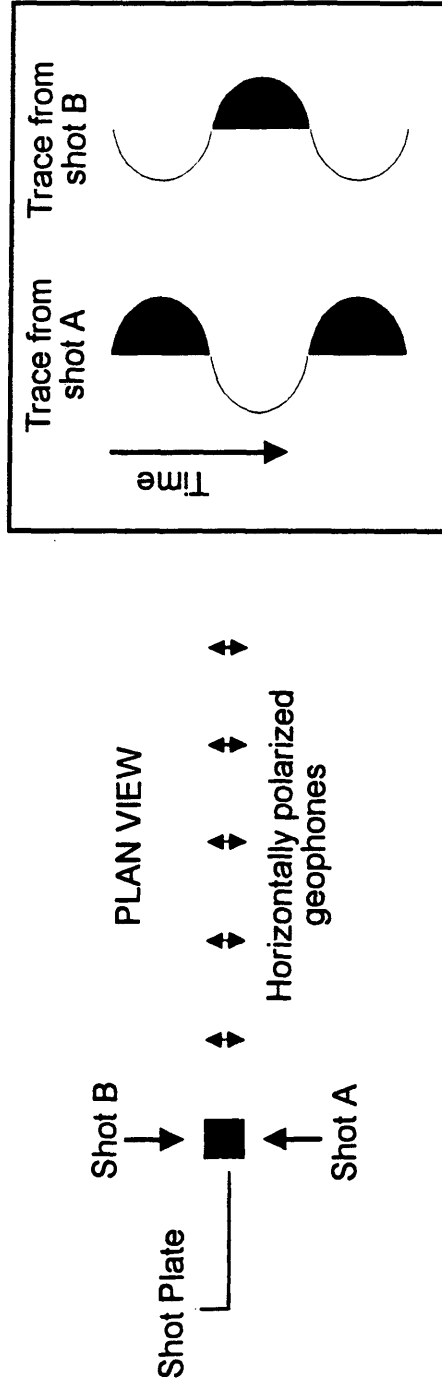


Figure 19. Reversing the direction of the sledge hammer impact reverses the polarity of the recorded SH-waves.

records, first arrivals were picked and input into the DRM refraction program, as described in the P-wave data processing section.

DC Sounding Acquisition

Sixteen Schlumberger soundings were acquired at the study site. Six soundings were acquired on each of Lines 1 and 2, and four soundings were acquired on Line 3. The two primary components of a resistivity system are a current source and a voltmeter. Soundings along Line 1 were initially completed using a current source and a digital averaging voltmeter manufactured by Bison Instruments. The source was capable of output currents as high as 100 milliAmperes (mA). Unfortunately, this amount of current is not large enough for the conductive units present at the site. As resistivity of earth materials decreases, the measured potential difference for any fixed amount of current between fixed electrode positions decreases. Potential differences over very conductive earth materials can be too small to measure because of ambient noise levels. Therefore, when performing resistivity soundings in very conductive material, larger currents are needed to measure accurate apparent voltages at large current electrode offsets. A current source developed by the U.S. Geologic Survey (USGS) is capable of producing current in excess of 400 mA, which is adequate for current electrode spacings up to 600 feet at the site. Soundings along Line 1 were repeated using the USGS source, and the results were significantly improved. The voltmeter with the USGS system was a Hewlett-Packard analog voltmeter with chart recorder output. The digital voltmeter from Bison averaged potential readings over time, so any self potential (SP) effects were averaged into the reading and caused inaccurate measurements. The Hewlett-Packard chart recorder output was useful because SP effects are visually observed as drift, with time, of the voltage reading as shown on the chart voltage record.

The Schlumberger electrode array was used for the DC soundings. This array consists of four electrodes: two current electrodes (**A** and **B**) and two potential electrodes (**M** and **N**) (see **Figure 12**, Chapter 3). The potential electrodes are placed near the center of the array, while the current electrodes are placed on either side of the pair of potential electrodes. Each data point is acquired by introducing a current into the ground at the current electrodes, and then measuring the potential difference between the potential electrodes. As the spacing between the current electrodes increases, the volume of earth sampled and depth of investigation increases. An apparent resistivity value is calculated from the input current, measured potential, and electrode spacing. The maximum separation of the current electrodes was 1200 feet (half spacing ($AB/2$)= 600 feet). Sounding centers were spaced approximately 360 feet apart along the three survey lines.

The only processing required for resistivity data was the calculation of apparent resistivity. The equation for apparent resistivity at the center of a Schlumberger electrode array is

$$\rho_{app} = \frac{\pi (s^2 - \frac{a^2}{4}) \Delta V}{a I}$$

where s is half of the current electrode separation, V is electrical potential, I is electrical current, and a is the separation of the potential electrodes. Apparent resistivity curves were created by plotting apparent resistivity versus current electrode separation.

Gravity Data Acquisition

Gravity measurements were made at 21 locations along Line 1. Gravity stations

were separated by approximately 100 feet. Where gravity measurements revealed possible anomalies, additional measurements were taken at smaller station intervals.

A modified LaCoste and Romberg Model G gravimeter, the Super-G® (EDCON, Inc.), was used for the gravity measurements. The Super G is nulled electronically and continuously monitors and corrects for level errors. A computer interface allows the meter readings to be recorded directly into a portable computer. Tidal corrections are applied to meter readings by the data acquisition software. The data acquisition software monitors the voltage required to null the beam of the gravimeter over a 1-second interval. These readings are averaged over a 15-second interval, and the value is recorded in a data file and then plotted on the computer screen. During any particular station occupation, a number of readings are recorded over a period of one to two minutes. The average of these readings is then taken as the meter reading for that particular occupation.

One station along the line was designated as a base station. The base station was occupied every 30 minutes throughout the survey so that meter drift could be observed through time. The meter drift was removed from the observed gravity readings. A free air correction of +94.06 $\mu\text{Gal}/\text{ft}$ and a Bouguer slab correction of $-12.77 \cdot (\text{density in } \text{g}/\text{cm}^3) \mu\text{Gal}/\text{ft}$ were applied to each drift-corrected gravity reading. Elevation was established relative to mean sea level. The density used for the Bouguer slab correction, $2.0 \text{ g}/\text{cm}^3$, was determined by Nettleton's method (Nettleton, 1983). A latitude correction was not necessary because the stations were located along an east-west profile. Local terrain corrections were not applied because the contribution of these corrections would be less than 10 percent of the targeted $50 \mu\text{Gal}$ anomaly. Terrain effects from large, distant terrain features such as the Front Range are assumed to be constant across the site.

Electromagnetic Data Acquisition

Geonics' EM-31 and EM-34 instruments were used to acquire terrain conductivity measurements at the site. Electromagnetic (EM) measurements were acquired at 89 locations along Line 1; stations were spaced at intervals of 30 ft along the line. The receiver coil was located directly over the station location, and the transmitter coil was located east of the receiver coil and along the survey line. No EM data were acquired on Lines 2 or 3 because after evaluating Line 1 data it was decided that the EM method (as implemented in this study) was not meeting the project objectives. EM measurements from different coil spacings and orientations were combined at each surface measurement point to form a sounding. The vertical resolution of the EM soundings (not to be confused with Time-Domain EM soundings) was not sufficient to accurately map the targeted units. The shortcomings of the EM survey are discussed in more detail in Chapter 5.

The only processing step prior to the interpretation of EM data was the removal of data values that were deemed to be corrupted either by cultural features, such as nearby fences or power lines, or by poor signal quality. In particular, the VMD (coils oriented in horizontal plane) data set for the 40-m coil spacing was very noisy, so those values were not used in the interpretation process.

Chapter 5

RESULTS AND INTERPRETATION

Introduction

In this chapter, the results of the geophysical surveys are presented and interpreted. Initially, each geophysical method is discussed with minimal reference to the results obtained from the other methods. The integrated interpretation is discussed in the final sections of this chapter. It should be noted that the order of the discussion in this chapter does not reflect the order of the interpretation process. The actual interpretation process was iterative and required an integrated approach from beginning to end.

Interpretation of P-wave Refraction Data

A visual inspection of each travel-time curve was required to define offset windows corresponding to the refracted wave arrival times. The offset window parameters were then input to the software along with the first break times. The offset window was needed because the algorithm did not automatically pick the number of layers to model, nor did it determine which arrival times corresponded to which layers. In other words, the algorithm did not know whether a particular arrival time corresponded to a direct arrival or a refraction until that information was specified by the interpreter.

As discussed previously, one refracted event is observed on all of the shot records in the P-wave data set. Therefore, the P-wave derived interpretation for the paleochannel

structure consists of two layers. Lateral variations in surface and refractor velocity are observed (**Figure 20**).

The interpreted P-wave refractor is shown in (**Figure 21**). The uppermost unit is interpreted to be unsaturated and unconsolidated. This dry surface layer is present on all of the survey lines. Velocities within this interval, as calculated from the direct arrivals, vary between 1,000 ft/s and 2,000 ft/s; 1,200 ft/s was used for the interpretation. This velocity is lower than the velocity of water (5,000 ft/s), which indicates that this unit is unsaturated. Source-generated airwave interference with the direct arrival occurs on many of the shot records. Unsuccessful attempts to minimize the recorded airwave included burying geophones and placing a rigid foam baffle-wall between the source gun and the geophones. Arrival times for energy traveling directly through the surface layer (direct wave) were difficult to pick where airwave energy interfered.

The refractor has an average velocity between 5,000 ft/s and 6,000 ft/s. Contrary to preliminary modeling results that suggested that this event would correspond to the surface of the Denver Formation, this refractor is interpreted to be the top of the saturated zone, primarily because the depth to the top of this refractor correlates with water table depths taken from well information along Line 1. Additionally, a sonic velocity log of the Denver Formation (Colog, 1991) shows that its velocity is in the range of 6,000 ft/s or even lower. Therefore, it is unlikely that the observed head wave is associated with the saturated alluvium/Denver interface because the velocity contrast between these two layers is small. The strong head wave observed on all records is interpreted to be due to the large velocity contrast between unsaturated alluvium and underlying saturated alluvium.

A subcrop of the Denver Formation above the level of the water table is interpreted in the western portion of Line 1. In this portion of the line, the refractor is

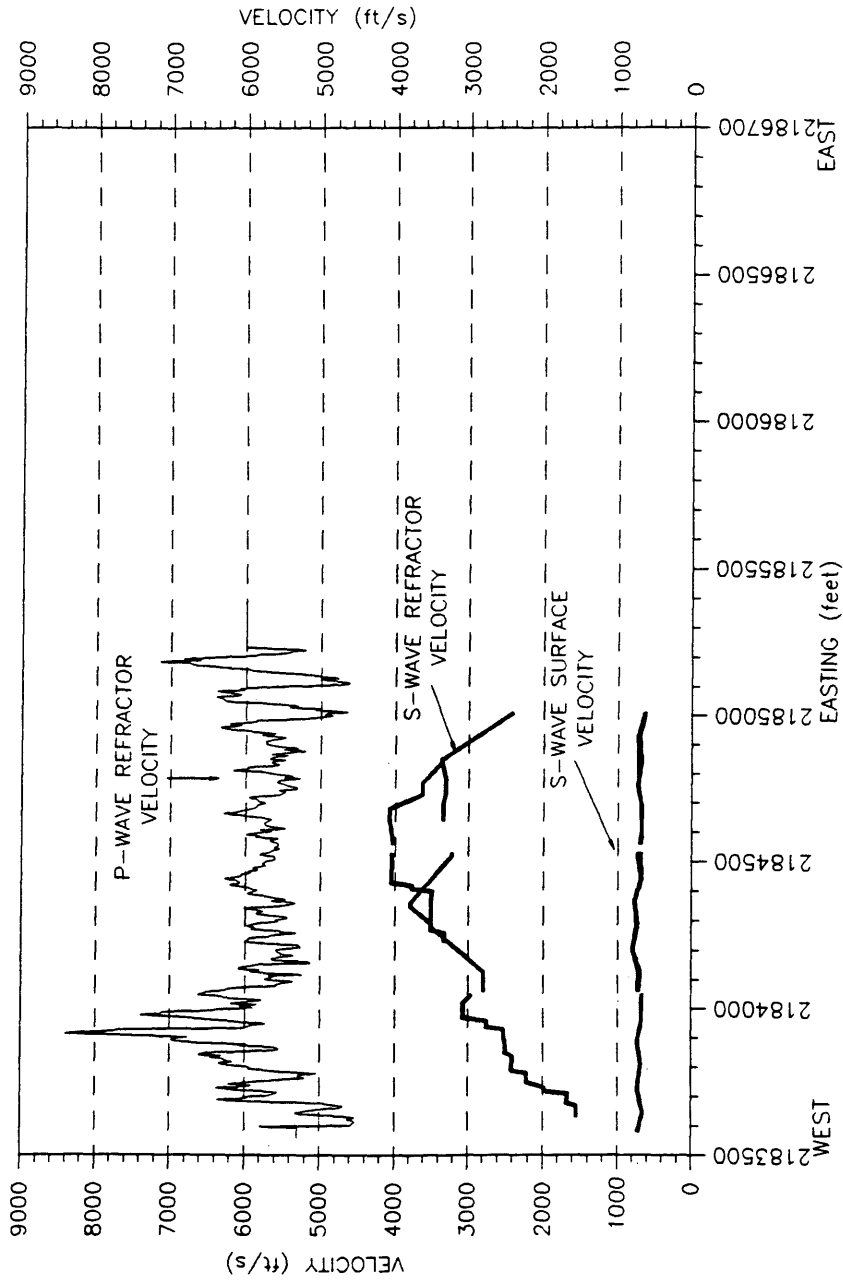


Figure 20. P-wave (refractor) and S-wave velocities for Line 1. P-wave velocity of surface layer was hand calculated and averaged 1,200 ft/s.

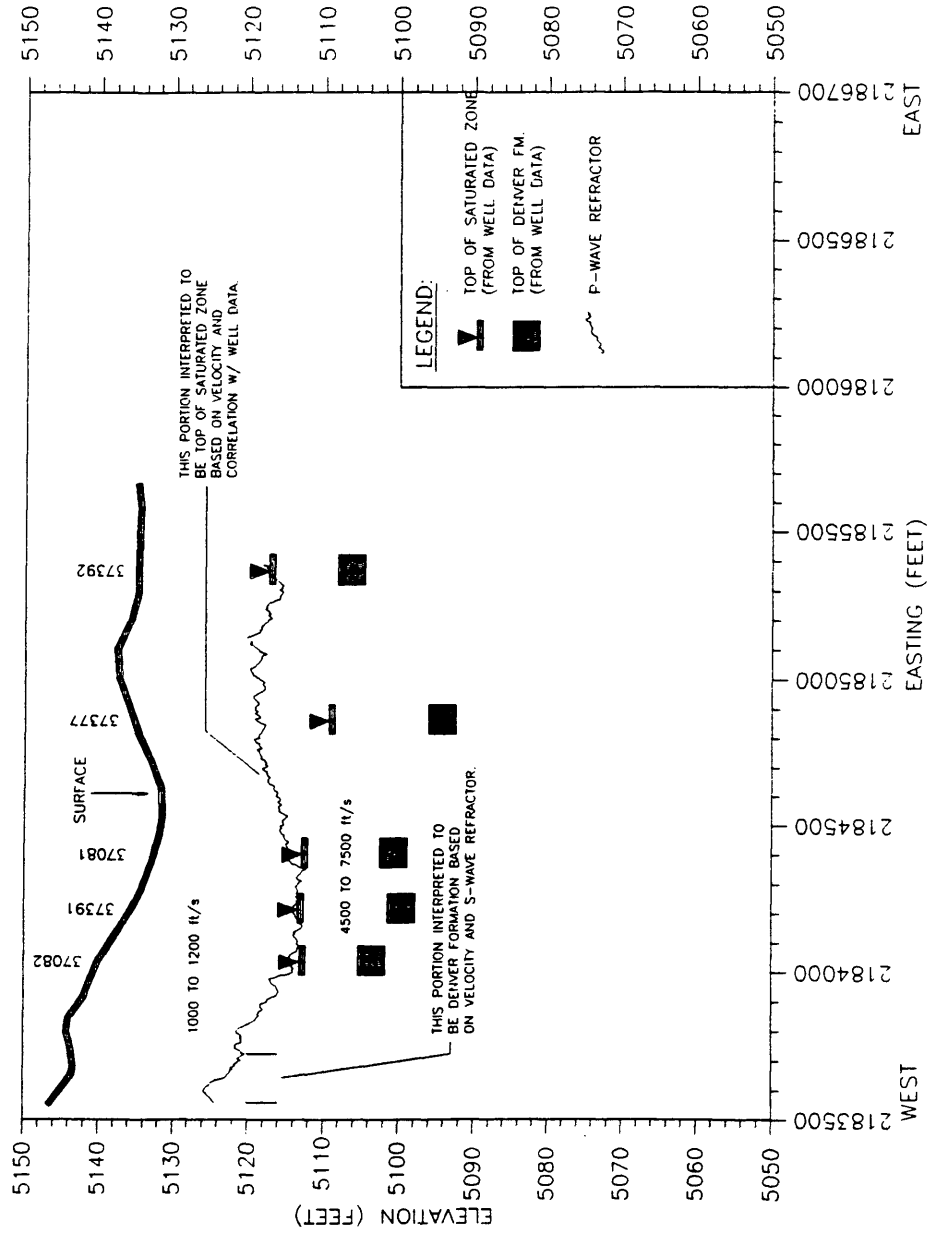


Figure 21. Interpreted P-wave refractor for Line 1, P1-1.

noticeably shallower, and its velocity is as low as 4,500 ft/s, which is consistent with that of a dry claystone (Clark, 1966), and is too low to be a saturated zone velocity. The fact that unsaturated Denver Formation is observed in well 37310 also supports this interpretation.

Additional velocity variations provide clues to the make-up of the unconsolidated alluvial material. The first velocity anomaly, a high-velocity zone, exists at the western end of Line 1 between 2,183,750 E and 2,184,100 E, just east of the Denver Formation high (**Figure 20**). The velocity of this region peaks near 7,000 ft/s, which is interpreted to be evidence of a significant, localized, lateral lithologic change in the saturated zone. This region may represent a lens of partially consolidated material.

A second area of interest is between 2,185,050 E and 2,185,250 E. In this region, a transition from high velocity (6,600 ft/s), to low velocity (5,000 ft/s) occurs very suddenly near 2,185,160 E. Within a few more stations to the east, the velocity returns (increases) to its previous value. This localized low velocity zone may be related to a bedrock high or a clay lens in the saturated zone. Interpreted P-wave sections are shown for Lines 2 and 3 in **Figure 22** and **Figure 23**, respectively.

Interpretation of S-wave Refraction Data

Analysis of S-wave data reveals the presence of one refracting interface. The velocity of the surface unit is near 500 ft/s along the length of Line 2 (**Figure 24**). The velocity of the refractor varies between 2,000 ft/s and 3,000 ft/s.

The refracting interface, labeled S2-1, is approximately 25 ft below ground surface (**Figure 25**). The average velocity of the refracting interface is 2,500 ft/s, which is a reasonable S-wave velocity for the Denver Formation if its P-wave velocity is 5,000 to 6,000 ft/s. Based on the depth and velocity of interface S2-1, the refractor is

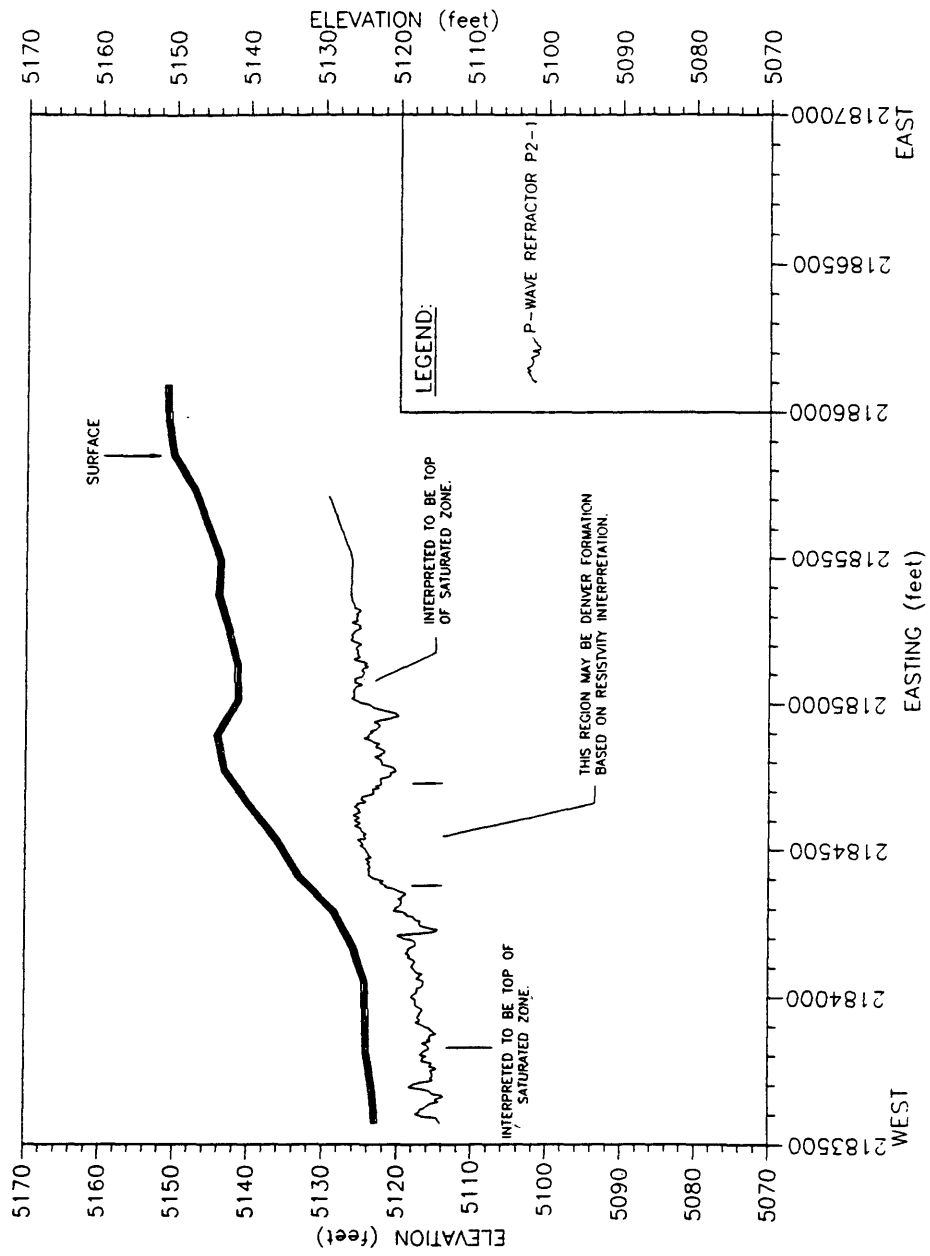


Figure 22. Interpreted P-wave refractor for Line 2, P2-1.

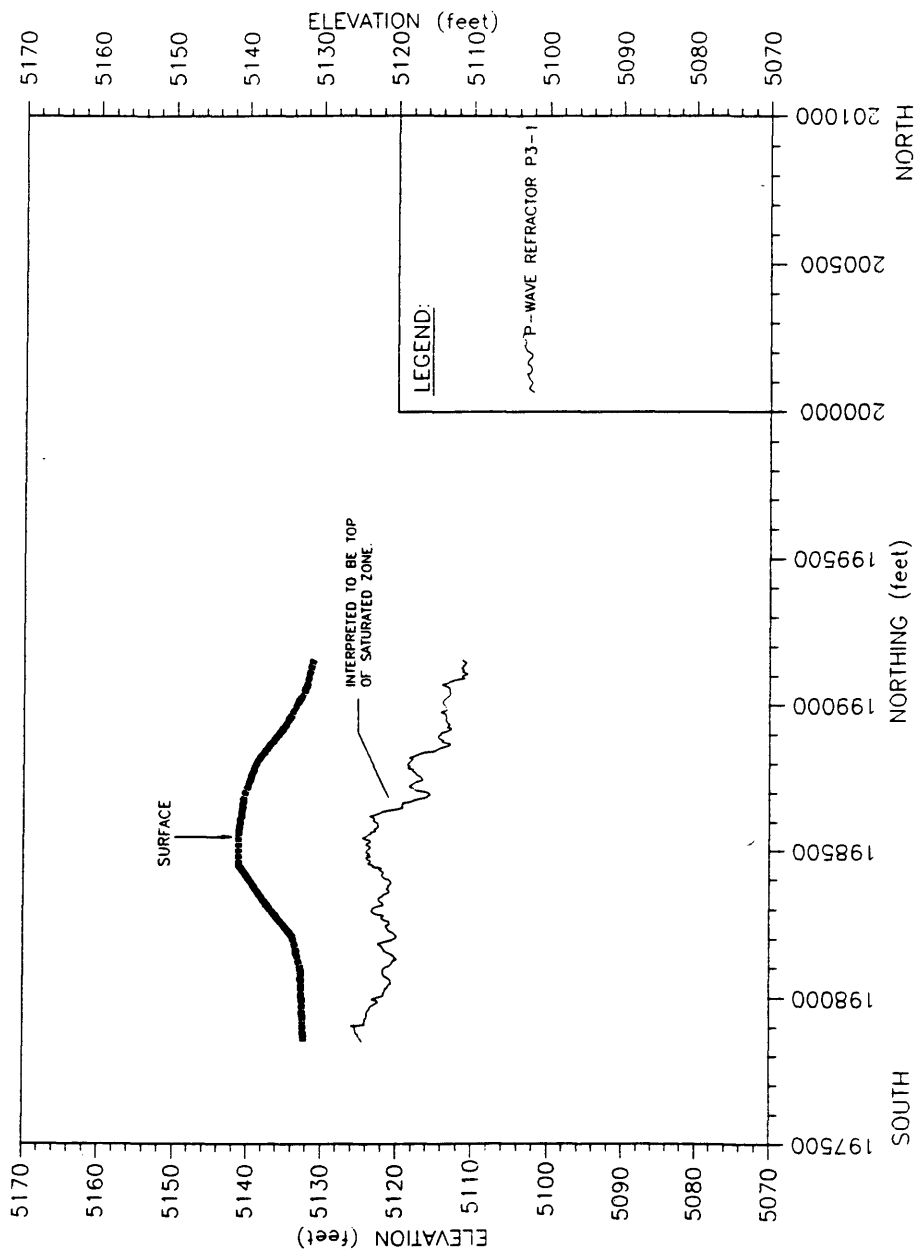


Figure 23. Interpreted P-wave refractor for Line 3, P3-1.

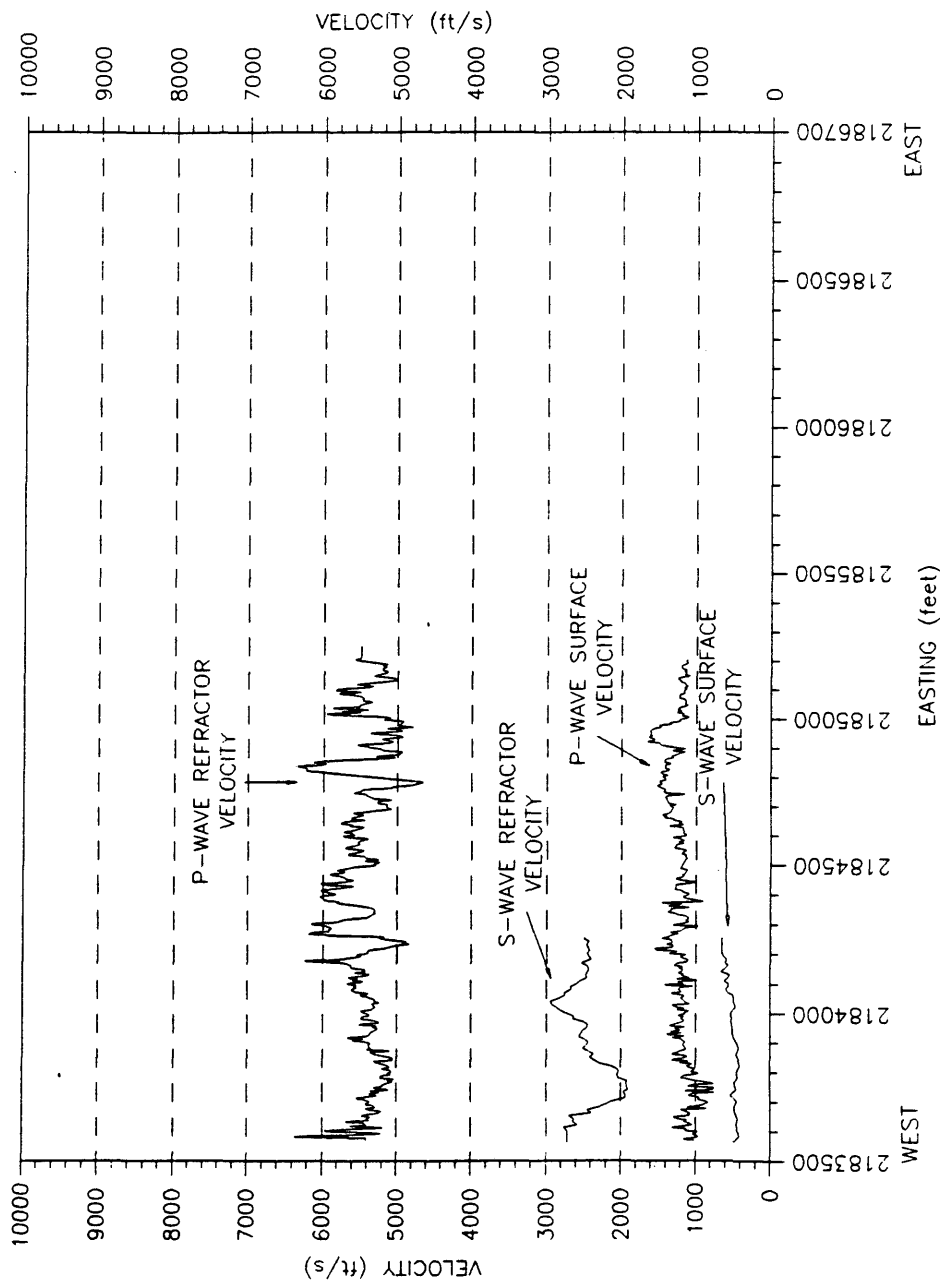


Figure 24. Calculated P-wave and S-wave velocities for Line 2.

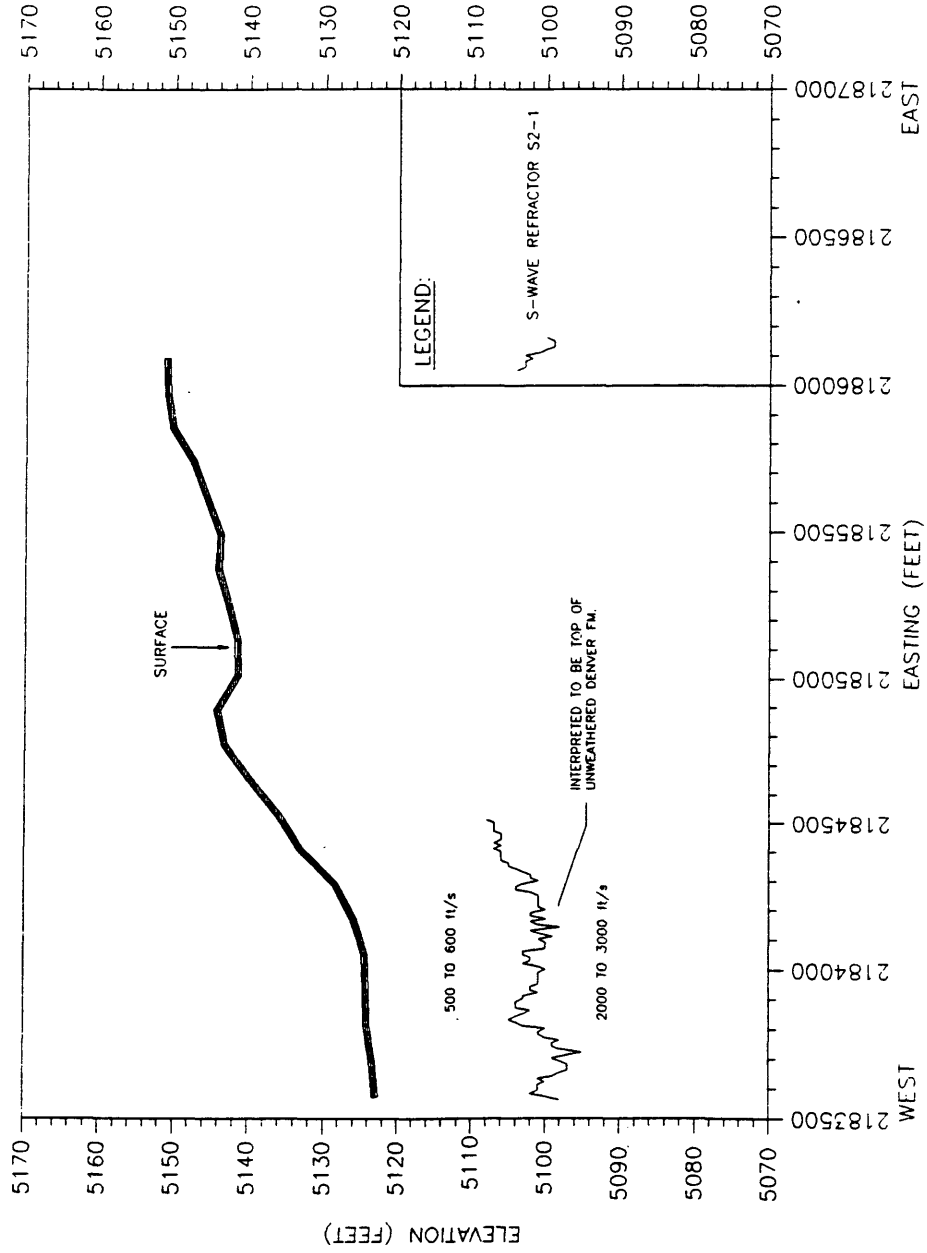


Figure 25. Interpreted S-wave refractor for Line 2, S2-1.

interpreted to be the bedrock surface. The interpreted S-wave refractor for Line 1 is shown in **Figure 26**. Based on this interpretation, the S-wave refraction method is a useful tool for determining the depth to the Denver Formation bedrock.

Interpretation of Direct Current Resistivity

As mentioned in Chapter 4, 16 Schlumberger soundings were acquired at the site. The initial resistivity model (Chapter 3) was a Q-type resistivity section ($\rho_1 > \rho_2 > \rho_3$), but the actual apparent resistivity curves reveal that the resistivity structure at the site varies from the initial model. A minimum of three and a maximum of five resistivity layers are observed on individual soundings.

Most of the apparent resistivity curves can be represented by one of two type-curves. Sounding type-1 is representative of a KH-type resistivity section ($\rho_1 < \rho_2 > \rho_3 < \rho_4$) and sounding type-2 is representative of a Q-type resistivity section. **Figure 27** shows examples of the two type-curves. Ironically, the two example curves are from adjacent sounding locations, which illustrates that the lateral resistivity structure can change rapidly in some areas at the site.

Using a one-dimensional inversion program (Resixp[®], Interpex Ltd.), each sounding is inverted to solve for layer resistivities and depths. Sounding interpretation is an iterative process which includes creating forward and inverse resistivity models. To begin the sounding interpretation process, a starting model is input that approximately fits the observed data; a starting model that does not fit the observed data within 10 to 30 percent leads to an inefficient and possibly inaccurate inversion process (Stoyer, 1987). At some point during the manual input of resistivity models, it becomes difficult to fine-tune all of the model parameters to get a very close fit, so the inversion algorithm is used

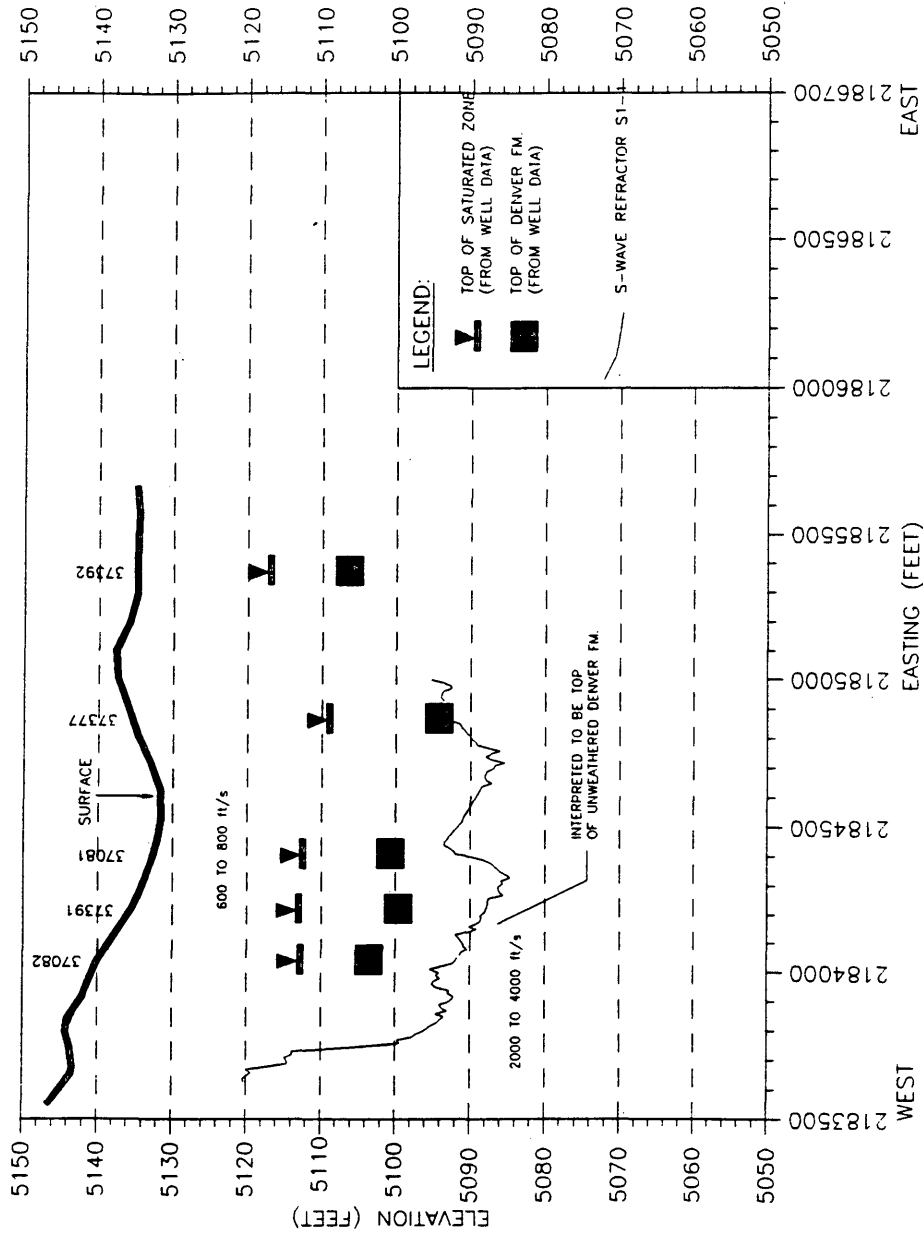


Figure 26. Interpreted S-wave refractor for Line 1, S1-1.

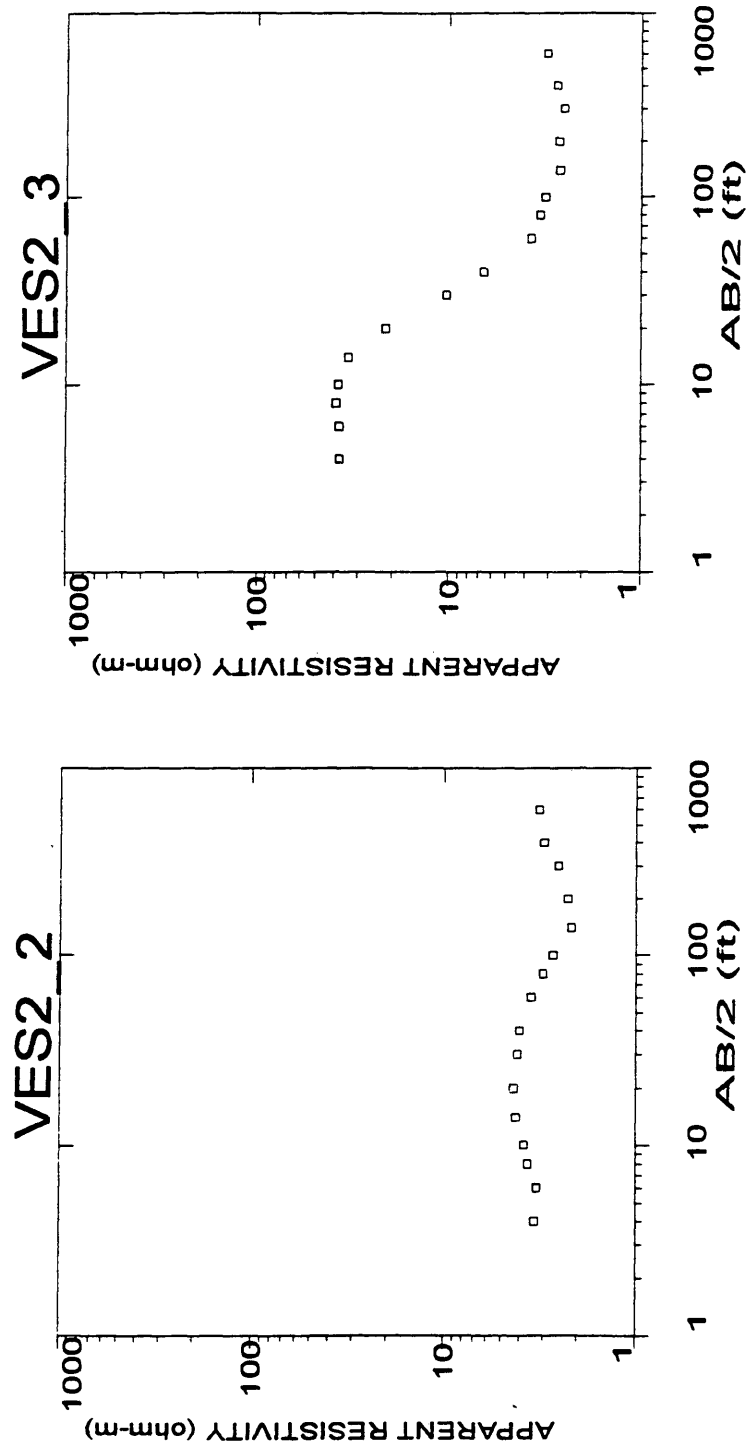


Figure 27. Two type-curves that are representative of the observed apparent resistivity curves. The apparent resistivity curve on the left is a KH-type curve, and the curve on the right is a Q-type curve.

to efficiently adjust the parameters. Resixp's® inverse modeling is performed using ridge regression (Inman, 1975). As a final step, a cross-section is created by correlating units from sounding to sounding.

The initial interpretation of the soundings was carried out on the group of soundings that were located near wells (Line 1 soundings). Interpretation of this first group of soundings was aided by the well information. Interpretation of the remaining soundings, which were located away from existing wells, was guided by the interpreted layer resistivities found in the first group of soundings and other geophysical data.

The most prominent feature of the all of the resistivity measurements is a very conductive layer (approximately 3 to 5 $\Omega\cdot\text{m}$), which is consistent with the resistivity expected for a saturated claystone (Keller and Frischnecht, 1966) (**Figure 28**). This unit is interpreted to be the Denver Formation. The interpreted resistivity-surface of the Denver Formation along Line 1 was constrained to honor the surface as defined by a combination of well information and data from S-wave refraction. However, a variety of acceptable interpretations can be created to honor the observed data. In order to map the surface of the Denver Formation to the degree of accuracy necessary to define the Northern Paleochannel, the interpretation of DC soundings must be supplemented with external information, such as well data or other geophysical data.

Generally, resistivity values for unconsolidated sediments commonly range from less than 1 $\Omega\cdot\text{m}$ for certain clays or sands saturated with saline water, to several thousand $\Omega\cdot\text{m}$ for dry basalt flows, dry sand, and gravel (Zohdy, 1974). The upper units at the site range in resistivity from approximately 10 to 50 $\Omega\cdot\text{m}$ and are interpreted to be unconsolidated alluvial material. The boundaries between upper units do not appear to correlate with the surface of the water table. In general, the base of the alluvial section is more resistive than the upper units, even though the upper units are unsaturated. It is

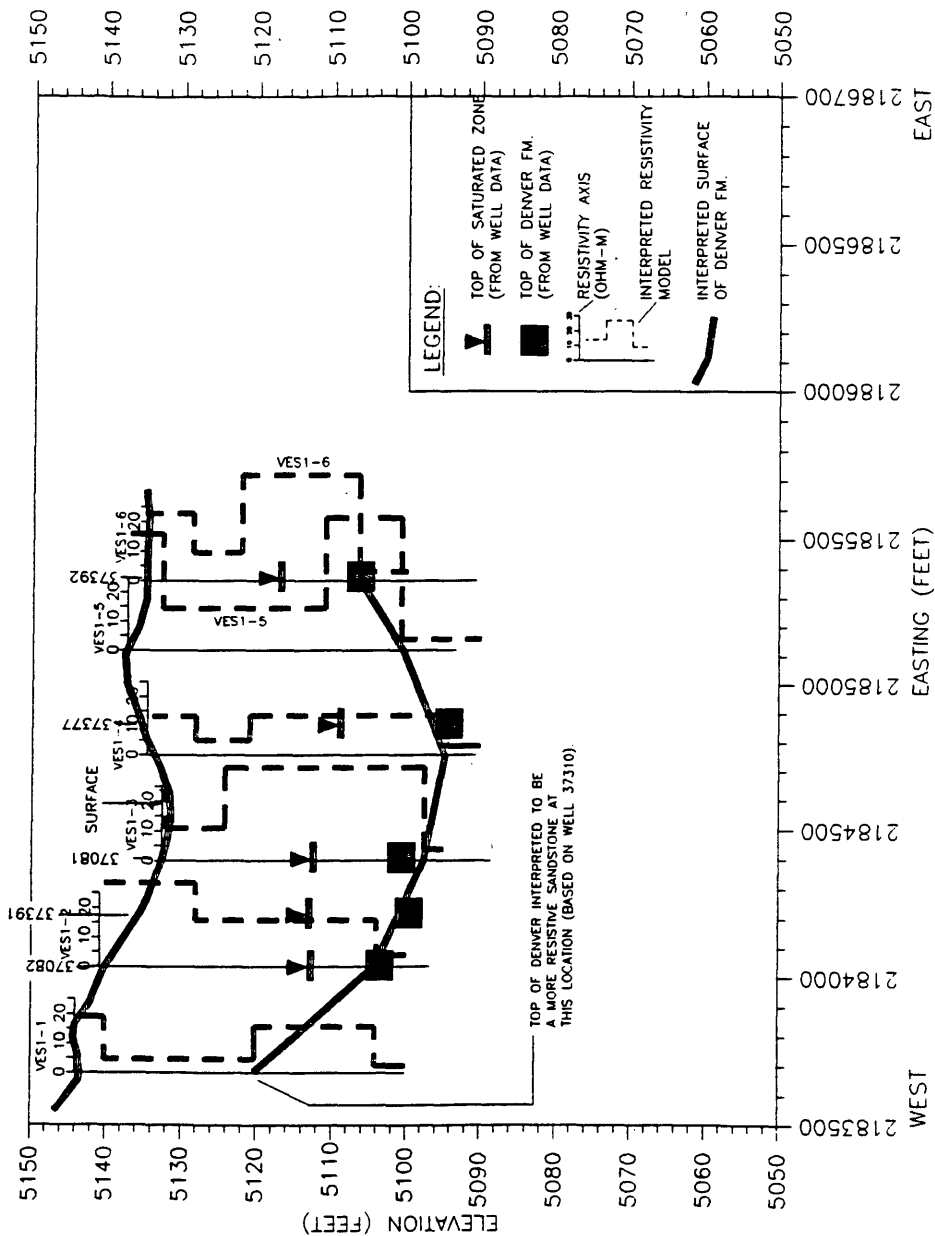


Figure 28. DC resistivity sounding interpretation for Line 1. The interpreted resistivity models are superimposed on the cross-section at each sounding location.

interpreted that the increase in resistivity with depth in the alluvial section is due to a decrease in clay content and salt content; precipitated salts are observed on the surface at the west end of Line 2 and, while not observed at the surface along Line 1, may be present in the sediments above the water table. Even a very small amount of moisture content in very salty soils can lower resistivity significantly.

The interpreted cross-section for Line 2 (**Figure 29**) shows a valley structure located between 2,184,700 E and 2,185,400 E. The topographic relief from the edges of the valley to the center is approximately 20 ft. The eastern edge of a second valley structure exists at the western end of the line and may correspond to the edge of the First Creek Paleochannel. Many smaller units are interpreted in the upper portion of the unconsolidated sediments. These units are small in lateral extent, which illustrates the complex depositional nature of these sediments. The depth to the top of the Denver Formation was constrained with the aid of interpreted depths obtained from P-wave and S-wave methods. VES2-4 is of particular interest because of a high-resistivity unit (420 $\Omega\cdot\text{m}$) interpreted overlying the bedrock surface. This unit may correspond to a dry sand or gravel lens.

The south end of Line 3 intersects Line 2 at a point located over the western edge of the Line 2 valley structure. The bedrock topography map shows the valley structure trending towards the northwest, so one would expect the valley to intersect Line 3. The interpreted cross-section for Line 3 supports this hypothesis (**Figure 30**); the south end of Line 3 shows the conductive bedrock to be near the surface, and then the bedrock surface dips down to the north as the path of the valley crosses Line 3. The interpreted depth to the top of the Denver Formation was constrained by the interpreted depths at the tie-points with Lines 1 and 2.

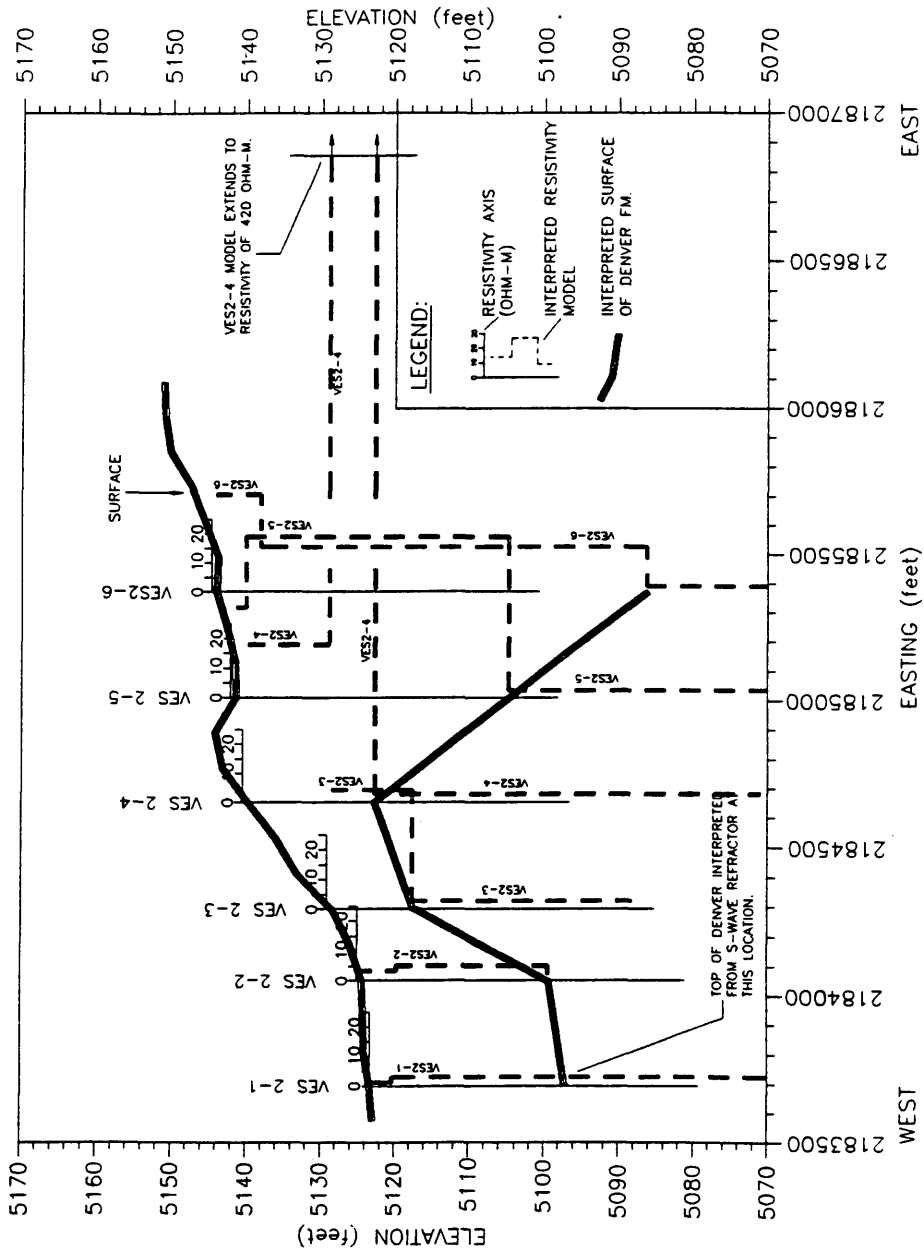


Figure 29. DC resistivity sounding interpretation for Line 2. The interpreted resistivity models are superimposed on the cross-section at each sounding location.

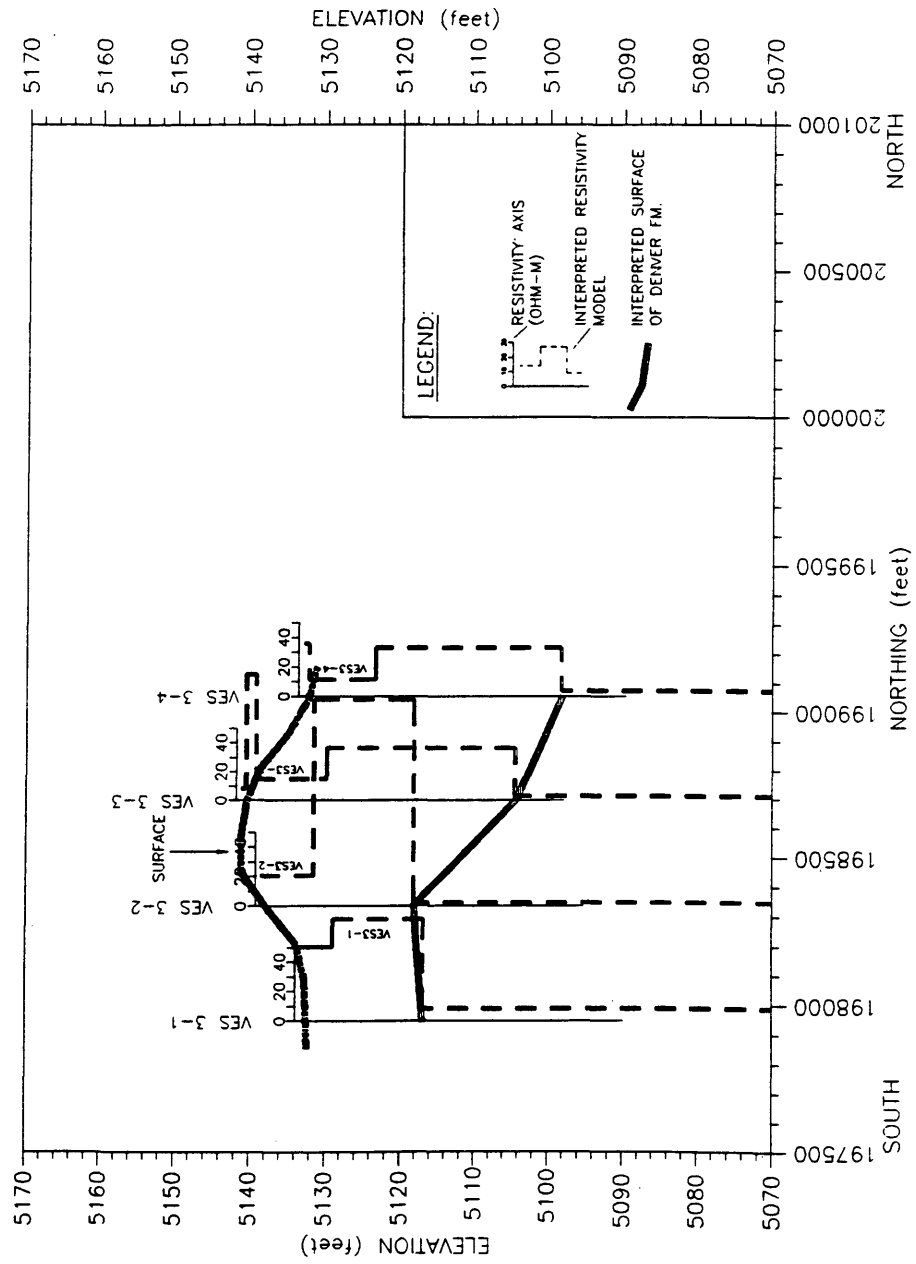


Figure 30. DC resistivity sounding interpretation for Line 3. The interpreted resistivity models are superimposed on the cross-section at each sounding location.

Not shown in any of the interpreted cross-sections is a deeper, resistive unit that was interpreted on several of the soundings and that may correspond either to a resistive sand unit within the Denver Formation or Arapahoe Formation. The Arapahoe-Denver contact is difficult to determine visually and is usually identified by detailed paleontological work and possibly a slight color change. The presence of volcanic material or the presence of a thick basal conglomerate (30 to 90 meters thick) (Kirkham and Ladwig, 1979) in the Arapahoe Formation may account for the high resistivity measurements.

Interpretation of Gravity Data

In Chapter 4, the gravity data processing was discussed through the point of the simple Bouguer anomaly; corrections were made for elevation and free-air effects. The interpretation of gravity data begins with the removal of the regional gravity field. The selection of a regional field is subjective and can affect interpretation results. An interpretation process, which includes forward modeling, inversion, and the input of any external geologic information, is based on the residual gravity anomaly.

The regional gravity field at the site is part of a large gravity low centered over the Rocky Mountains. The regional low is an isostatic effect caused by the lowering of the earth's mantle under the thickened crust of the Rocky Mountain region. RMA is located within the eastern flank of the gravity low, so the regional gravity field increases in magnitude toward the east. The slope of the simple Bouguer anomaly gravity acquired along Line 1 agrees with the estimated slope determined from the Bouguer gravity map for Colorado (Behrendt and LaCretia, 1974). Therefore, a straight-line, least-squares fit

to the simple Bouguer anomaly was subtracted as the regional gravity field. The slope of the removed regional is 0.242 $\mu\text{gal}/\text{ft}$.

The residual gravity anomaly was interpreted using Magixp® (Interpex Ltd.). As in the interpretation of DC resistivity data, a starting depth/density model is input to Magixp® and a forward model is generated. Next, the model is fine-tuned via an iterative process that involves the integration of geology and other geophysical results with the gravity model. Once the model parameters are difficult to refine any further, an inversion algorithm fine-tunes the depth/density values.

Gravity data along Line 1 were fit with a two-dimensional, two-layer model (**Figure 31**). The density contrast between the model layers is 0.3 g/cm^3 . The interpreted surface of the Denver Formation agrees with the initial geologic model in that a Denver Formation high is interpreted at the west end of Line 1 (2,183,500 E to 2,183,900 E). A smaller Denver Formation high (approximately 5 ft of relief) is interpreted from 2,184,700 E through 2,185,200 E.

Interpretation of Electromagnetic Data

The outputs of the EM-31 and EM-34 survey were terrain conductivity (related to the quadrature component of the secondary magnetic field). The secondary magnetic field is a complicated function of the intercoil spacing, the operating frequency, and the ground conductivity. The relationship is simplified when certain constraints, defined as "operation at low induction number", are met (McNeill, 1980). When the low induction number constraints are not satisfied, the measured quadrature and inphase responses deviate from expected values. In very conductive terrain ($>300 \text{ mS}/\text{m}$), or in the presence of metal, the quadrature component of the received magnetic

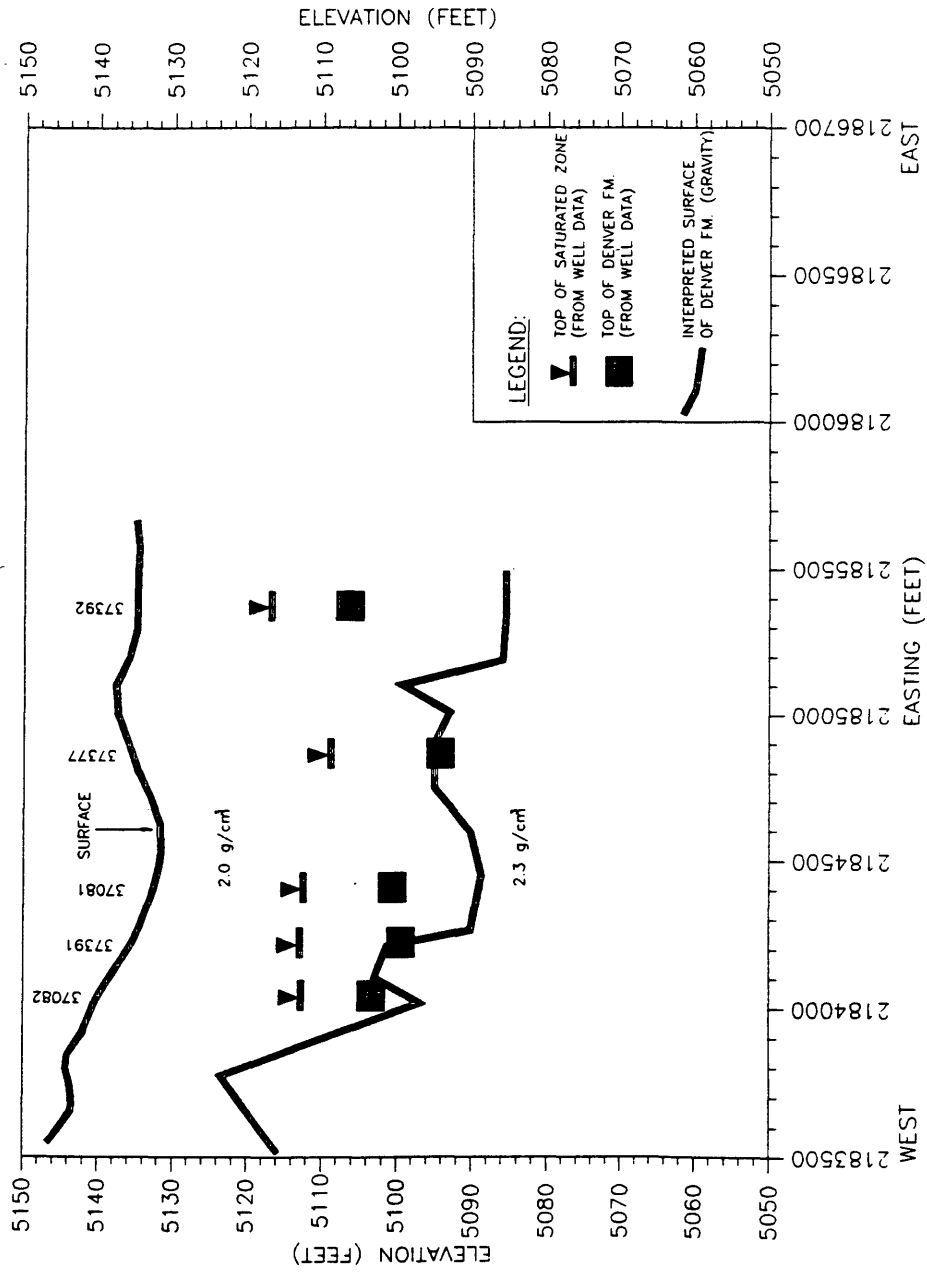


Figure 31. Interpreted surface of the Denver Formation from gravity data.

field is not linearly proportional to the terrain conductivity. Therefore, the conductivity readings reported by the EM instruments are not accurate in all conditions.

To understand the depth of investigation of the EM-31 and EM-34, it is useful to consider a homogeneous halfspace with the addition of a thin layer at some depth. For VMD orientation, a layer located at a depth of 0.4 times the coil spacing gives the most contribution to the response; however, deeper layers (as deep as 1.5 times the spacing) still contribute a significant amount to the response (McNeil, 1980). The response for HMD orientation is greatest for a layer at the surface (McNeil, 1980). Perhaps more useful than looking at the effect of one layer at depth is to look at the instrument response for all layers below a given depth. **Figure 16** (Chapter 3) shows this function for both coil orientations and illustrates that the VMD orientation has approximately twice the exploration depth of the HMD orientation (McNeill, 1980).

Figure 32 and **Figure 33** show the HMD and VMD (respectively) data sets for the EM survey along Line 1. Qualitatively, conductivities are greater with larger coil spacing which agrees with the geologic model presented in Chapter 2. Assuming that lateral changes in conductivity are relatively small in any given layer, it is expected that most of the lateral variation in the observed data will correspond to changes in depths and thicknesses of the layers. The shape of the conductivity curve in **Figure 32** suggests that conductive material is closer to the surface at the west end of Line 1 (approximately 2,183,700 E), which agrees with the interpretation of a Denver Formation high in that region.

In **Figure 33**, it is shown that data from the VMD orientation with coil spacings of 20 m and 40 m are particularly noisy, which illustrates the sensitivity of VMD measurements to small coil misalignments. HMD data is less sensitive to coil alignment

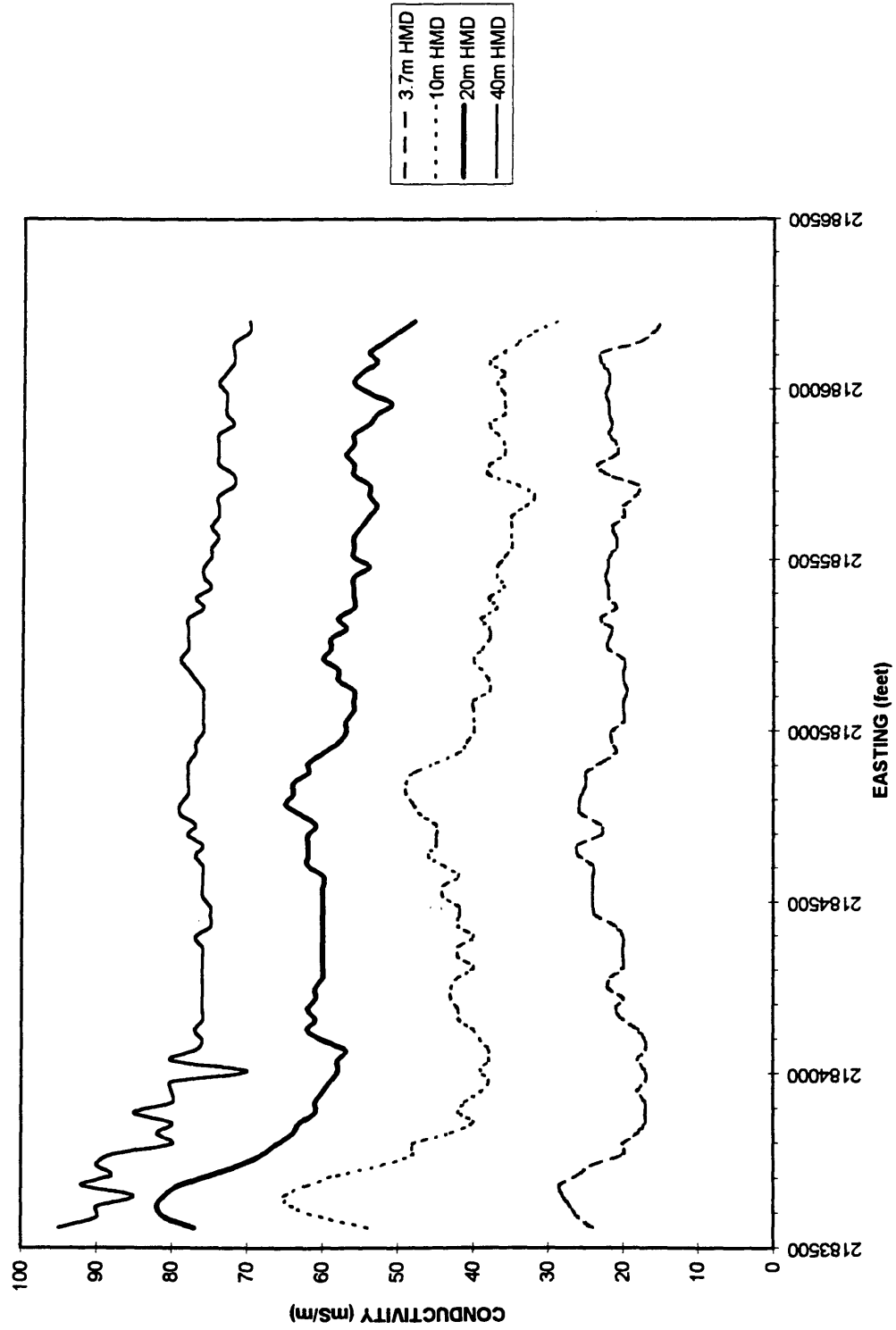


Figure 32. HMD conductivity measurements for Line 1 (EM-31 and EM-14).

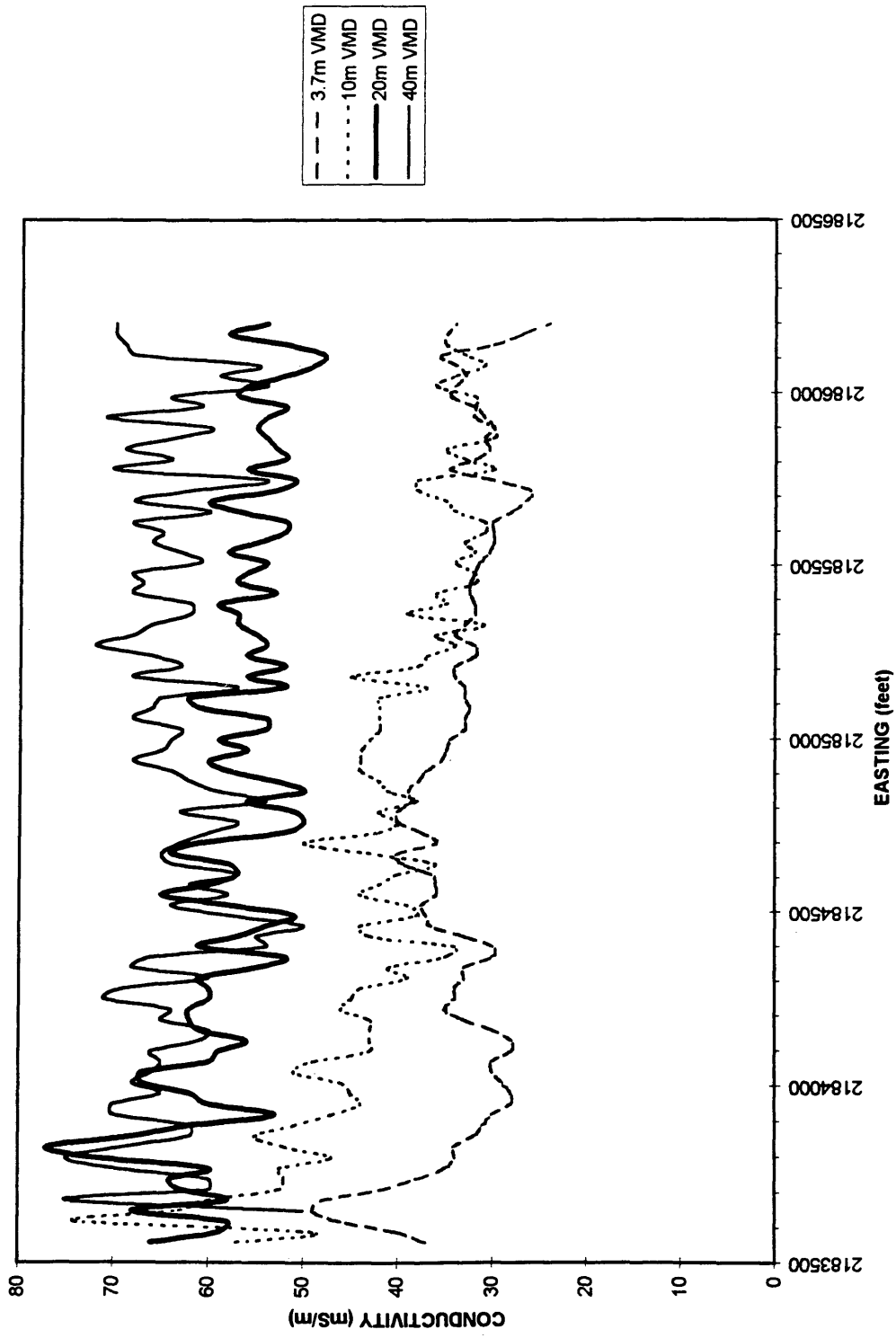


Figure 33. VMD conductivity data for Line 1 (EM-31 and EM-34).

(McNeill, 1980) and is therefore more useful in the quantitative interpretation. Quantitative interpretation was performed with the aid of Emix34p[®] (Interpex Ltd.) interpretation software. To facilitate interpretation of a conductivity-depth model, all EM measurements at a single surface location (maximum of 8 measurements) are compiled to create an EM sounding. A one-dimensional layered model is created that fits the observed data and any external data. The modeling process is similar to the process carried out for the interpretation of DC resistivity soundings; once an input model matches the observed data to within 10 to 30 percent, an inversion algorithm is used to fine-tune conductivity and depth parameters. Modeled EM responses are calculated using a method described by Patra and Mallick (1980), and inverse modeling is performed using ridge regression (Inman, 1975).

Due to the limited number of data points for each sounding, the only prudent model that can be constructed for this data set is a two-layer model. Given the noise level present in the VMD data, these data were excluded from the final inversion process. Preliminary interpretations that included the VMD data resulted in irregularly varying layer thicknesses, but roughly conformed to the interpretation obtained with only HMD data. The final interpreted conductivity cross-section is shown in **Figure 34**. It was not possible to fix the depth of the deepest layer to agree with the depth to the Denver Formation as determined from well information, but the general shape of the interpreted curve suggests a Denver Formation high to the west and shows the Northern Paleochannel to the east. The question arises as to whether the layer interpreted from EM measurements is actually the Denver Formation or just a conductive clay or saturated zone within the alluvium. As will be discussed in the integration of all of the geophysical results, a strong correlation of the EM model with the interpreted gravity model and S-wave model (except for a DC shift) suggests that the lower layer of the EM model is

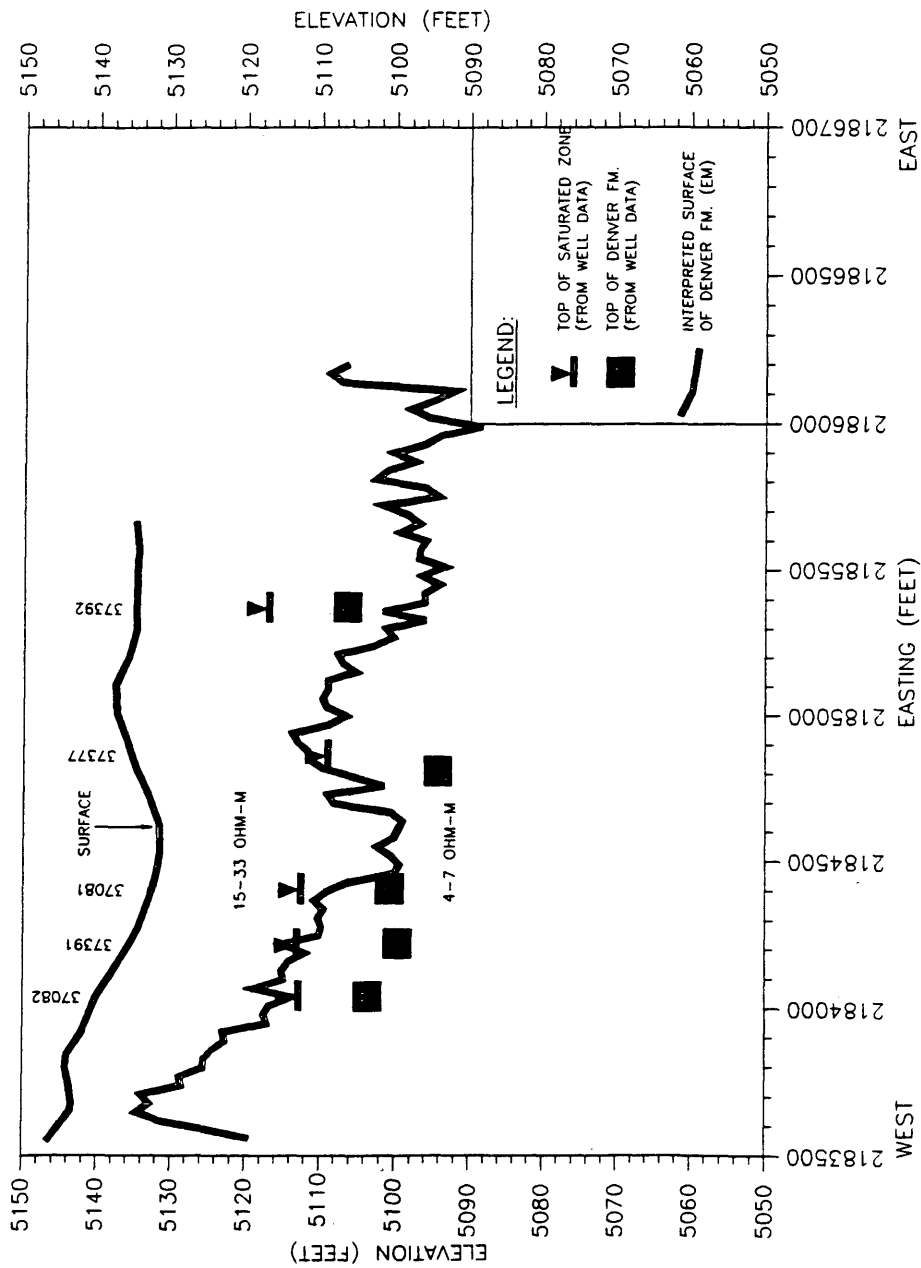


Figure 34. Interpreted surface of the Denver Formation along Line 1 based only on EM data.

related to the Denver Formation. The layer conductivities (**Figure 35**) were allowed to vary slightly across the line and are similar to the alluvial and Denver Formation resistivities interpreted from the DC soundings. Alluvial resistivities range from 15 to 33 $\Omega\cdot\text{m}$, and Denver Formation resistivity varies from 4 to 7 $\Omega\cdot\text{m}$.

Integrated Geologic Interpretation

The ultimate goal of this geophysical investigation is to characterize shallow geologic features that, in turn, will aid the understanding of groundwater/contaminant flow at RMA. It is clear from the individual geophysical interpretations that one method cannot provide all of the information necessary to characterize the alluvial zone, saturated zone, and Denver Formation. This section presents all of the geophysical results together, in order to form one geologic interpretation.

In general, P-wave refraction is used to map the surface of the water table in regions where the Denver Formation is lower than the water table surface. In areas where the Denver Formation subcrops above the water table, P-wave refraction will define its surface. S-wave refraction, DC soundings, gravity, and EM methods are used to map the surface of the Denver Formation. If all four methods correlate, the interpretation is considered very reliable because three independent physical parameters are utilized: shear modulus, resistivity, and density. DC resistivity gives clues as to the composition of alluvial materials in that more resistive materials are interpreted to have lower clay content and higher permeability, and materials with low resistivity are interpreted as less permeable clays and silts. Although correlating alluvial resistivities with the specific alluvial lithologies found in the wells is difficult, DC methods may provide a broad picture of alluvial composition.

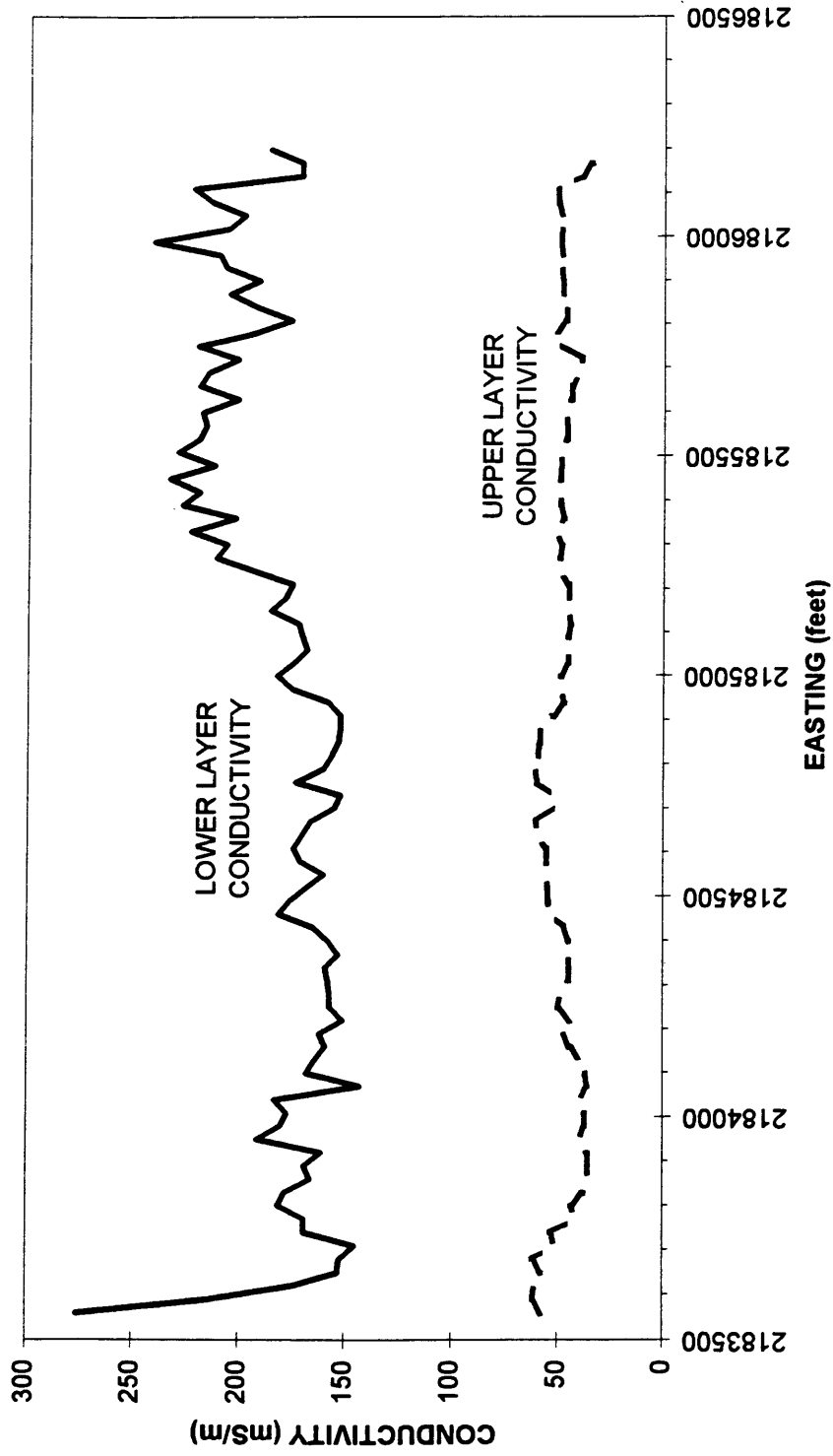


Figure 35. Interpreted conductivities for Line 1.

Figure 36 shows the combined geophysical interpretations and well data for Line 1, with the exception of the EM interpretation. The surface of the water table is delineated via P-wave refraction, while the S-wave refractor surface is interpreted to show the surface of the Denver Formation. The surface of the Denver Formation is also interpreted from gravity and DC resistivity data. The surface interpreted from EM data does not match the depth of the Denver Formation, but a strong correlation exists between the shape of the interpreted EM surface and the surface interpreted from gravity data.

Figure 37 shows the combined geophysical interpretations for Line 2. Limited S-wave coverage and a lack of gravity or EM data on Line 2 result in a roughly defined bedrock surface. The high in the Denver Formation (2,184,400 E to 2,184,700 E) interpreted from DC soundings VES2-3 and VES2-4 appears to be confirmed by a localized high in the P-wave refractor surface, P2-1. It is interpreted that the Denver Formation may be at or above the water table in this region. Either S-wave refraction, gravity, or EM data would be useful in confirming this interpretation because DC sounding interpretations can vary widely with little external control and because the topographic variation in the surface P2-1 is small.

Figure 38 shows the combined geophysical interpretations and well data for Line 3. DC resistivity soundings are interpreted to delineate the surface of the Denver Formation and yield clues to the lithology of alluvial units. P-wave refractor P3-1 is interpreted to be the surface of the saturated zone. Either S-wave refraction, gravity, or EM data would be useful in confirming the apparent Denver low from 198,300 N to 199,100 N.

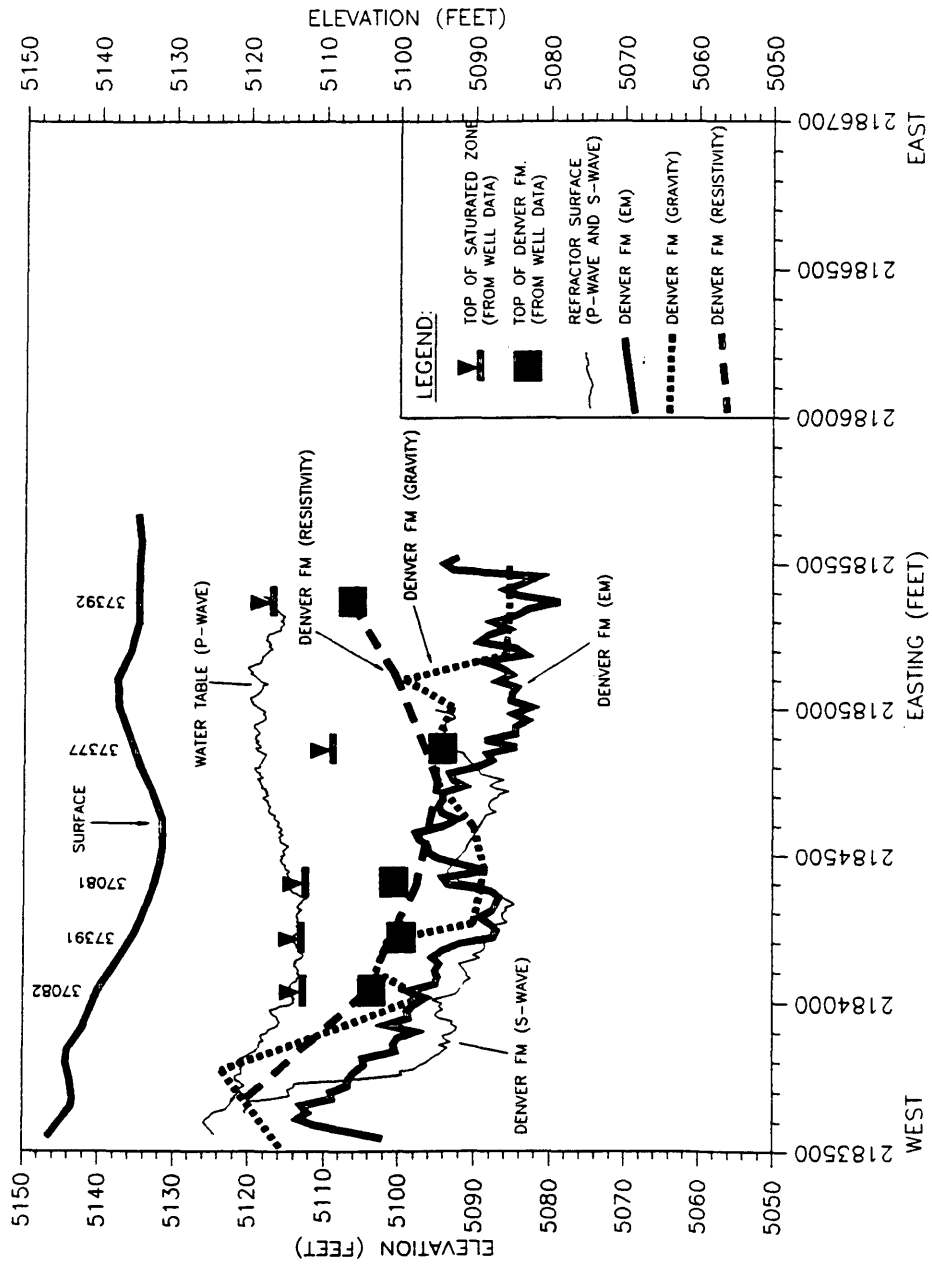


Figure 36. Integrated interpretation for Line 1. The EM surface has been manually shifted downward to agree with S-wave and gravity interpretations.

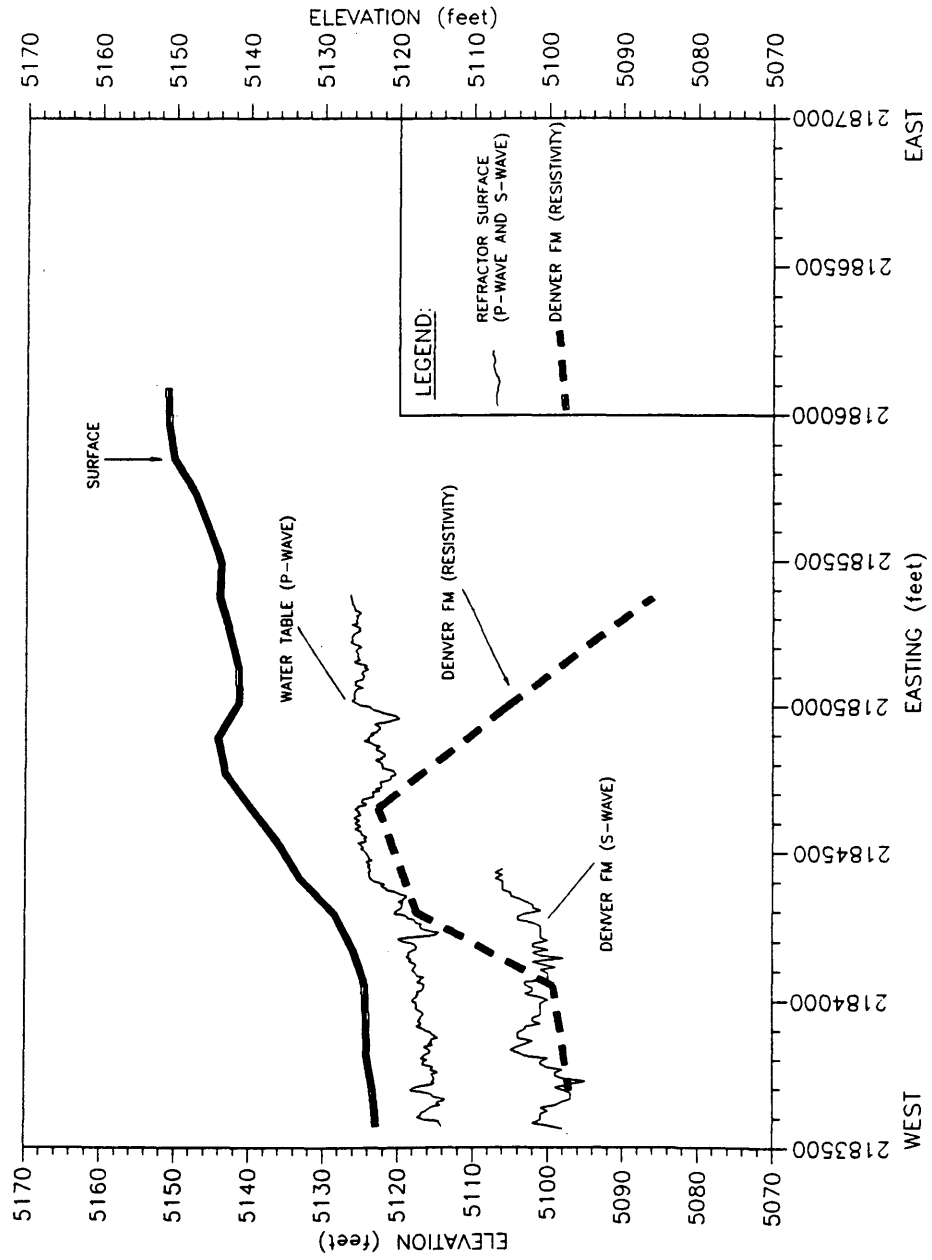


Figure 37. Integrated interpretation for Line 2.

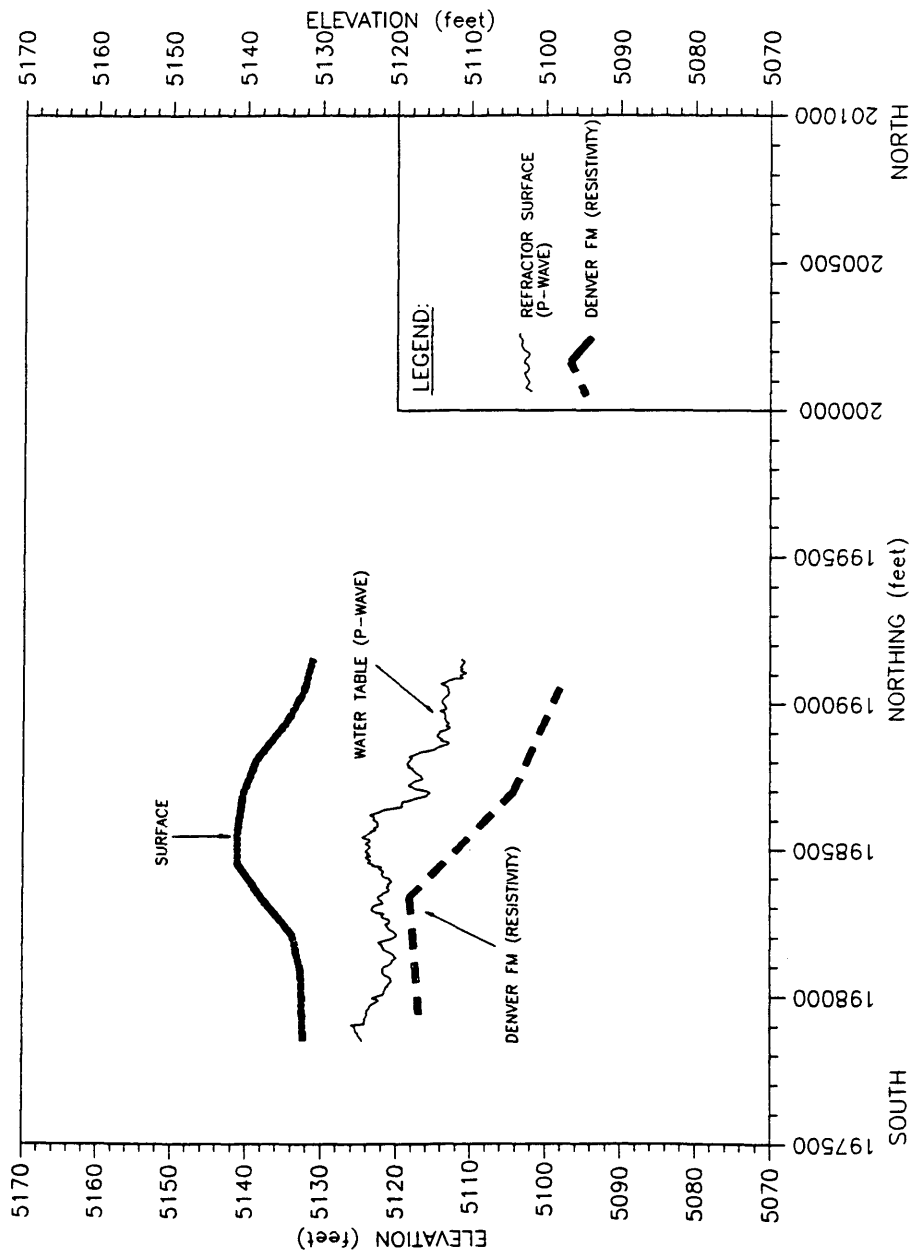


Figure 38. Integrated interpretation for Line 3.

Chapter 6

CONCLUSIONS

An integrated geophysical investigation was conducted in the Offpost Study Area of Rocky Mountain Arsenal. The goal of the investigation was to find geophysical methods that would help characterize the geologic environment of a shallow, contaminated aquifer. Forward modeling, based on a geologic model that was determined from pre-existing well information, was used to select geophysical methods that were likely to succeed. The following methods were selected for testing: P-wave and S-wave seismic reflection, P-wave and S-wave seismic refraction, DC resistivity soundings, microgravity, and frequency-domain electromagnetics. A combination of modeling and field tests were used to design the geophysical surveys. The acquisition of data took place during the summer of 1992.

The integrated geophysical investigation was shown to be a viable method for characterizing several components of the shallow geology of the Northern Paleochannel: the surface of the Denver Formation, the surface of the saturated zone, and the clues to the composition of alluvial materials that overly the Denver Formation. Geophysical interpretations agreed with well information along Line 1 and were extended into areas with no well data along Lines 2 and 3. The most successful combination of geophysical tools in the investigation were determined to be seismic refraction, microgravity, and DC resistivity soundings. Little useful quantitative information (such as depth or layer-conductivity) was gained from EM profiling, and no success was obtained with seismic reflection methods. Future geophysical investigations at RMA may be guided by

the findings of this study. Therefore, it is useful to evaluate the effectiveness and limitations of the geophysical methods as they were applied in this investigation.

P-wave seismic methods are often the first methods that are considered when the objective is to map shallow bedrock. However, the results of this investigation revealed that P-wave methods achieved only limited success in the detection of the Denver Formation claystone. P-wave seismic methods failed for two reasons. First, the shallow Denver claystone is likely weathered and has a relatively low P-wave velocity (approximately 6,000 ft/s) which is contrary to what is often associated with the term "bedrock". P-wave velocity of overlying, saturated, unconsolidated sediment ranged from 5,000 ft/s to 6,500 ft/s (with few exceptions), and consequently little or no P-wave velocity contrast exists between the two units. P-wave refraction succeeded in mapping the surface of the Denver Formation only in areas where the Denver Formation subcrops above the water table.

A second reason for the limited success of P-wave methods is the shallow depth of the targeted units (Denver Formation and water table). Even if the Denver Formation possessed a significantly higher P-wave velocity ($> 6,800$ ft/s), the water table would be a hidden layer; that is, the layer would be too thin to detect without a very small geophone interval (< 5 ft). Refracted arrivals from the water table could be detected only in a very narrow offset range; it is often cost-prohibitive to carry out refraction surveys with geophone intervals smaller than five feet. Regardless, in this case the Denver Formation does not have a high enough P-wave velocity, so only the water table was mapped in the region of the aquifer. The primary success achieved with P-wave refraction was the mapping of the surface of the water table. The P-wave reflection method failed because reflected arrivals were overwhelmed by surface waves and air waves that occupied the same time/offset window in the shot records. Had the water table been significantly

deeper (approximately 2 to 3 times deeper), the reflection method might have had more success.

The S-wave refraction method was successful in mapping the unweathered surface of the Denver Formation because a significant S-wave velocity contrast occurs at this surface. S-wave refraction methods were limited by two factors. The first factor was attenuation. High attenuation of S-wave energy made it difficult to record refracted arrivals at distant geophones (approximately greater than 150 to 200 ft offset). The second limiting factor was dispersion. Dispersion of S-wave energy resulted in difficult-to-pick first breaks, that is, the first breaks appeared very "emergent" and consequently first arrivals were sometimes picked incorrectly during the first attempt.

The S-wave reflection method failed in this investigation because of interference from high-amplitude surface-wave energy and low recorded frequency content.

DC resistivity soundings were effective in mapping the approximate depth to the Denver Formation because of the significant contrast in resistivity at that interface. The resistivity of overlying unconsolidated sediments was found to be (with localized exceptions such as the shallow clay layers found in VES1-1 and VES1-4) greater than 10 $\Omega\cdot\text{m}$. The underlying Denver Formation resistivity is 3 to 5 $\Omega\cdot\text{m}$. Resistivity soundings provided the most information about the unconsolidated sediments because the vertical resolution of resistivity measurements is greatest near the surface. However, it was found that the unconsolidated sediments change rapidly in the lateral direction, so it is impossible to create a cross-sectional interpretation with the sparse spatial sampling afforded by the soundings in this investigation. Future resistivity investigations should include resistivity profiling in order to reduce the lateral sampling interval. Data acquisition on a grid is also recommended for the future because it would create a better three-dimensional picture of the resistivity changes.

The major limitation of DC resistivity soundings was the amount of ambiguity in the interpretations. Some depths and resistivities had to be fixed in the inversion process to yield results that fit observed well data and independent geophysical data. Unconstrained inversions were not reliable. A second limitation of the DC resistivity soundings in this investigation was that the resistivities of all the earth materials at the site are relatively low, which means that either a high-power transmitter or a more sophisticated digital resistivity meter is required.

The EM survey was successful as a qualitative tool for mapping Denver Formation highs and lows, but it failed to delineate shallow alluvial features or a quantitative depth to the Denver Formation. The EM method (as applied in this investigation) failed because of a lack of vertical resolution. Only eight data points were acquired at each station, which are not enough to characterize a complicated, multi-layer environment. Also, the coil separations and operating frequencies of the EM equipment were fixed, so the EM survey could not be fine-tuned for small, shallow targets (e.g., clay and sand lenses). Frequency-domain EM methods would be more useful as a reconnaissance tool for defining lateral conductivity changes. It is recommended in the future that EM measurements should be acquired on a grid to facilitate mapping lateral features.

The gravity method was successful in delineating the structure of the Denver formation. Gravity data is useful in combination with resistivity and EM data because it helps to limit the ambiguity of the interpretation. Areas where conductivity anomalies correlate with gravity anomalies (e.g., high conductivity and high gravity at the west end of Line 1) can be interpreted as structural changes in the Denver Formation. A conductivity anomaly in the absence of a gravity anomaly may indicate a lithologic change rather than a structural change. The primary limitations of the gravity method are

that the method lacks the resolution of the other methods, and that density contrasts among alluvial sands and clays are small and unmeasurable.

An important lesson learned from this investigation is that an integrated geophysical approach is necessary because of the inherent non-uniqueness of geophysical interpretations and because each of the targets of this investigation is defined by different physical parameters. For example, the interface between alluvial material and the Denver Formation is best characterized by a contrast in S-wave velocity, density, and resistivity, while the top of the saturated zone is best characterized by a significant change in P-wave velocity. No single geophysical method is capable of characterizing all of the geologic targets.

In summary, future investigations at RMA may benefit from the use of refraction, DC resistivity, gravity, and electromagnetic methods. However, seismic reflection methods are ineffective and expensive exploration tools for this purpose.

REFERENCES CITED

- Aki, K., P. Richards. 1980. Quantitative Seismology. W.H. Freeman.
- Burger, H.R. 1992. Exploration Geophysics of the Shallow Subsurface. Englewood Cliffs, NJ: Prentice-Hall.
- Clark, Sydney P. Jr. 1966. Handbook of physical constants. revised ed. Geological Society of America: mem 97.
- Colog Inc. 1991. Velocity log and neutron-density log from Denver Formation at Rocky Mountain Arsenal (exact location unknown). Golden, CO.
- Domenico, S.N. 1976. Effect of brine-gas mixture on velocity in an unconsolidated sand reservoir. Geophysics. Vol. 41. No. 5: 882-894.
- Docherty, P. 1991. Cshot: Common-shot modeling program. Golden, CO: Center for Wave Phenomena, Colorado School of Mines: CWP-U08R (documentation).
- EDCON, 1993. Promotional material for Super G gravimeter. Lakewood, CO.
- Environmental Science and Engineering, Inc. (ESE). 1988. Offpost Operable Unit, remedial investigation and chemical specific applicable or relevant and appropriate requirements, Task 39, Final report, Version 3.1. Denver, CO: Prepared for Office of Program Manager, Rocky Mountain Arsenal Contamination Cleanup.
- Guest, P.R. 1988. Case Study: An assessment of ground-water flow in the Denver Formation beneath a ground-water containment system at the Rocky Mountain Arsenal, Denver, Colorado. Unpublished Master's Thesis. Colorado School of Mines. Golden, CO.
- Gulunay, N. 1985. (Abstract) A new method for the surface consistent decomposition of statics using diminishing residual matrices (DRM). 55th meeting of the International Society of Exploration Geophysicists. Washington, D.C.

- Harding Lawson Associates (HLA). 1991. Groundwater monitoring program: Final annual groundwater monitoring report for 1991. Denver, CO: Program Manager for Rocky Mountain Arsenal.
- Inman, J.R. 1975. Resistivity inversion with ridge regression. Geophysics 40.
- Keller, G.V., F.C. Frischnecht. 1966. Electrical methods in geophysical prospecting Elmsford, NY: Permagon Press: 39-43.
- Kirkham, R.M., L.R. Ladwig. 1979. Coal resources of the Denver and Cheyenne Basins, Colorado. Denver, CO: Colorado Geological Survey Department of Natural Resources.
- Lindvall, R.M. 1971. Geologic map of the Sable Quadrangle, Adams, and Denver counties, Colorado. Reston, VA: U.S. Geological Survey Map Gq-1567.
- Lindvall, R.M. 1980. Geologic map of the Sable Quadrangle, Adams, and Denver counties, Colorado. Reston, VA: U.S. Geological Survey Map Gq-1180.
- Lindvall, R.M. 1983. Geologic map of the Sable Quadrangle, Adams, and Denver counties, Colorado. Reston, VA: U.S. Geological Survey Map Gq-1567.
- May, J.H., D.W. Thompson, P.K. Law, and R.E. Wahl. 1980. Hydrogeologic assessment of Denver sands along the North Boundary of Rocky Mountain Arsenal. Vicksburg, MS: U.S. Army Corps of Engineers Waterways Experiment Station.
- McNeill, J.D. 1980. Electromagnetic terrain conductivity measurement at low induction numbers. Geonics Technical Note TN-6. Mississauga, Ontario, Canada: Geonics Ltd.
- Nettleton, L.L. 1983. Elementary gravity and magnetics for geologists and seismologists. Monograph Series 1. 4th ed. Tulsa, OK: Society of Exploration Geophysicists.
- Patra, Mallick. 1980. Geosounding principles II. NY: Elsevier Publishing.
- Romero, J.C. 1976. Report on the ground-water resources of the bedrock aquifer of the Denver Basin, Colorado. Denver, CO: Colorado Department of Natural Resources.

Sheriff, R. E. 1973. Encyclopedic dictionary of exploration geophysics. 2nd ed. Tulsa, OK: Society of Exploration Geophysics.

Stoyer, C.H.. 1987. Resixp users manual. Golden, CO: Interpex Limited.

Talwani, M., J.L. Worzel, M. Landisman. 1959. Rapid gravity computations for two-dimensional bodies with application to the Mandocino Submarine Fracture Zone. Journal of Geophysical Research, 64.

Zohdy, A.A.R., G.P. Eaton, D.R. Mabey. 1974. Techniques of water-resources investigation of the United States Geological Survey: Application of surface geophysics to ground-water investigations. Book 2. Chapter D1. Denver, CO: United States Government Printing Office.

APPENDIX

DC Resistivity Data and Sounding Curves

DATA SET: VES1-1

CLIENT: ROCKY MOUNTAIN ARSENAL	DATE:
LOCATION:	SOUNDING: 1
COUNTY: COMMERCE CITY, COLORADO	AZIMUTH: 0
PROJECT: MS THESIS - NWHITE	EQUIPMENT: USGS
ELEVATION: 5143.30	
SOUNDING COORDINATES: X: 2183679.0000 Y: 199055.0000	

Schlumberger Configuration

FITTING ERROR: 8.218 PERCENT

L #	RESISTIVITY (ohm-m)	THICKNESS (feet)	ELEVATION (feet)	LONG. COND. (Siemens)	TRANS. RES. (Ohm-m ²)
			5143.2		
1	18.66	3.19 *	5140.1	0.0521	18.15
2	4.91	19.80 *	5120.2	1.22	29.65
3	13.57	16.83	5103.4	0.377	69.64
4	2.52				

*" INDICATES FIXED PARAMETER

PARAMETER BOUNDS FROM EQUIVALENCE ANALYSIS

	LAYER	MINIMUM	BEST	MAXIMUM
RHO	1	16.348	18.663	21.199
	2	4.323	4.912	5.678
	3	6.306	13.575	105.827
	4	2.131	2.528	2.933
THICK	1	3.191	3.191	3.191
	2	19.809	19.809	19.809
	3	1.913	16.831	41.811
DEPTH	1	3.191	3.191	3.191
	2	23.000	23.000	23.000
	3	24.913	39.831	64.811

No.	SPACING (ft)	RHO-A (ohm-m)		DIFFERENCE (percent)
		DATA	SYNTHETIC	
1	3.00	19.78	17.13	13.38
2	4.00	15.00	15.72	-4.84

----- VES1-1

----- PAGE 2

No.	SPACING (ft)	RHO-A (ohm-m)		DIFFERENCE (percent)
		DATA	SYNTHETIC	
3	6.00	10.71	12.56	-17.31
4	8.00	9.45	9.93	-5.10
5	10.00	8.85	8.14	7.98
6	14.00	7.53	6.37	15.29
7	20.00	5.43	5.68	-4.63
8	30.00	5.21	5.71	-9.75
9	40.00	5.80	5.94	-2.57
10	60.00	6.03	6.09	-1.05
11	80.00	6.06	5.78	4.48
12	100.0	5.32	5.28	0.602
13	140.0	4.22	4.30	-2.05
14	200.0	3.38	3.39	-0.377
15	300.0	2.87	2.83	1.25
16	400.0	2.63	2.67	-1.65

PARAMETER RESOLUTION MATRIX:

"F" INDICATES FIXED PARAMETER

P 1	0.99							
P 2	0.00	0.99						
P 3	-0.01	0.02	0.59					
P 4	0.00	0.00	-0.01	0.98				
F 1	0.00	0.00	0.00	0.00	0.00			
F 2	0.00	0.00	0.00	0.00	0.00	0.00		
T 3	0.00	-0.02	0.44	0.03	0.00	0.00	0.48	
	P 1	P 2	P 3	P 4	F 1	F 2	T 3	

----- VES1-2

----- PAGE 2

No.	SPACING (ft)	RHO-A (ohm-m)		DIFFERENCE (percent)
		DATA	SYNTHETIC	
7	20.00	23.66	24.04	-1.61
8	30.00	19.57	20.18	-3.13
9	40.00	15.65	16.95	-8.36
10	60.00	11.84	12.22	-3.21
11	80.00	9.61	9.09	5.40
12	100.0	7.69	7.12	7.36
13	140.0	5.29	5.24	0.763
14	200.0	4.63	4.43	4.19
15	300.0	4.03	4.15	-3.06
16	400.0	3.28	4.08	-24.40
17	600.0	3.78	4.03	-6.72

PARAMETER RESOLUTION MATRIX:

"F" INDICATES FIXED PARAMETER

P 1	1.00					
P 2	0.00	1.00				
P 3	0.00	0.00	1.00			
F 1	0.00	0.00	0.00	0.00		
F 2	0.00	0.00	0.00	0.00	0.00	
	P 1	P 2	P 3	F 1	F 2	

----- VES1-3

----- PAGE 2

No.	SPACING (ft)	RHO-A (ohm-m)		DIFFERENCE (percent)
		DATA	SYNTHETIC	
3	4.00	11.88	12.41	-4.53
4	6.00	12.10	11.87	1.87
5	8.00	12.15	12.09	0.429
6	10.00	13.04	12.62	3.22
7	14.00	14.12	14.02	0.638
8	20.00	15.91	16.17	-1.66
9	30.00	18.42	18.56	-0.797
10	40.00	19.43	19.42	0.0505
11	60.00	18.25	18.21	0.178
12	80.00	15.50	15.39	0.675
13	100.0	12.36	12.47	-0.901
14	140.0	8.27	8.17	1.15
15	200.0	5.27	5.28	-0.211
16	300.0	4.04	4.10	-1.55
17	400.0	3.86	3.87	-0.468
18	600.0	3.84	3.77	1.76

PARAMETER RESOLUTION MATRIX:

"F" INDICATES FIXED PARAMETER

P 1 0.71

P 2 -0.01 0.97

P 3 0.01 -0.01 0.75

P 4 0.00 0.00 -0.01 0.99

T 1 0.31 0.07 0.01 0.00 0.44

T 2 -0.04 -0.06 -0.19 0.00 0.16 0.71

T 3 -0.01 0.02 0.28 0.02 -0.02 0.23 0.66

P 1 P 2 P 3 P 4 T 1 T 2 T 3

DATA SET: VES1-4

CLIENT: ROCKY MOUNTAIN ARSENAL	DATE:
LOCATION:	SOUNDING: 4
COUNTY: COMMERCE CITY, COLORADO	AZIMUTH: 90
PROJECT: MS THESIS - NWHITE	EQUIPMENT: USGS
ELEVATION: 5134.00	
SOUNDING COORDINATES: X: 2184759.0000 Y: 199064.0000	

Schlumberger Configuration

FITTING ERROR: 3.652 PERCENT

L #	RESISTIVITY (ohm-m)	THICKNESS (feet)	ELEVATION (feet)	LONG. COND. (Siemens)	TRANS. RES. (Ohm-m ²)
			5134.0		
1	13.34 *	5.73	5128.2	0.131	23.33
2	5.03 *	7.16	5121.0	0.434	10.98
3	13.65 *	26.41	5094.6	0.589	109.9
4	3.08 *	153.9	4940.6	15.22	144.7
5	5.52				

"*" INDICATES FIXED PARAMETER

PARAMETER BOUNDS FROM EQUIVALENCE ANALYSIS

LAYER	MINIMUM	BEST	MAXIMUM
RHO	1	13.312	13.345
	2	5.031	5.031
	3	32.755	13.659
	4	3.000	3.084
	5	3.935	5.528
THICK	1	5.347	5.737
	2	8.669	7.164
	3	9.392	26.414
	4	81.454	153.994
DEPTH	1	5.347	5.737
	2	14.369	12.901
	3	24.156	39.315
	4	106.419	193.309

No.	SPACING	RHO-A (ohm-m)	DIFFERENCE
-----	---------	---------------	------------

----- VES1-4

----- PAGE 2

	(ft)	DATA	SYNTHETIC	(percent)
1	3.00	12.16	13.17	-8.31
2	4.00	13.37	12.96	3.00
3	6.00	12.54	12.32	1.74
4	8.00	12.04	11.47	4.66
5	10.00	11.01	10.61	3.58
6	14.00	8.86	9.26	-4.62
7	20.00	8.32	8.42	-1.29
8	30.00	8.48	8.53	-0.591
9	40.00	9.14	8.82	3.47
10	60.00	8.77	8.60	1.82
11	80.00	7.85	7.75	1.18
12	100.0	6.65	6.78	-2.07
13	140.0	5.01	5.27	-5.23
14	200.0	4.03	4.20	-4.46
15	300.0	3.97	3.91	1.50
16	400.0	4.01	4.06	-1.47

PARAMETER RESOLUTION MATRIX:
 "F" INDICATES FIXED PARAMETER

F 1	0.00									
F 2	0.00	0.00								
F 3	0.00	0.00	0.00							
F 4	0.00	0.00	0.00	0.00						
P 5	0.00	0.00	0.00	0.00	0.94					
T 1	0.00	0.00	0.00	0.00	0.00	1.00				
T 2	0.00	0.00	0.00	0.00	0.00	0.00	1.00			
T 3	0.00	0.00	0.00	0.00	0.00	0.00	0.00	1.00		
T 4	0.00	0.00	0.00	0.00	-0.08	0.00	0.00	0.00	0.88	
	F 1	F 2	F 3	F 4	P 5	T 1	T 2	T 3	T 4	

----- VES1-5 -----

----- PAGE 2 -----

PARAMETER RESOLUTION MATRIX:

"F" INDICATES FIXED PARAMETER

P 1 0.98

P 2 -0.01 0.95

P 3 0.01 0.06 0.47

P 4 0.00 0.00 0.00 0.99

T 1 0.03 0.06 -0.06 0.00 0.87

T 2 -0.02 -0.11 0.12 0.02 0.12 0.59

T 3 0.00 0.04 0.42 0.00 -0.04 0.19 0.40

P 1 P 2 P 3 P 4 T 1 T 2 T 3

----- VES1-6

----- PAGE 2

No.	SPACING (ft)	RHO-A (ohm-m)		DIFFERENCE (percent)
		DATA	SYNTHETIC	
3	4.00	23.32	22.48	3.59
4	6.00	23.48	21.74	7.38
5	8.00	20.87	20.74	0.596
6	10.00	19.42	19.67	-1.33
7	14.00	18.24	17.94	1.62
8	20.00	16.21	16.84	-3.88
9	30.00	16.53	16.90	-2.26
10	40.00	17.19	16.77	2.41
11	60.00	14.43	14.50	-0.499
12	80.00	11.58	11.39	1.63
13	100.0	9.10	8.72	4.11
14	140.0	5.40	5.48	-1.64
15	200.0	3.49	3.78	-8.33
16	300.0	3.18	3.23	-1.58
17	400.0	3.15	3.12	0.664
18	600.0	3.30	3.07	6.83

PARAMETER RESOLUTION MATRIX:

"F" INDICATES FIXED PARAMETER

P 1	0.99							
P 2	0.00	0.61						
P 3	0.00	0.12	0.57					
P 4	0.00	0.00	-0.01	0.99				
T 1	0.02	0.16	-0.05	0.00	0.76			
T 2	0.00	-0.40	-0.07	0.01	0.14	0.37		
T 3	0.00	-0.07	0.45	0.01	0.07	0.15	0.50	
	P 1	P 2	P 3	P 4	T 1	T 2	T 3	

----- VES2-1

----- PAGE 2

No.	SPACING (ft)	RHO-A (ohm-m)		DIFFERENCE (percent)
		DATA	SYNTHETIC	
7	20.00	4.48	4.58	-2.30
8	30.00	4.79	4.73	1.14
9	40.00	4.77	4.76	0.190
10	60.00	4.61	4.64	-0.767
11	80.00	4.49	4.41	1.58
12	100.0	4.14	4.15	-0.287
13	140.0	3.57	3.64	-2.22
14	200.0	2.51	3.13	-24.99
15	300.0	2.73	2.75	-1.05

PARAMETER RESOLUTION MATRIX:

"F" INDICATES FIXED PARAMETER

P 1	1.00				
P 2	0.00	1.00			
P 3	0.00	0.00	1.00		
T 1	0.00	0.00	0.00	0.97	
T 2	0.00	0.00	0.00	0.01	0.98
	P 1	P 2	P 3	T 1	T 2

----- VES2-2 -----

----- PAGE 2 -----

No.	SPACING (ft)	RHO-A (ohm-m)		DIFFERENCE (percent)
		DATA	SYNTHETIC	
3	8.00	3.62	3.65	-0.923
4	10.00	3.80	3.81	-0.523
5	14.00	4.21	4.08	3.02
6	20.00	4.30	4.28	0.421
7	30.00	4.12	4.26	-3.51
8	40.00	4.03	4.03	-0.0452
9	60.00	3.49	3.43	1.62
10	80.00	3.04	2.96	2.52
11	100.0	2.69	2.66	0.928
12	140.0	2.16	2.39	-10.73
13	200.0	2.26	2.31	-2.58
14	300.0	2.53	2.46	2.50
15	400.0	3.00	2.74	8.65
16	600.0	3.20	3.38	-5.80

PARAMETER RESOLUTION MATRIX:

"F" INDICATES FIXED PARAMETER

P 1	0.98						
P 2	0.00	0.96					
P 3	0.00	-0.02	0.92				
P 4	0.00	0.01	-0.02	0.81			
T 1	-0.07	-0.09	-0.01	0.01	0.46		
T 2	0.01	0.08	0.11	-0.01	0.21	0.72	
T 3	0.00	-0.02	-0.16	-0.24	-0.01	0.17	0.40
	P 1	P 2	P 3	P 4	T 1	T 2	T 3

----- VES2-3

----- PAGE 2

No.	SPACING (ft)	RHO-A (ohm-m)		DIFFERENCE (percent)
		DATA	SYNTHETIC	
7	30.00	10.35	11.59	-12.05
8	40.00	6.60	6.44	2.30
9	60.00	3.71	3.47	6.44
10	80.00	3.33	2.98	10.30
11	100.0	3.13	2.87	8.08
12	140.0	2.63	2.81	-7.03
13	200.0	2.65	2.79	-5.38
14	300.0	2.49	2.79	-12.43
15	400.0	2.73	2.83	-3.77
16	600.0	3.08	2.96	3.74

PARAMETER RESOLUTION MATRIX:

"F" INDICATES FIXED PARAMETER

P 1	1.00				
P 2	0.00	1.00			
P 3	0.00	0.00	0.13		
T 1	0.00	0.00	0.00	1.00	
T 2	0.00	0.00	-0.31	0.00	0.76
	P 1	P 2	P 3	T 1	T 2

DATA SET: VES2-4

CLIENT: ROCKY MOUNTAIN ARSENAL	DATE:
LOCATION:	SOUNDING: 4
COUNTY: COMMERCE CITY, COLORADO	AZIMUTH: 90
PROJECT: MS THESIS - NWHITE	EQUIPMENT: USGS
ELEVATION: 5134.80	
SOUNDING COORDINATES: X: 2184653.0000 Y: 197985.0000	

Schlumberger Configuration

FITTING ERROR: 5.929 PERCENT

L #	RESISTIVITY (ohm-m)	THICKNESS (feet)	ELEVATION (feet)	LONG. COND. (Siemens)	TRANS. RES. (Ohm-m ²)
			5134.7		
1	53.69	10.81	5123.9	0.0613	176.9
2	419.9	6.00	5117.9	0.00436	768.0
3	2.81	309.9	4808.0	33.49	266.3
4	4.13				

ALL PARAMETERS ARE FREE

PARAMETER BOUNDS FROM EQUIVALENCE ANALYSIS

LAYER	MINIMUM	BEST	MAXIMUM
RHO	1	49.399	57.698
	2	156.854	4737.058
	3	2.468	3.250
	4	2.786	24.862
THICK	1	8.848	13.047
	2	0.517	16.298
	3	139.451	8596.806
DEPTH	1	8.848	13.047
	2	12.697	26.563
	3	156.359	8613.228

No.	SPACING (ft)	RHO-A (ohm-m)		DIFFERENCE (percent)
		DATA	SYNTHETIC	
1	3.00	51.53	53.86	-4.52
2	4.00	59.19	54.09	8.61

----- VES2-4 -----

----- PAGE 2 -----

No.	SPACING (ft)	RHO-A (ohm-m)		DIFFERENCE (percent)
		DATA	SYNTHETIC	
3	6.00	55.85	54.96	1.57
4	8.00	53.62	56.45	-5.29
5	10.00	56.27	58.51	-3.99
6	14.00	61.89	63.74	-2.99
7	20.00	75.83	71.62	5.53
8	30.00	80.57	78.19	2.95
9	40.00	79.30	75.90	4.28
10	60.00	56.00	58.56	-4.58
11	80.00	37.67	39.48	-4.81
12	100.0	24.77	25.09	-1.29
13	140.0	9.87	10.12	-2.58
14	200.0	4.70	4.15	11.60
15	300.0	2.98	3.07	-3.13
16	400.0	2.76	3.06	-10.90
17	600.0	3.40	3.21	5.35

PARAMETER RESOLUTION MATRIX:

"F" INDICATES FIXED PARAMETER

P 1	1.00							
P 2	0.00	0.51						
P 3	0.00	0.00	1.00					
P 4	0.00	0.00	0.00	0.77				
T 1	0.00	-0.02	0.00	0.00	0.99			
T 2	0.00	0.50	0.00	0.00	0.03	0.49		
T 3	0.00	-0.01	-0.02	-0.37	0.00	0.01	0.23	
	P 1	P 2	P 3	P 4	T 1	T 2	T 3	

----- VES2-5 ----- PAGE 1

DATA SET: VES2-5

CLIENT: ROCKY MOUNTAIN ARSENAL	DATE:
LOCATION:	SOUNDING: 5
COUNTY: COMMERCE CITY, COLORADO	AZIMUTH: 90
PROJECT: MS THESIS - NWHITE	EQUIPMENT: USGS
ELEVATION: 5141.40	
SOUNDING COORDINATES: X: 2185012.0000 Y: 197999.0000	

Schlumberger Configuration

FITTING ERROR: 7.724 PERCENT

L #	RESISTIVITY (ohm-m)	THICKNESS (feet)	ELEVATION (feet)	LONG. COND. (Siemens)	TRANS. RES. (Ohm-m ²)
			5141.3		
1	30.65	1.28	5140.1	0.0127	11.97
2	54.96	35.12	5104.9	0.194	588.4
3	2.42	408.2	4696.7	51.38	301.3
4	5.99				

ALL PARAMETERS ARE FREE

PARAMETER BOUNDS FROM EQUIVALENCE ANALYSIS

LAYER		MINIMUM	BEST	MAXIMUM
RHO	1	12.535	30.654	42.408
	2	49.762	54.964	62.269
	3	1.936	2.422	2.888
	4	2.135	5.998	44.027
THICK	1	0.318	1.282	3.003
	2	30.880	35.123	38.769
	3	194.213	408.248	1480.386
DEPTH	1	0.318	1.282	3.003
	2	32.861	36.405	39.687
	3	231.504	444.653	1515.311

No.	SPACING (ft)	RHO-A (ohm-m)		DIFFERENCE (percent)
		DATA	SYNTHETIC	
1	3.00	37.42	38.91	-3.99
2	4.00	40.11	42.23	-5.28

----- VES2-5

----- PAGE 2

No.	SPACING (ft)	RHO-A (ohm-m)		DIFFERENCE (percent)
		DATA	SYNTHETIC	
3	6.00	47.71	46.60	2.31
4	8.00	51.45	49.08	4.60
5	10.00	52.74	50.54	4.16
6	14.00	55.80	51.91	6.96
7	20.00	56.86	52.05	8.44
8	30.00	51.10	49.71	2.70
9	40.00	43.93	45.37	-3.28
10	60.00	28.33	34.05	-20.21
11	80.00	21.33	23.33	-9.40
12	100.0	15.83	15.35	3.02
13	140.0	7.17	6.91	3.59
14	200.0	3.78	3.38	10.54
15	300.0	2.49	2.66	-7.18
16	400.0	2.47	2.67	-8.34
17	600.0	3.06	2.90	5.00

PARAMETER RESOLUTION MATRIX:

"F" INDICATES FIXED PARAMETER

P 1	0.81						
P 2	0.01	0.98					
P 3	0.00	-0.01	0.96				
P 4	0.00	0.01	0.04	0.12			
T 1	-0.30	-0.03	-0.01	0.01	0.22		
T 2	0.01	0.01	0.01	-0.01	0.05	0.98	
T 3	0.00	-0.01	-0.09	-0.20	-0.02	0.02	0.33
	P 1	P 2	P 3	P 4	T 1	T 2	T 3

----- VES2-6 -----

----- PAGE 2 -----

No.	SPACING (ft)	RHO-A (ohm-m)		DIFFERENCE (percent)
		DATA	SYNTHETIC	
3	6.00	31.93	31.33	1.85
4	8.00	31.13	29.42	5.48
5	10.00	28.32	27.32	3.51
6	14.00	23.83	23.52	1.30
7	20.00	18.49	19.74	-6.77
8	30.00	16.33	16.85	-3.22
9	40.00	15.29	15.48	-1.29
10	60.00	13.92	13.44	3.44
11	80.00	13.65	11.34	16.89
12	100.0	9.50	9.30	2.07
13	140.0	6.28	6.06	3.35
14	200.0	3.33	3.56	-6.98
15	300.0	2.39	2.48	-3.85
16	400.0	2.46	2.44	0.480
17	600.0	2.84	2.83	0.151

PARAMETER RESOLUTION MATRIX:

"F" INDICATES FIXED PARAMETER

P 1	0.98							
P 2	-0.01	0.98						
P 3	0.00	-0.01	0.93					
P 4	0.00	0.01	0.05	0.18				
T 1	0.03	0.04	0.02	-0.01	0.86			
T 2	0.00	0.02	0.03	-0.03	-0.02	0.97		
T 3	0.00	-0.02	-0.13	-0.26	0.03	0.05	0.40	
	P 1	P 2	P 3	P 4	T 1	T 2	T 3	

----- VES3-1

----- PAGE 1

DATA SET: VES3-1

CLIENT: ROCKY MOUNTAIN ARSENAL	DATE:
LOCATION:	SOUNDING: 1
COUNTY: COMMERCE CITY, COLORADO	AZIMUTH: 0
PROJECT: MS THESIS - NWHITE	EQUIPMENT: USGS
ELEVATION: 5133.20	
SOUNDING COORDINATES: X: 2184413.0000 Y: 197977.0000	

Schlumberger Configuration

FITTING ERROR: 4.442 PERCENT

L #	RESISTIVITY (ohm-m)	THICKNESS (feet)	ELEVATION (feet)	LONG. COND. (Siemens)	TRANS. RES. (Ohm-m ²)
			5133.2		
1	44.42	4.23	5128.9	0.0290	57.37
2	62.97	12.03	5116.9	0.0582	230.9
3	2.39	319.7	4797.1	40.64	233.6
4	7.79				

ALL PARAMETERS ARE FREE

No.	SPACING (ft)	RHO-A (ohm-m)		DIFFERENCE (percent)
		DATA	SYNTHETIC	
1	3.00	50.16	44.92	10.42
2	4.00	44.72	45.47	-1.68
3	6.00	46.38	46.92	-1.17
4	8.00	49.43	48.35	2.16
5	10.00	49.17	49.32	-0.317
6	14.00	47.98	49.32	-2.80
7	20.00	41.03	45.20	-10.17
8	30.00	31.10	33.44	-7.53
9	40.00	22.30	22.22	0.327
10	60.00	9.64	9.15	5.07
11	80.00	4.85	4.54	6.33
12	100.0	3.40	3.13	7.68
13	140.0	2.62	2.58	1.14
14	200.0	2.49	2.53	-1.66
15	300.0	2.65	2.63	0.668
16	400.0	2.82	2.82	-0.173
17	600.0	3.35	3.32	0.648

----- VES3-1 -----

----- PAGE 2 -----

PARAMETER RESOLUTION MATRIX:

"F" INDICATES FIXED PARAMETER

P 1	0.98							
P 2	0.02	0.93						
P 3	0.00	-0.01	0.98					
P 4	0.00	0.00	0.01	0.15				
T 1	-0.03	-0.04	-0.01	0.00	0.17			
T 2	-0.01	0.07	0.02	-0.01	0.30	0.84		
T 3	0.00	-0.02	-0.05	-0.29	-0.01	0.03	0.65	
	P 1	P 2	P 3	P 4	T 1	T 2	T 3	

----- VES3-2 -----

----- PAGE 1 -----

DATA SET: VES3-2

CLIENT: ROCKY MOUNTAIN ARSENAL	DATE:
LOCATION:	SOUNDING: 2
COUNTY: COMMERCE CITY, COLORADO	AZIMUTH: 0
PROJECT: MS THESIS - NWHITE	EQUIPMENT: USGS
ELEVATION: 5138.50	
SOUNDING COORDINATES: X: 2184410.0000 Y: 198336.0000	

Schlumberger Configuration

FITTING ERROR: 2.661 PERCENT

L #	RESISTIVITY (ohm-m)	THICKNESS (feet)	ELEVATION (feet)	LONG. COND. (Siemens)	TRANS. RES. (Ohm-m ²)
			5138.5		
1	20.52	6.90	5131.5	0.102	43.16
2	141.5	13.38	5118.2	0.0288	577.3
3	2.26	161.6	4956.6	21.74	111.5
4	4.82				

ALL PARAMETERS ARE FREE

No.	SPACING (ft)	RHO-A (ohm-m)		DIFFERENCE (percent)
		DATA	SYNTHETIC	
1	3.00	20.89	20.82	0.345
2	4.00	21.03	21.21	-0.844
3	6.00	23.28	22.58	2.99
4	8.00	25.05	24.66	1.55
5	10.00	32.54	27.22	16.33
6	14.00	33.04	32.76	0.830
7	20.00	39.84	39.89	-0.124
8	30.00	44.09	46.30	-5.01
9	40.00	46.28	47.07	-1.70
10	60.00	40.49	39.79	1.72
11	80.00	29.87	29.37	1.66
12	100.0	21.71	20.36	6.24
13	140.0	9.59	9.45	1.54
14	200.0	4.02	4.08	-1.62
15	300.0	3.02	3.00	0.497
16	400.0	3.22	3.17	1.27
17	600.0	3.76	3.61	3.91

CURRENT RESOLUTION MATRIX NOT AVAILABLE

----- VES3-3 -----

----- PAGE 1 -----

DATA SET: VES3-3

CLIENT: ROCKY MOUNTAIN ARSENAL	DATE:
LOCATION:	SOUNDING: 3
COUNTY: COMMERCE CITY, COLORADO	AZIMUTH: 0
PROJECT: MS THESIS - NWHITE	EQUIPMENT: USGS
ELEVATION: 5141.10	
SOUNDING COORDINATES: X: 2184407.0000 Y: 198696.0000	

Schlumberger Configuration

FITTING ERROR: 2.749 PERCENT

L #	RESISTIVITY (ohm-m)	THICKNESS (feet)	ELEVATION (feet)	LONG. COND. (Siemens)	TRANS. RES. (Ohm-m ²)
			5141.1		
1	8.24	0.521	5140.5	0.0192	1.31
2	86.89	1.36	5139.2	0.00478	36.11
3	14.97	9.38	5129.8	0.191	42.86
4	36.45	25.35	5104.4	0.212	281.7
5	3.06	380.2	4724.2	37.86	354.6
6	6.90				

ALL PARAMETERS ARE FREE

PARAMETER BOUNDS FROM EQUIVALENCE ANALYSIS

	LAYER	MINIMUM	BEST	MAXIMUM
RHO	1	0.659	8.243	18.009
	2	46.495	86.897	225.544
	3	20.784	14.977	24.349
	4	2.026	36.452	3.282
	5	3.489	3.060	14.499
	6	0.044	6.900	1.114
THICK	1	0.242	0.522	1.879
	2	46.953	1.364	57.768
	3	70.860	9.389	619.786
	4	0.000	25.359	0.000
	5	0.000	380.202	0.000
DEPTH	1	0.044	0.522	1.114
	2	0.722	1.885	2.360
	3	48.157	11.275	59.056

4	128.525	36.634	669.586
5	0.000	416.836	0.000

No.	SPACING (ft)	RHO-A (ohm-m)		DIFFERENCE (percent)
		DATA	SYNTHETIC	
1	2.00	22.57	22.41	0.717
2	3.00	28.20	27.73	1.67
3	4.00	30.25	30.39	-0.475
4	6.00	30.12	31.05	-3.10
5	8.00	29.08	29.07	0.0340
6	10.00	26.32	26.62	-1.16
7	14.00	23.79	23.07	3.02
8	20.00	21.76	21.36	1.86
9	30.00	21.38	21.94	-2.62
10	40.00	21.65	22.38	-3.36
11	60.00	20.14	20.56	-2.07
12	80.00	17.34	16.98	2.03
13	100.0	14.13	13.36	5.44
14	140.0	8.01	8.14	-1.60
15	200.0	4.51	4.75	-5.19
16	300.0	3.68	3.53	3.91
17	400.0	3.39	3.44	-1.71
18	600.0	3.73	3.70	0.762

PARAMETER RESOLUTION MATRIX:
"F" INDICATES FIXED PARAMETER

P 1	0.50									
P 2	0.04	0.50								
P 3	-0.02	0.09	0.72							
P 4	0.01	-0.03	0.08	0.69						
P 5	0.00	0.00	0.01	-0.02	0.96					
P 6	0.00	0.00	-0.01	0.03	0.05	0.17				
T 1	-0.48	-0.06	0.04	-0.02	0.00	0.00	0.47			
T 2	-0.03	0.45	0.10	-0.04	0.00	0.00	0.02	0.42		
T 3	-0.02	0.08	-0.31	-0.14	0.01	-0.01	0.03	0.10	0.40	
T 4	0.00	0.01	-0.03	0.34	0.04	-0.04	0.02	0.03	0.23	0.60
T 5	0.00	0.00	0.02	-0.04	-0.09	-0.23	0.00	0.00	0.02	0.07

0.32

T 5

P 1 P 2 P 3 P 4 P 5 P 6 T 1 T 2 T 3 T 4

----- VES3-4

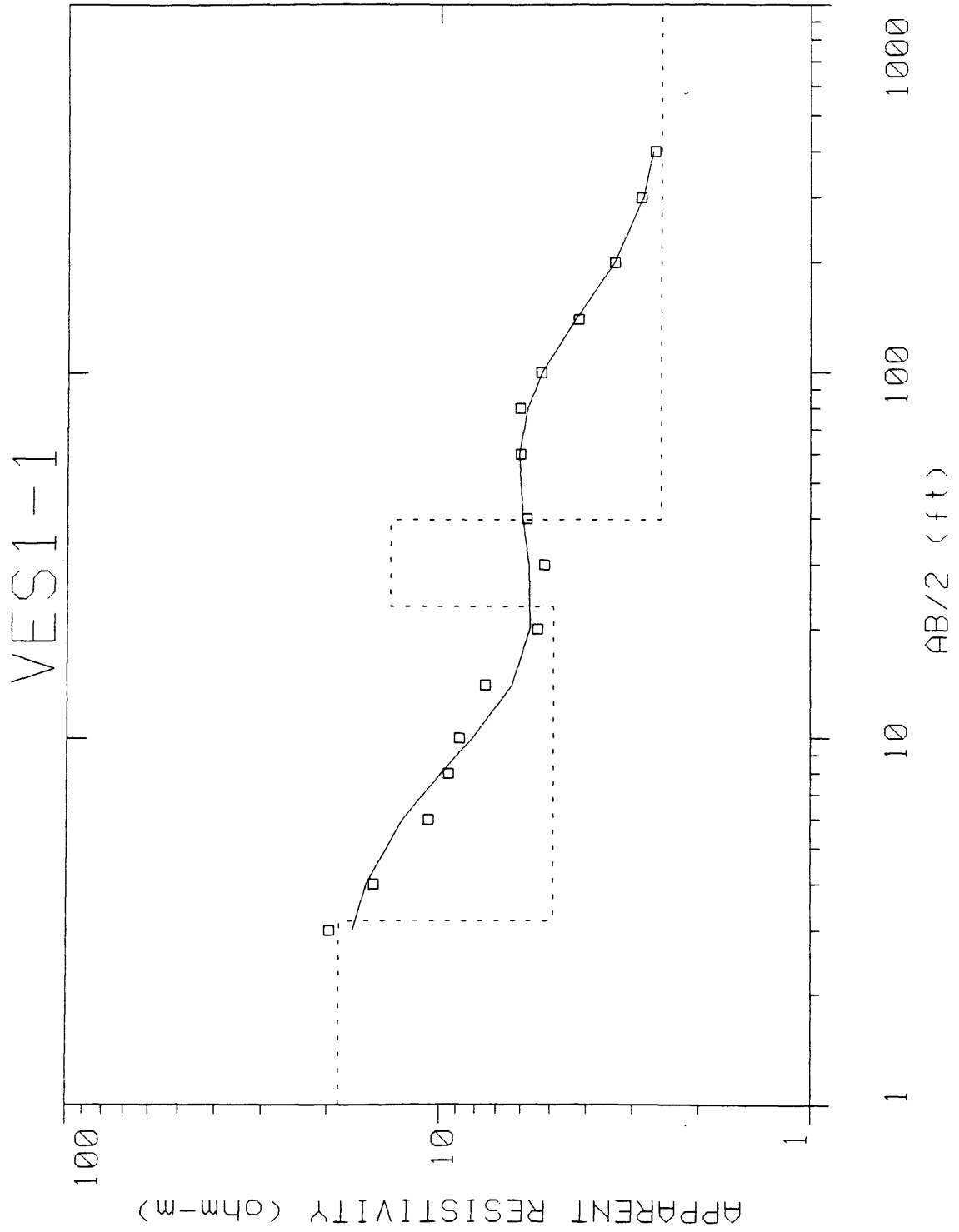
----- PAGE 2

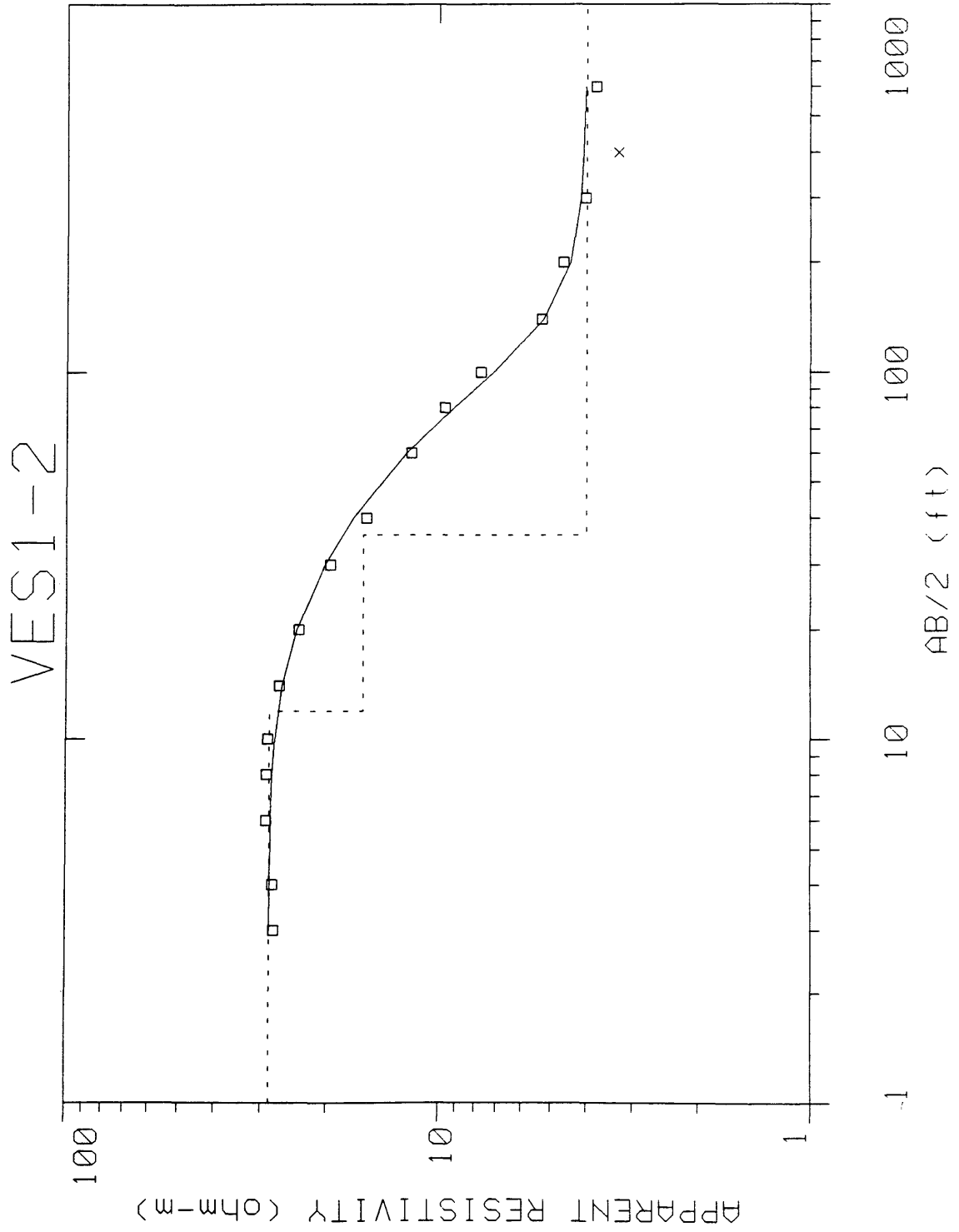
No.	SPACING (ft)	RHO-A (ohm-m)		DIFFERENCE (percent)
		DATA	SYNTHETIC	
3	4.00	11.88	12.47	-4.97
4	6.00	12.10	12.11	-0.0477
5	8.00	12.15	12.33	-1.41
6	10.00	13.04	12.78	1.95
7	14.00	14.12	14.04	0.576
8	20.00	15.91	16.06	-0.925
9	30.00	18.42	18.44	-0.133
10	40.00	19.43	19.35	0.432
11	60.00	18.25	18.21	0.208
12	80.00	15.50	15.41	0.581
13	100.0	12.36	12.49	-1.06
14	140.0	8.27	8.19	0.991
15	200.0	5.27	5.28	-0.330
16	300.0	4.04	4.10	-1.58
17	400.0	3.86	3.88	-0.542
18	600.0	3.84	3.77	1.67

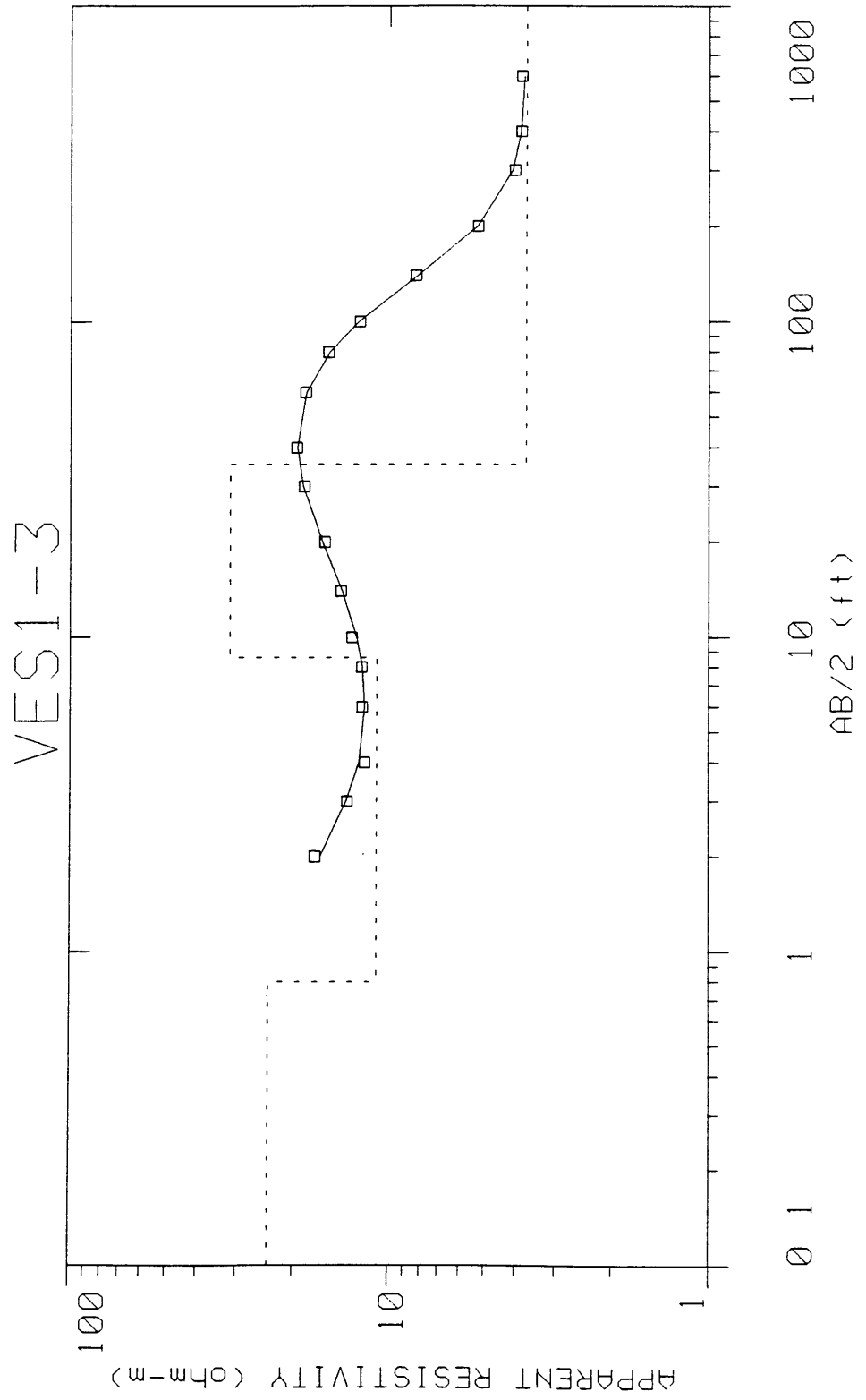
PARAMETER RESOLUTION MATRIX:

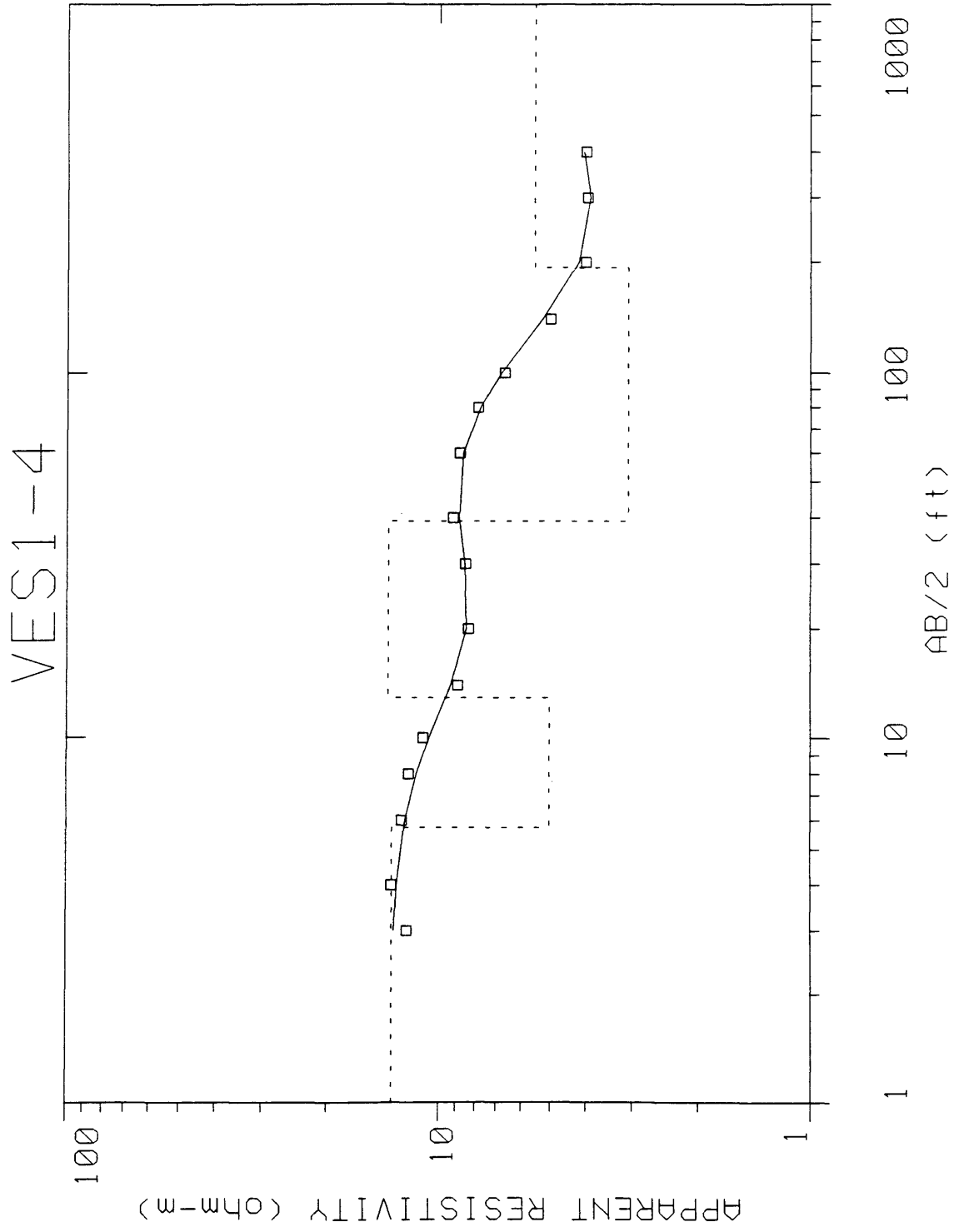
"F" INDICATES FIXED PARAMETER

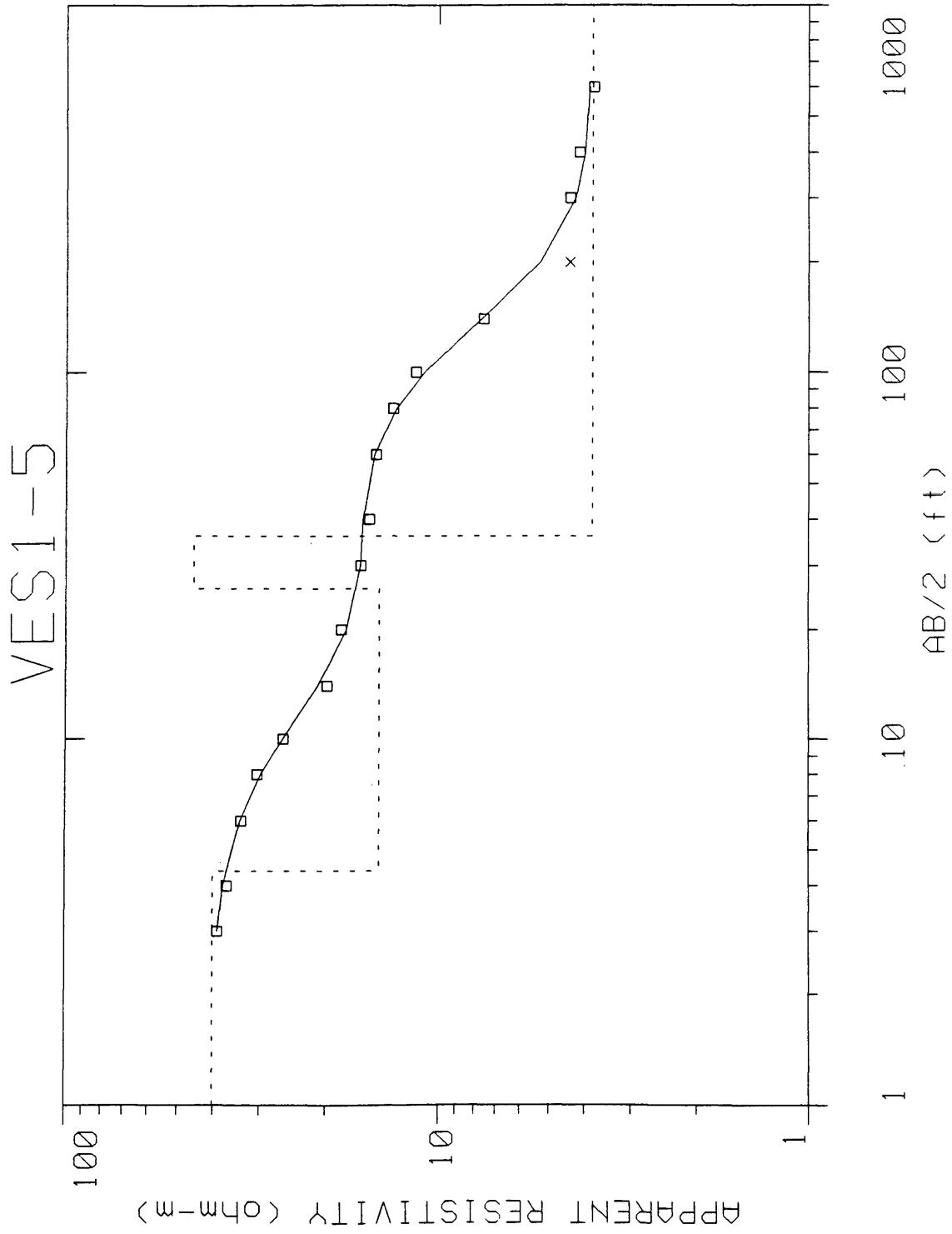
P 1	0.81							
P 2	-0.01	1.00						
P 3	-0.02	0.00	0.96					
P 4	0.00	0.00	0.00	1.00				
T 1	0.10	0.01	0.02	0.00	0.94			
T 2	-0.04	-0.01	-0.04	0.00	0.03	0.95		
T 3	0.03	0.01	0.05	0.00	-0.02	0.05	0.94	
	P 1	P 2	P 3	P 4	T 1	T 2	T 3	

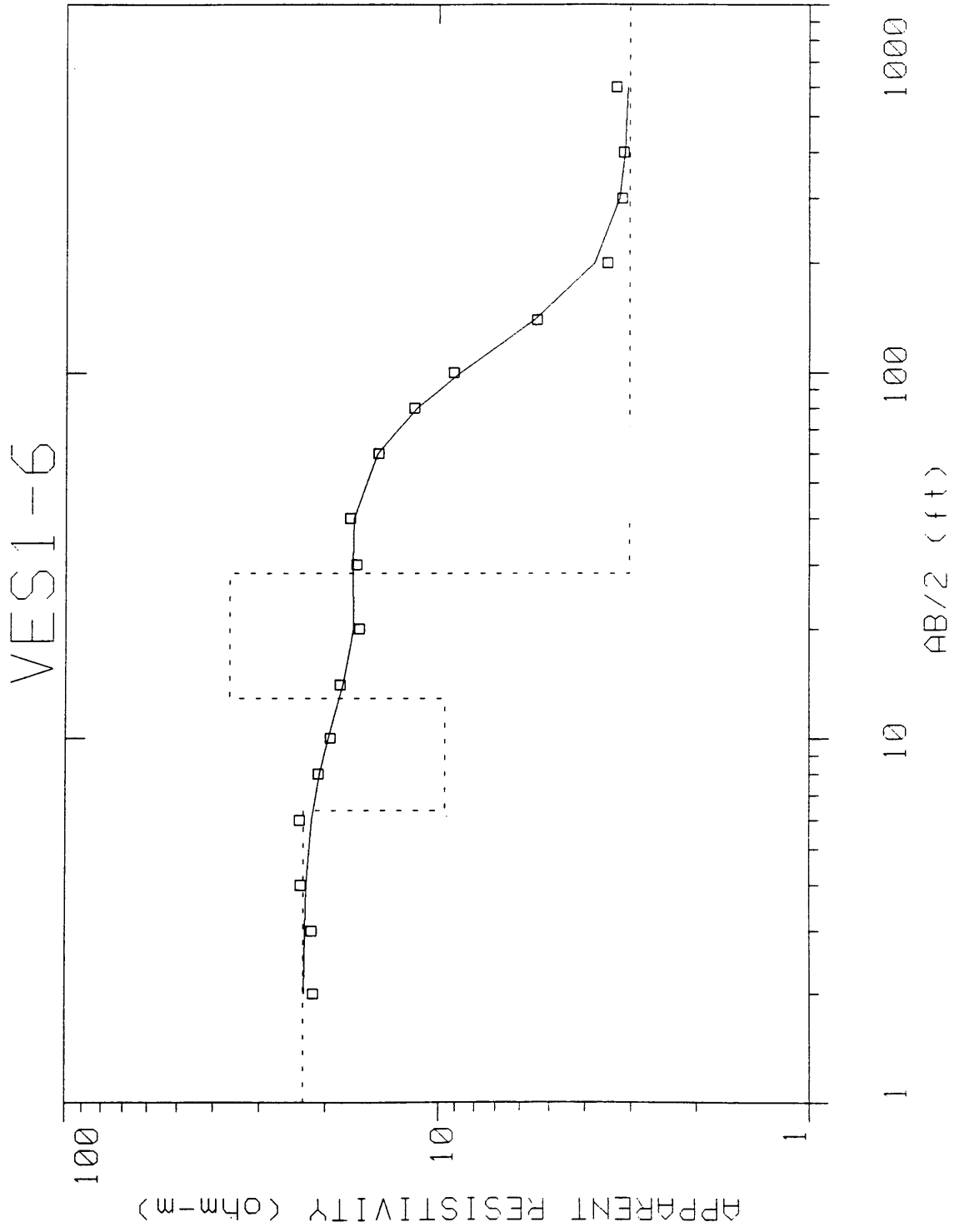


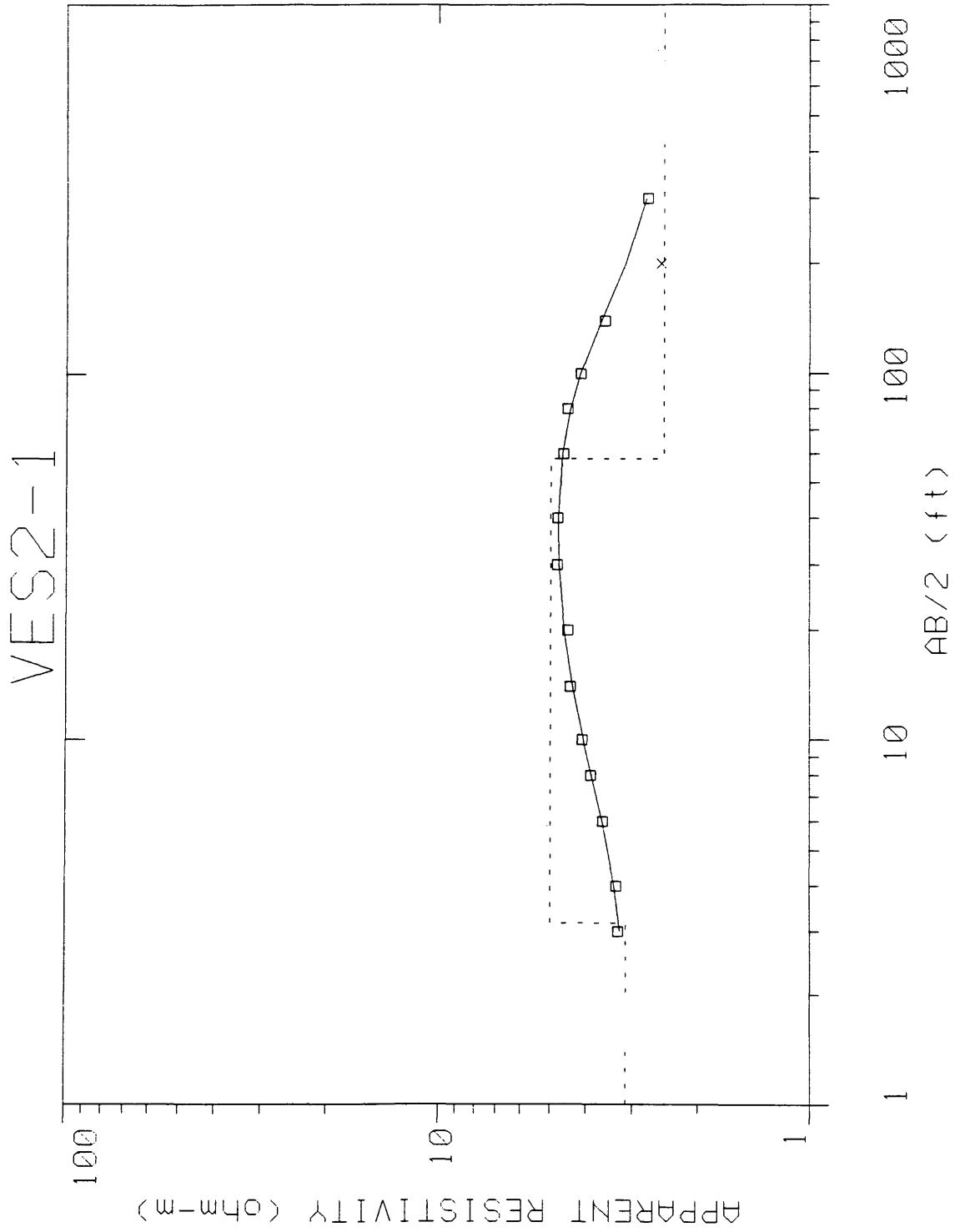


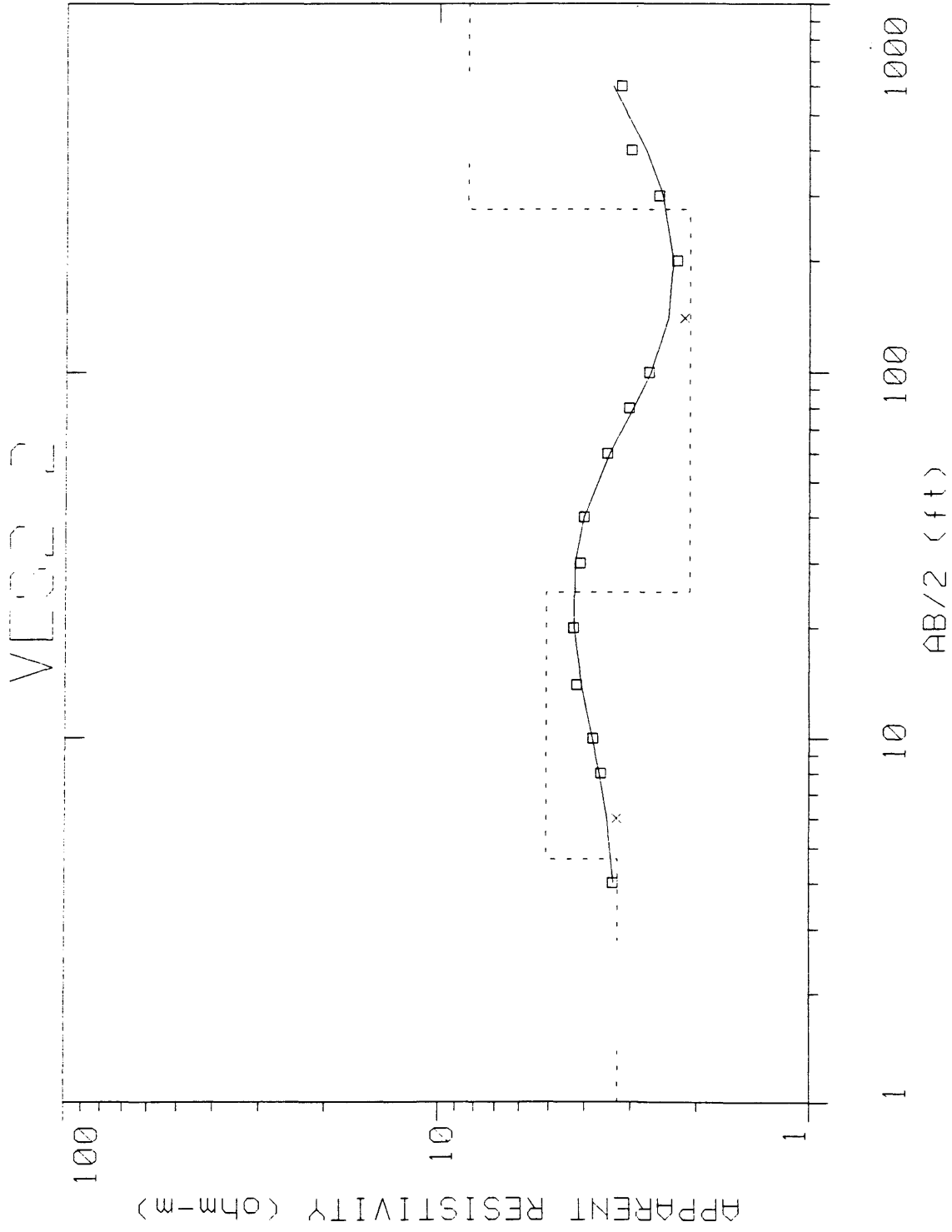


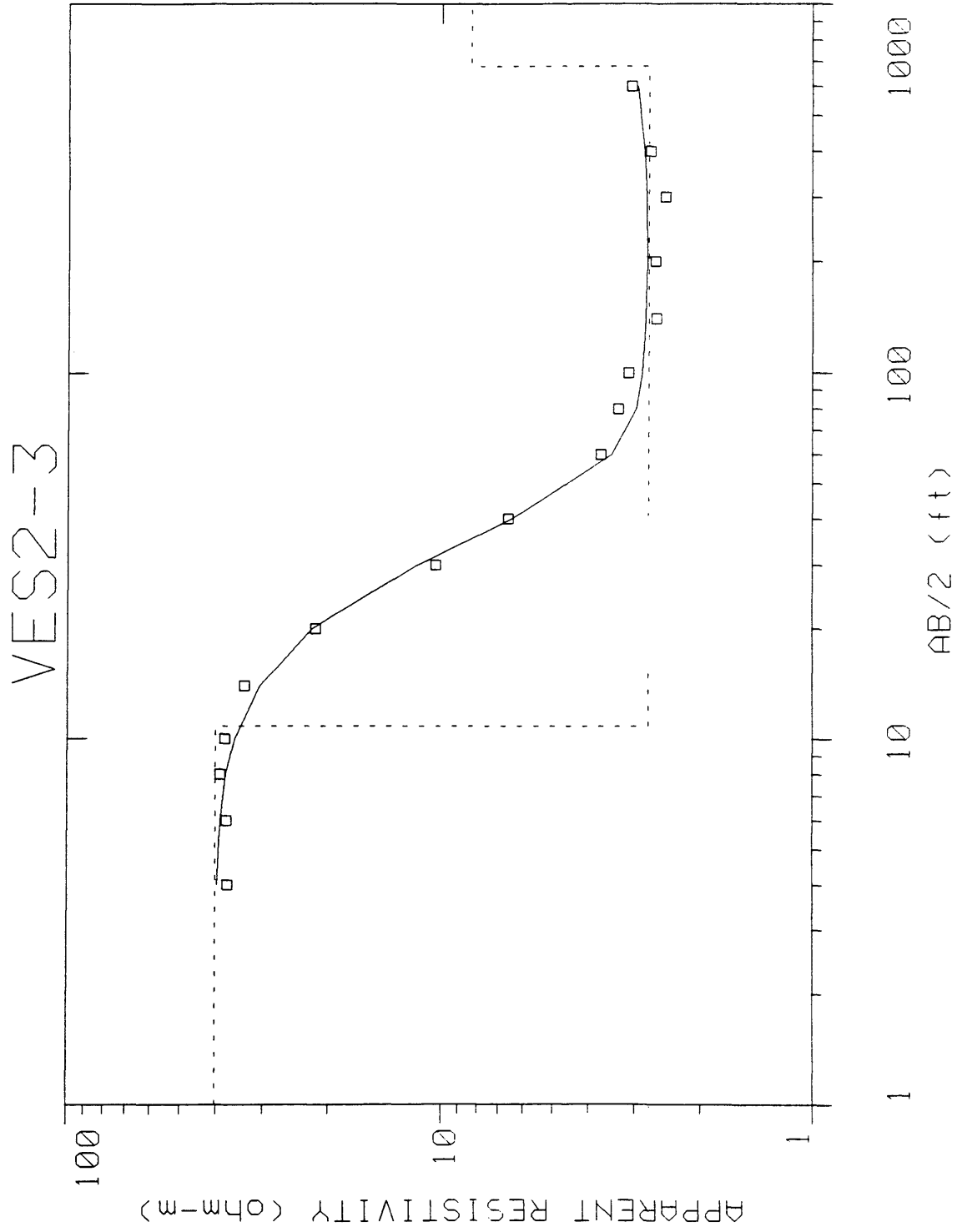


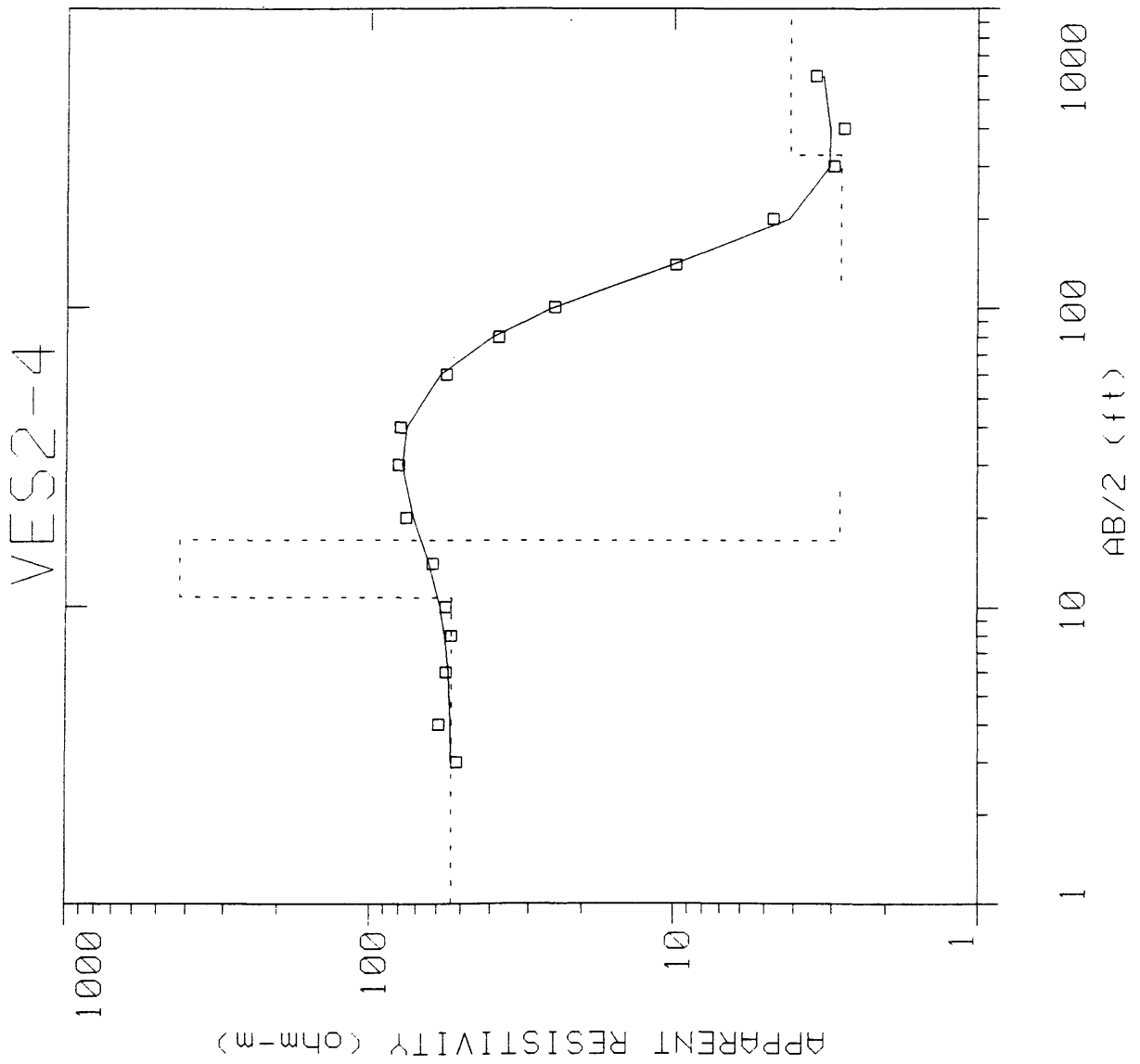


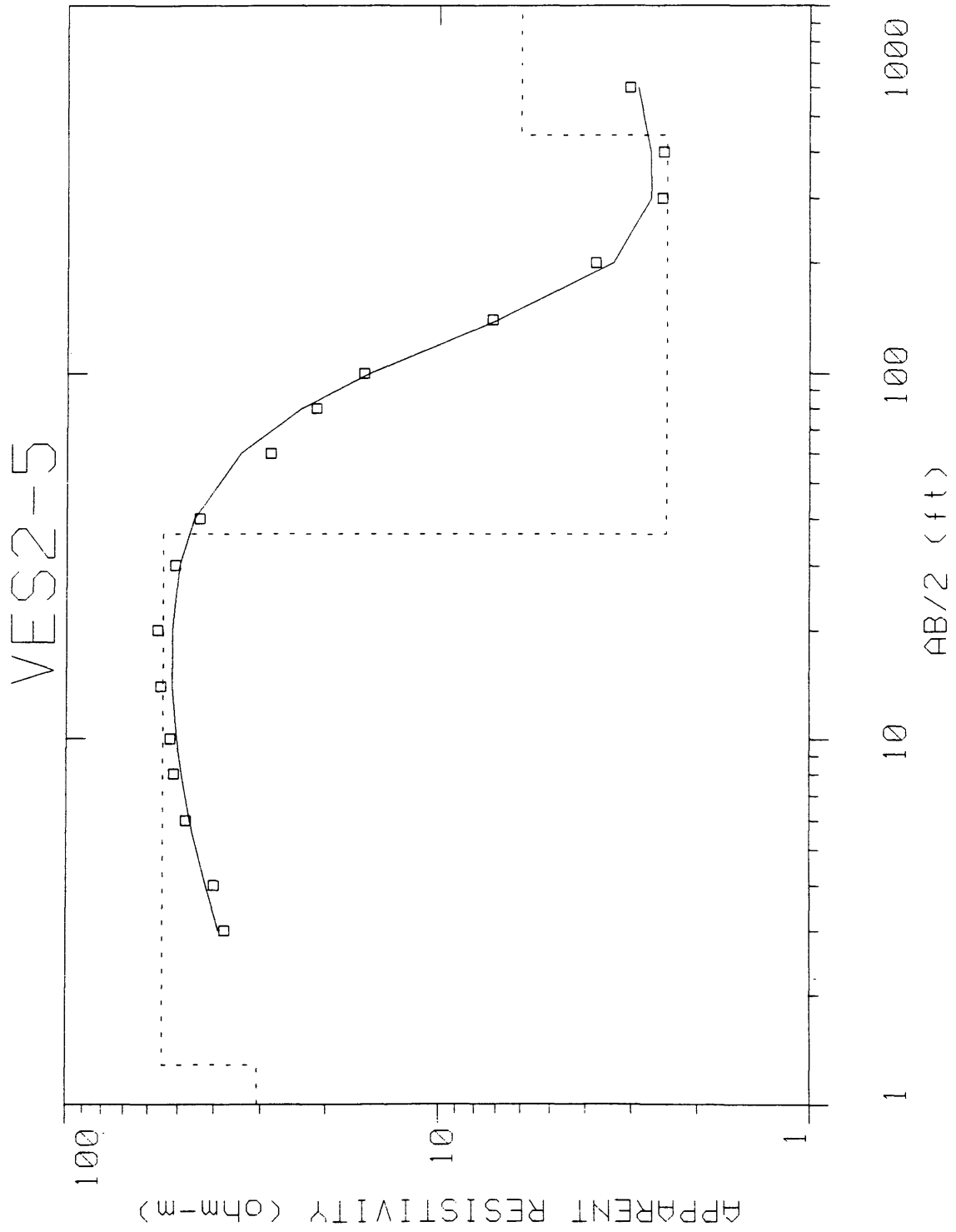


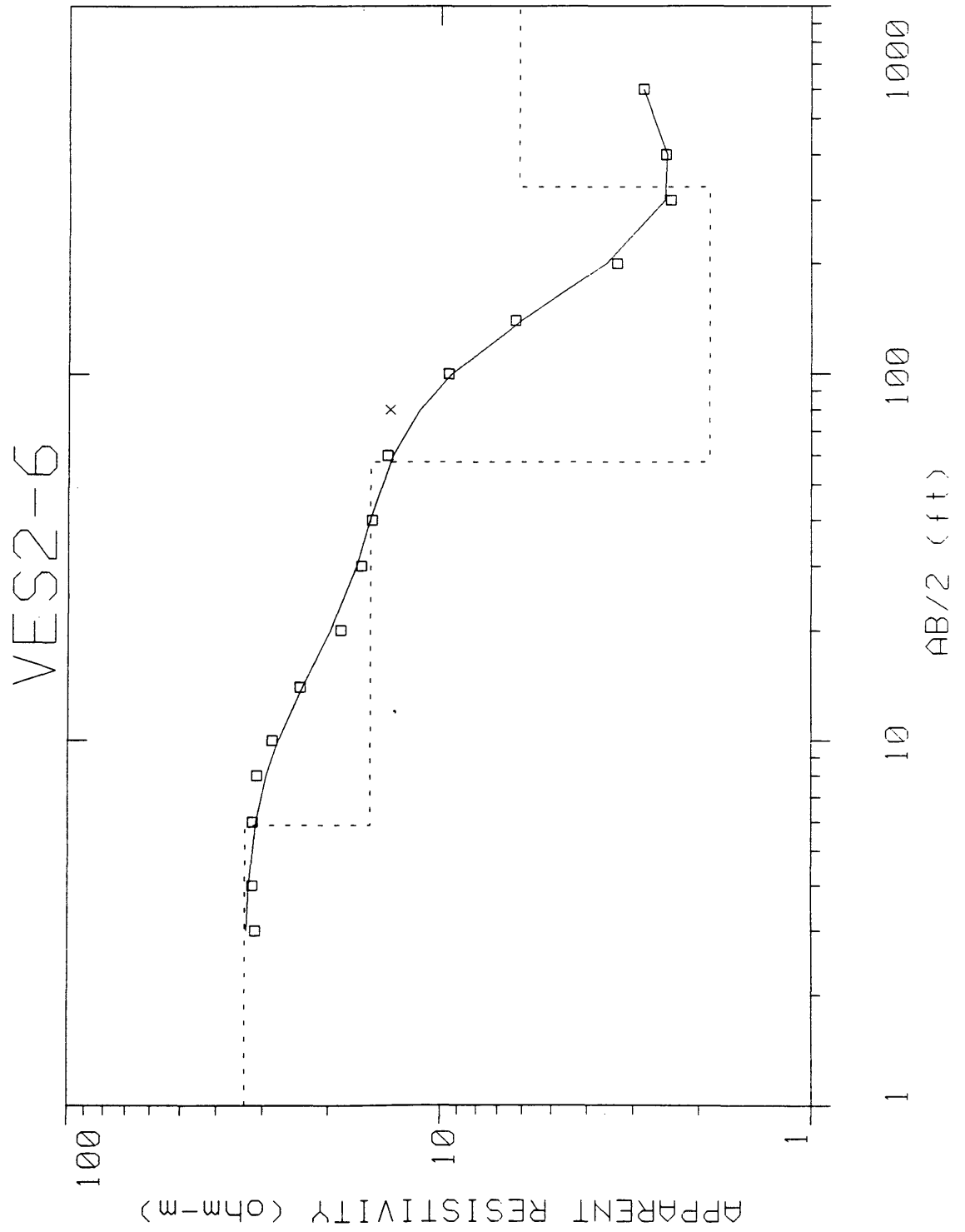


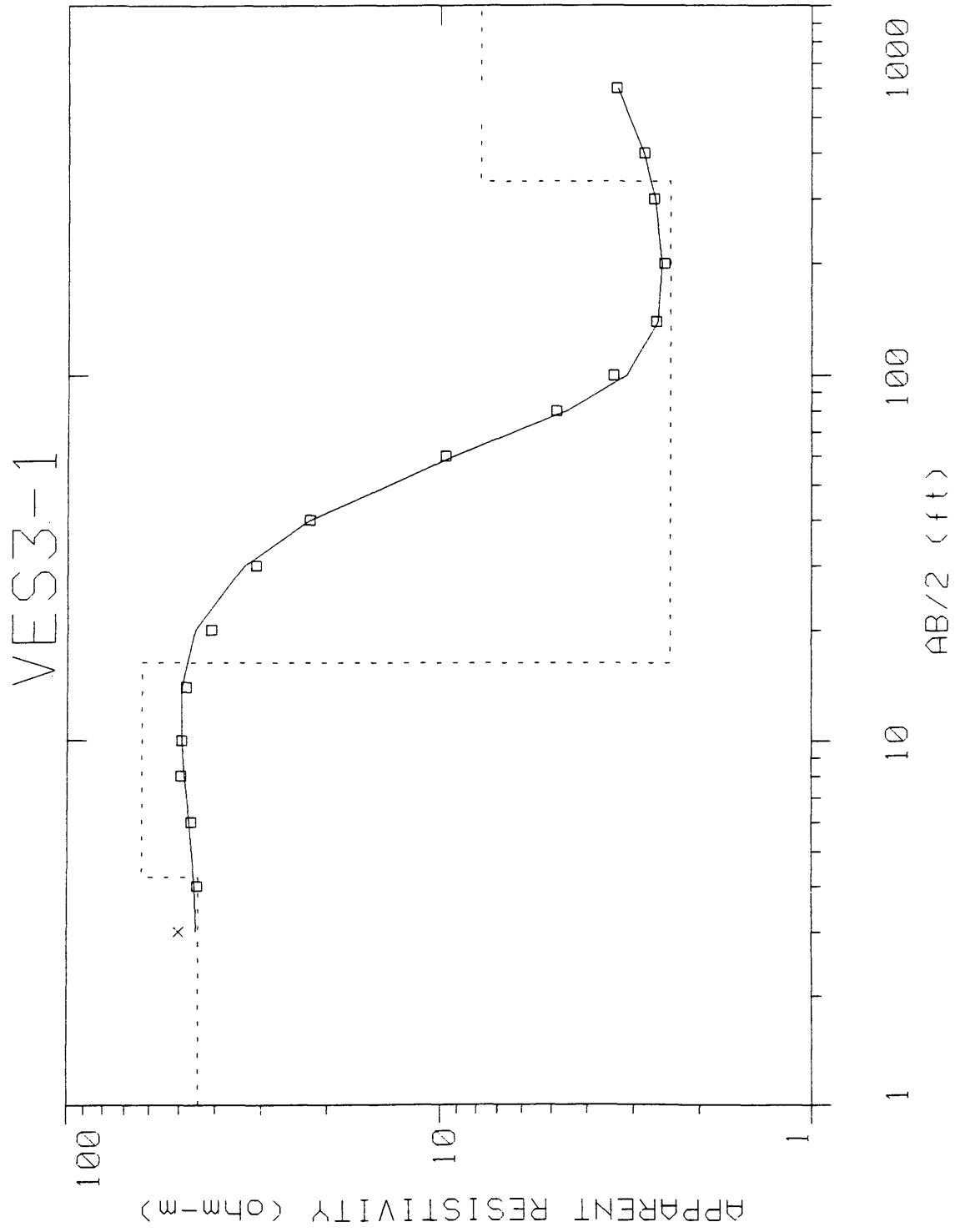


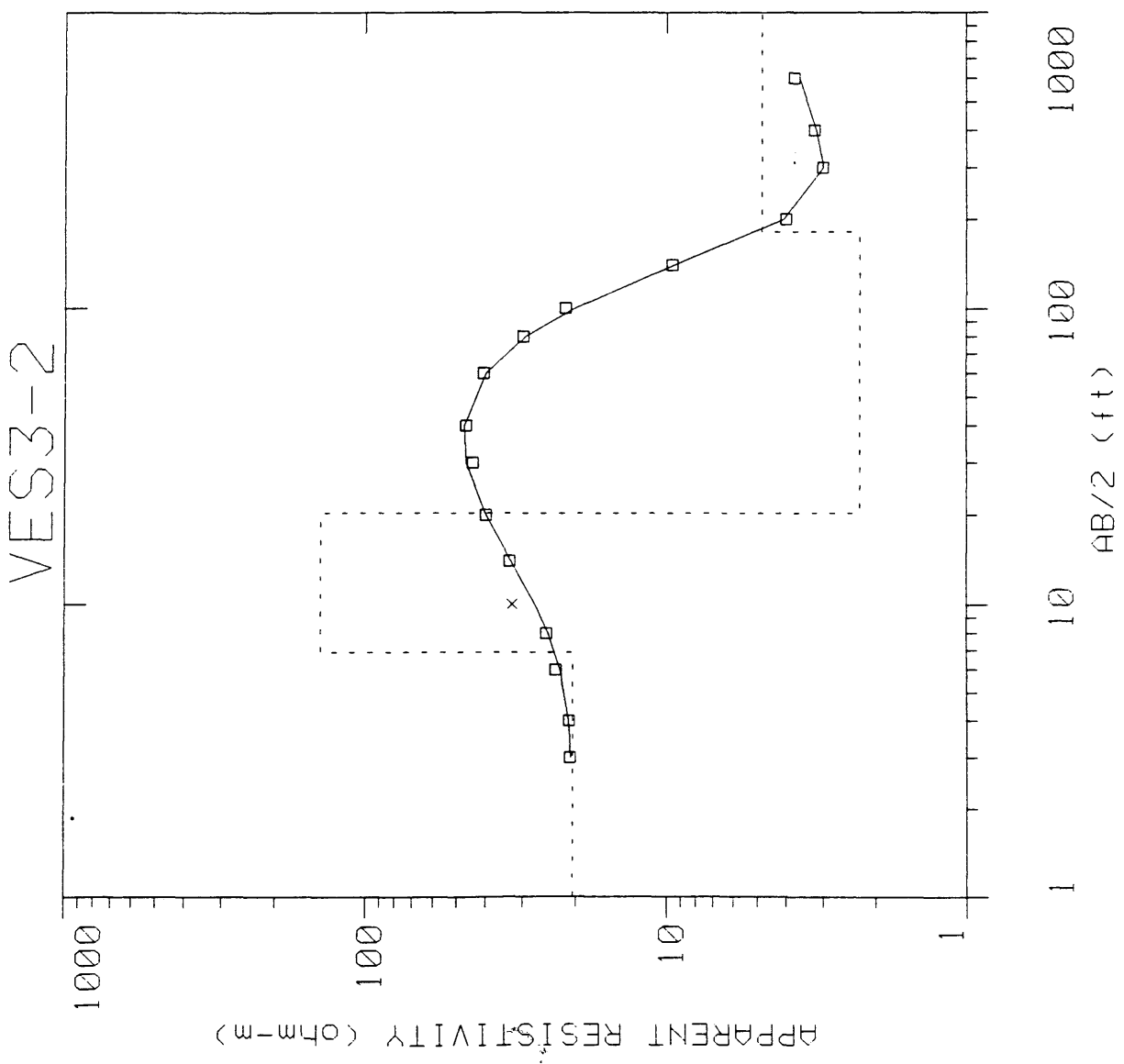


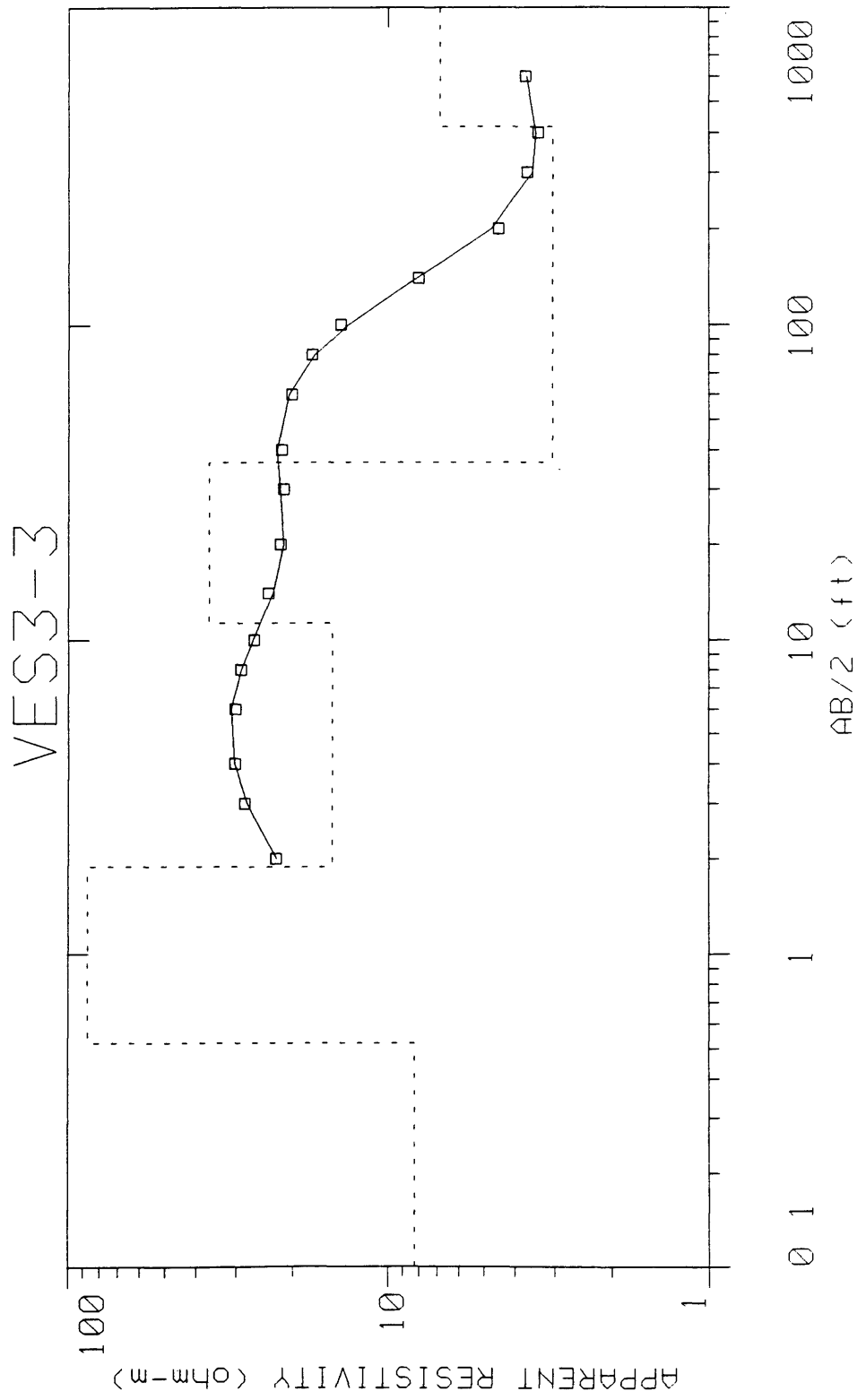


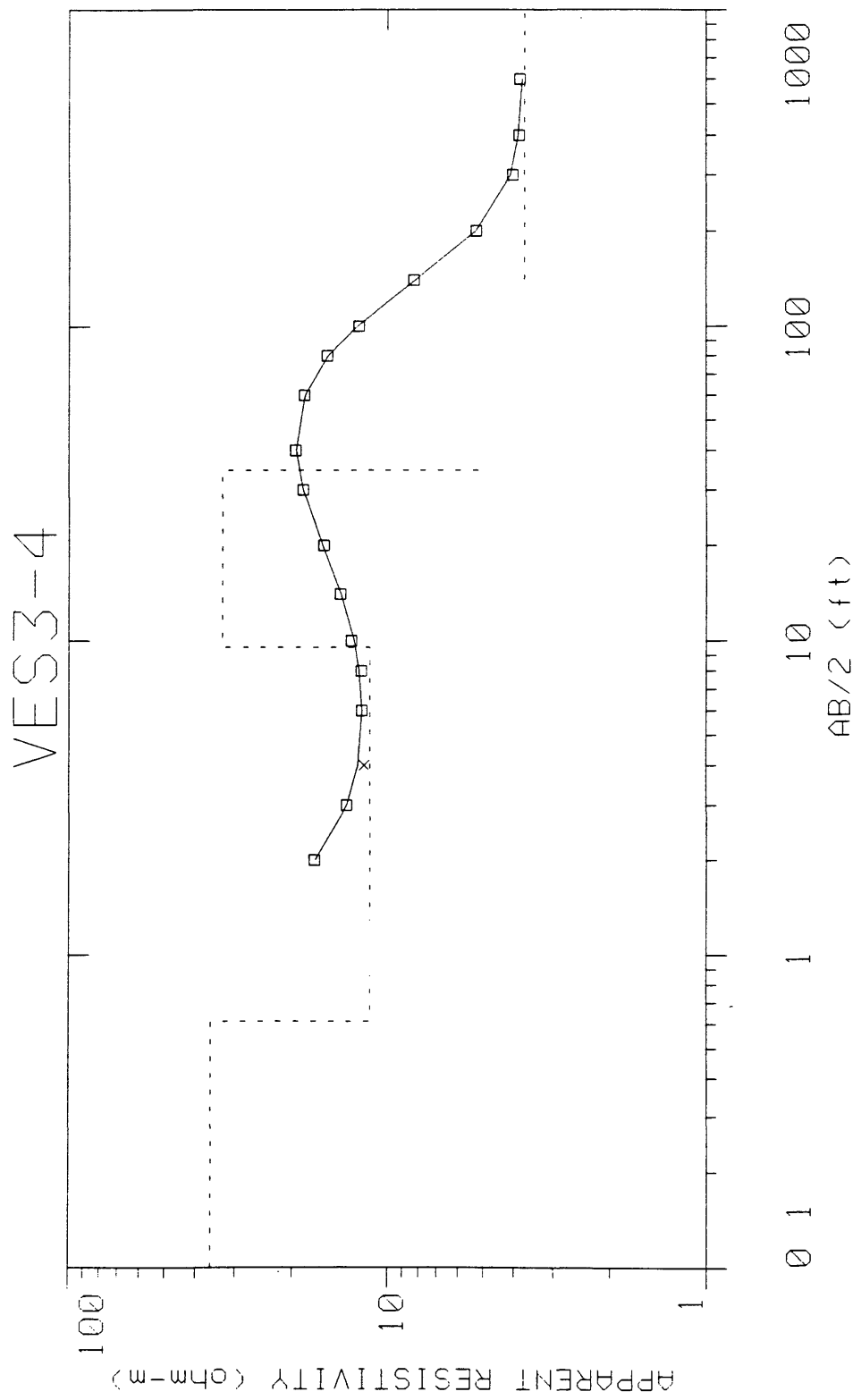












Gravity Data

ROCKY MOUNTAIN ARSENAL GEOPHYSICAL INVESTIGATION
GRAVITY DATA

LINE 1 SUMMER 1991

LaCOSTE AND ROMBERG/ EDCON SUPERG

EDITED (Deleted stations 12-20 from MAY19th)

EASTING (feet)	BOUGUER GRAVITY (mGal)	AVERAGE of REPEATS (mGal)	STD. DEV. of REPEATS (mGal)
2183655	3264.890	3264.890	
2183748	3264.920	3264.920	
2183844	3264.926	3264.926	
2183943	3264.930	3264.931	0.002
2183943	3264.933		
2184040	3264.934	3264.934	
2184136	3264.978	3264.978	
2184227	3264.995	3264.995	
2184281	3264.990	3264.990	
2184333	3264.995	3265.000	0.004
2184333	3265.002		
2184333	3265.001	3265.001	
2184383	3265.024	3265.024	
2184407	3265.024	3265.024	
2184431	3265.037	3265.033	0.006
2184431	3265.029		
2184474	3265.049	3265.049	
2184531	3265.053	3265.049	0.005
2184531	3265.046		
2184625	3265.087	3265.091	0.013
2184625	3265.105		
2184625	3265.080		
2184722	3265.107	3265.114	0.008
2184722	3265.113		
2184722	3265.123		
2184816	3265.142	3265.138	0.006
2184816	3265.134		
2184912	3265.148	3265.151	0.004
2184912	3265.154		
2185009	3265.175	3265.172	0.004
2185009	3265.169		
2185104	3265.213	3265.208	0.007
2185104	3265.203		
2185199	3265.221	3265.215	0.008
2185199	3265.209		
2185295	3265.247	3265.248	0.001
2185295	3265.249		

EASTING (feet)	BOUGUER GRAVITY (mGal)	AVERAGE of REPEATS (mGal)	STD. DEV. of REPEATS (mGal)
2185390	3265.263	3265.263	0.001
2185390	3265.262		
AVERAGE STANDARD DEVIATION=			<u>0.005</u>

Electromagnetic Data

ROCKY MOUNTAIN ARSENAL GEOPHYSICAL INVESTIGATION
 EM DATA
 LINE 1 SUMMER 1991
 GEONICS EM-31 AND EM-34

EASTING (feet)	CONDUCTIVITY							
	3.7m HMD (mS/m)	3.7m VMD (mS/m)	10m HMD (mS/m)	10m VMD (mS/m)	20m HMD (mS/m)	20m VMD (mS/m)	40m HMD (mS/m)	40m VMD (mS/m)
2183559	24	37	54	57	77	66	95	
2183589	26	40	60	49	81	59	90	
2183619	27	46	64	74	82	58	90	
2183649	28	49	65	63	81	68	85	50
2183679	29	48	62	60	79	58	92	75
2183709	26	42	58	53	75	63	88	60
2183739	24	38	52	52	71	64	90	60
2183769	20	35	48	53	68	60	88	70
2183799	20	34	48	47	66	72	80	75
2183829	18	34	43	52	64	77	82	69
2183859	17	32	40	55	63	68	80	62
2183889	17	31	42	51	61	62	85	62
2183919	17	30	41	47	61	53	80	70
2183949	18	28	39	44	60	60	80	70
2183979	17	28	38	45	59	62	80	65
2184009	17	29	39	46	58	67	70	68
2184039	18	30	38	51	58	67	80	66
2184069	17	30	38	49	57	60	77	65
2184099	17	28	39	43	60	59	76	66
2184129	18	28	40	43	62	56	77	61
2184159	20	30	42	43	61	61	76	60
2184189	21	33	42	43	62	62	76	65
2184219	20	35	43	46	61	62	76	64
2184249	22	34	43	45	61	60	76	71
2184279	22	34	42	44	60	60	76	69
2184309	20	33	40	39	60	61	76	60
2184339	20	33	42	41	60	55	76	68
2184369	20	30	42	35	60	52	76	66
2184399	20	30	40	34	60	61	77	54
2184429	21	33	42	43	60	57	75	55
2184459	24	37	42	44	60	54	75	50
2184489	24	37	42	38	60	51	75	58
2184519	24	38	44	39	60	58	76	64
2184549	24	36	44	44	60	65	76	58
2184579	24	36	42	42	60	60	76	62
2184609	24	37	44	40	62	57	76	57
2184639	26	40	46	36	62	58	77	64
2184669	26	40	45	43	62	64	76	65
2184699	23	36	45	50	62	61	78	63

EASTING (feet)	CONDUCTIVITY							
	3.7m HMD (mS/m)	3.7m VMD (mS/m)	10m HMD (mS/m)	10m VMD (mS/m)	20m HMD (mS/m)	20m VMD (mS/m)	40m HMD (mS/m)	40m VMD (mS/m)
2184729	23	38	45	42	61	52	77	60
2184759	26	40	47	40	63	50	79	57
2184789	26	40	48	42	65	51	79	63
2184819	26	39	49	38	64	56	78	54
2184849	25	39	49	41	64	50	78	59
2184879	25	38	48	42	62	53	78	62
2184909	23	37	45	44	62	58	78	64
2184939	21	36	42	44	60	60	77	68
2184969	22	35	41	44	58	56	77	65
2184999	22	35	40	43	57	59	76	64
2185029	20	33	40	42	57	54	76	63
2185059	20	33	40	42	56	54	76	68
2185089	20	33	40	42	56	61	76	66
2185119	20	33	38	42	56	62	76	65
2185149	20	33	38	37	58	52	77	57
2185179	20	34	39	45	58	56	78	68
2185209	20	34	40	38	60	52	79	63
2185239	22	32	39	37	59	56	78	66
2185269	22	32	38	34	59	54	78	72
2185299	22	34	38	36	57	55	78	68
2185329	23	33	39	31	58	57	78	66
2185359	21	32	37	39	56	57	76	62
2185389	22	32	38	35	56	59	77	62
2185419	22	33	36	36	56	53	75	68
2185449	23	33	37	32	56	57	76	67
2185479	22	32	37	32	54	56	76	68
2185509	22	32	36	34	56	54	75	61
2185539	21	31	35	32	56	58	75	63
2185569	21	30	35	33	56	55	74	66
2185599	22	30	35	31	55	52	75	65
2185629	20	30	35	31	54	52	74	68
2185659	20	28	33	34	53	57	74	60
2185689	19	27	32	35	54	60	74	68
2185719	18	26	34	38	54	53	72	62
2185749	22	30	38	38	56	51	72	54
2185779	24	35	38	30	56	56	74	70
2185809	21	32	36	33	57	52	74	64
2185839	21	31	36	35	56	53	74	69
2185869	22	31	37	30	56	54	74	64
2185899	22	30	38	30	54	55	72	60
2185929	22	31	36	32	53	54	73	71
2185959	22	32	36	32	51	52	73	61
2185989	23	35	36	32	54	57	73	64

EASTING (feet)	CONDUCTIVITY							
	3.7m HMD (mS/m)	3.7m VMD (mS/m)	10m HMD (mS/m)	10m VMD (mS/m)	20m HMD (mS/m)	20m VMD (mS/m)	40m HMD (mS/m)	40m VMD (mS/m)
2186019	22	34	37	36	56	56	74	54
2186049	22	33	36	34	55	52	73	59
2186079	23	34	38	31	53	49	72	55
2186109	23	36	36	33	54	48	72	68
2186139	18	30	34	35	52	52	72	69
2186169	16	27	32	35	50	58	70	70
2186199	15	24	29	34	48	54	70	70